TERTIARY IMIDAZOLE PHOSPHINE LIGANDS AND THEIR TRANSITION METAL COMPLEXES

by

ZHIXIAN WANG, B.Sc.

A Thesis

Submitted to the Faculty of Graduate Studies in Partial Fulfilment of the Requirements for the Degree

Doctor of Philosophy

McMaster University

January, 1994

DOCTOR OF PHILOSOPHY (1994) McMASTER UNIVERSITY
Department of Chemistry Hamilton, Ontario

TITLE: Tertiary Imidazole Phosphine Ligands and Their Transition Metal Complexes

AUTHOR: Zhixian Wang, B.Sc. (Shanghai Institute of Chemical Technology)

SUPERVISOR: Professor C.J.L. Lock

NUMBER OF PAGES: xiv, 175

ACKNOWLEDGEMENTS

I would like to thank Professor Colin Lock for his invaluable instructions, constant encouragement and friendship, which guided me through years of work.

I would like to thank the members of my committee, Drs. M. McGlinchey and J. Barbier for their guidance of my work.

I would like to thank Dr J.F. Britten for his generous help of the X-ray crystallographic work, Dr R.A. Bell for the help of organic synthesis, Drs B. Sayer and D. Hughes for the help of the NMR work, Dr H.E. Howard-Lock and G. Timmins for the help of the vibrational spectroscopy, Dr C. Frampton for collecting data and solving structure of some complexes.

I would like to thank our research group members, Dr Alon Guest, Hosen Alarabi, Yi Wei, Daren LeBlanc, Theresa Fauconnier, John Valliant, Christian Scholten, Byron DeLaBarre, Erika Wheeler, Paolo Vigna, Diana Copping, and Timor Seidel for providing a friendly atmosphere and various assistances.

Financial assistance is acknowledged from NSERC and the Department of Chemistry in the form of scholarships and teaching assistantships.

Abstract

Gold(I) phosphine complexes have been used in the treatment of rheumatoid arthritis. One such complex, auranofin [triethylphosphinegold(I) 2,3,4,6-tetra-O-acetyl-1-thio-β-glucopyranoside] is a commercially available drug. It is possible to replace the triethylphosphine by other phosphines, hence changing the chemical and physical properties of the compounds. Tertiary imidazole phosphines are multidentate ligands containing both "soft" and "hard" binding sites. By use of such ligands, it is possible to make complexes that can bring two different metal ions into the biological system at once.

In this work, a number of tertiary imidazole phosphine ligands and their metal complexes have been prepared and characterized by the X-ray diffraction method and other spectroscopic methods. The chemical properties of the phosphine ligands have been investigated.

The phosphines which have the phosphorus atom connected to the C2 carbon atom of the imidazole ring are poor σ-bases with respect to the phosphorus atom and are subject to chemical attack in the presence of some metal cations. Complexes of these ligands with hard or soft metal ion have been obtained, but no complexes with both a hard and a soft metal ion have been isolated for these phosphines. A new phosphine with the phosphorus atom connected to the C5(4) carbon atom of the imidazole ring has been synthesized, which readily binds to both hard and soft metal ions. A complex of this ligand

with gold(I) and copper(II) has been prepared and characterized.

Some gold(I) and platinum(II) complexes with ligands related to the decomposition products of the tertiary imidazole phosphines have also been prepared and characterized. The dynamic and static Jahn-Teller effects of the copper(II) complexes studied in this work are discussed.

Abbreviations

aq	aqueous
BIP	bis(imidazol-2-yl)phosphinic acid
$(BIP)_2Pt{\cdot}4H_2O$	bis[di(imidazol-2-yl)phosphinato-$N^3,N^{3'}$]platinum(II) tetrahydrate
bipy	bipyridine
^tBu	t-butyl
CI	chemical ionization
DMSO	dimethylsuphoxide
D-pen	D-penicillamine
EI	electron impact
en	ethylenediamine
e.s.d.	estimated standard deviation
Et	ethyl
EtMeinH	2-ethyl-4-methylimidazole
$HBpz_3$	hydrotris(1-pyrazolyl)borate
imH	imidazole
IR	infrared
Me	methyl
Me_2imH	4,5-dimethylimidazole
$(MeO)_3PAuCl$	chloro(trimethylphosphite-P)gold(I)
NMR	nuclear magnetic resonance
NOE	nuclear Overhauser enhancement
Ph	phenyl
phen	1,10-phenanthroline
ppm	parts per million
pyO	pyridine N-oxide

RA	rheumatoid arthritis
s	solid
TDMIP	tris(4,5-dimethylimidazol-2-yl)phosphine
TDMIP-5	tris(1,2-dimethylimidazol-5-yl)phosphine
TEMIP	tris(2-ethyl-4(5)-methylimidazol-5(4)-yl)phosphine
$[(TEMIPAuCl)_2Cu](NO_3)_2$	bis{chloro[tris(2-ethyl-5-methylimidazol-4-yl)phosphine-P]gold(I)-N^3,$N^{3'}$,$N^{3''}$}copper(II) dinitrate dihydrate
$[(TEMIP)_2Cu](NO_3)_2$	bis[tris(2-ethyl-5-methylimidazol-4-yl)phosphine-N^3,$N^{3'}$,$N^{3''}$]copper(II) dinitrate
TGT	1-thio-β-D-glucose tetraacetate
THF	tetrahydrofuran
TIP	tris(imidazol-2-yl)phosphine
$[(TIP)_2Cu](NO_3)_2$	bis[tris(imidazol-2-yl)phosphine-N^3,$N^{3'}$,$N^{3''}$]copper(II) dinitrate
$[(TIP)_2M](NO_3)_2$	bis[tris(imidazol-2-yl)phosphine-N^3,$N^{3'}$,$N^{3''}$]M(II) dinitrate
TMIP	tris(1-methylimidazol-2-yl)phosphine
TMIPAuCl	chloro[tris(1-methylimidazol-2-yl)phosphine-P]gold(I)
$[(TMIP)_2Ni](AuI_2)_2$	bis[tris(1-methylimidazol-2-yl)phosphine-N^3,$N^{3'}$,$N^{3''}$]nickel(II) di[diiodoaurate(I)]
TMS	tetramethylsilane
TPP	tris(2-pyridyl)phosphine
ttcn	trithiacyclononane

Table of Contents

List of Tables

List of Figures

Chapter 1

Introduction

1.1 The Chemistry of Tertiary Phosphines

Tertiary imidazole phosphine ligands are of particular interest because they are multidentate ligands containing both "soft" and "hard" binding sites. Such ligands can bind to both soft and hard metal ions simultaneously. The aromatic nitrogen atoms of the imidazole ring is a relatively hard ligand; it tends to form stable complexes with hard metal ions such as Cu(II), Ni(II) and Fe(III). The phosphorus atom of the phosphine is a relatively soft ligand; it tends to form stable complexes with soft metal ions such as Au(I), Ag(I) and Cu(I).

The hardness and softness of an acid or a base is generally described by electronic interactions. Hard acids and bases tend to have more ionic interactions while soft ones are more covalent. These can be interpreted in terms of frontier orbital separation. When the separation is small, the electron distribution is easily rearranged by some energy perturbations to give a covalent bond and the molecule is soft. When the separation is large, the electronic structures are barely perturbable and the interaction is mainly electrostatic; the molecule is hard (1). Some examples of hard and soft acids and bases are listed in **Table 1.1**.

Phosphines are well known to chemists. They are important ligands in studying organometallic and coordination chemistry. Phosphines have important

Table 1.1 The classification of Lewis acids and bases*

	Hard	Borderline	Soft
Acids	H^+, Li^+, Na^+, K^+, Be^{2+}, Mg^{2+}, Ca^{2+}, Cr^{3+}, SO_3, BF_3	Fe^{2+}, Co^{2+}, Ni^{2+}, Cu^{2+}, Zn^{2+}, Pb^{2+}, SO_2, BBr_3	Cu^+, Ag^+, Au^+, Tl^+, Hg^+, Pd^{2+}, Cd^{2+}, Pt^{2+}, Hg^{2+}, BH_3
Bases	F^-, OH^-, H_2O, NH_3, CO_3^{2-}, NO_3^- O^{2-}, SO_4^{2-}, $PO_4^{3-}ClO_4^-$	NO_2^-, SO_3^{2-}, Br^-, N_3^-, N_2, C_6H_5N, SCN^-	H^-, R^-, CN^-, CO, I^-, SCN^-, R_3P, R_2S

* For SCN^-, the italicized element is the site of attachment to which the classification refers. Adapted from reference 1.

applications in organic synthesis (2). Transition metal phosphine complexes are extensively used as catalysts for various chemical reactions (3). The chemistry of phosphines has been reviewed annually by the Royal Society of Chemistry in the journal "Organophosphorus Chemistry".

Some laboratory methods for preparing tertiary phosphines are (4):

(i) Reaction of phosphorus halides with Grignard reagents, such as:

$$PCl_3 + 3RMgBr \longrightarrow PR_3 + 3MgClBr$$

Sometimes organolithium derivatives can be used as an alternative.

(ii) Reduction of phosphorus compounds with lithium aluminum hydride, such as:

$$4R_3PO + LiAlH_4 \longrightarrow 4R_3P + LiAl(OH)_4$$

(iii) From metal phosphides, such as:

$$NaPR_2 + R'X \longrightarrow R_2PR' + NaX$$

Metal phosphides can be prepared by reacting the metal with the appropriate phosphine in liquid ammonia:

$$2R_2PH + 2Na \xrightarrow{NH_3} 2R_2PNa + H_2$$

(iv) Nucleophilic addition towards polarized carbon-carbon multiple bonds (2),

$$RPH_2 + 2CH_2{=}CHY \longrightarrow RP(CH_2CH_2Y)_2 \qquad (Y = CN, COR', CO_2R', CONH_2, \text{etc.})$$

The products can be further reacted with alkyl halides to give new kinds of phosphines, such as (5):

$$PhP(CH_2CH_2CN)_2 + RBr + NaOEt \longrightarrow PhRP(CH_2CH_2CN) + NaBr + EtOCH_2CH_2CN$$

$$PhRP(CH_2CH_2CN) + R'Br + NaOEt \longrightarrow PhRR'P + NaBr + EtOCH_2CH_2CN$$

Phosphines are good σ-donor and to some extent, π-acceptor ligands. The relative σ-basicity and π-acidity of such ligands is still an area of controversy (6).

The σ-basicity has been assumed to follow the order (7):

$$P^tBu_3 > PMe_3 > PMe_2Ph > PMePh_2 > PPh_3 > PH_3$$

This is in accord with the lone pair donor ability of PR_3 towards protons in solution (8). Puddephatt and coworkers have suggested that such an order should actually be reversed on the bases of relative lone pair ionization potentials and proton-affinities of these phosphines in the gas phase (9).

The σ-basicity of phosphine ligands is also associated with steric and electronic effects. For example, increasing the steric bulkiness of substituents on the phosphorus atom opens up the C-P-C angles, hence increasing the s-character in the P-C bonds and decreasing the s-character of the lone pair. Also, the percentage of s-character of the phosphorus lone pair will increase with increasing electronegativity of the substituents (7).

The π-basicity of phosphine ligands is thought to follow the sequence below (10):

$PH_3 > PPh_3 \sim PR_3 > P^tBu_3$

Bonding in metal-phosphine complexes is generally described (11) in terms of the Dewar-Chatt model (12). According to this model, the phosphorus atom donates charge to the metal atom through its lone pair, and the metal atom filled or partly filled d-orbitals back donate charge into the empty phosphorus atom 3d-orbitals. Such a π-π bonding interaction is important when the metal is in a low valence state (7).

It has been shown by recent studies that the antibonding orbitals of the phosphines themselves can act as accepting orbitals without invoking a direct participation of the phosphorus 3d-orbitals (1, 13), but Pacchioni and coworkers found that the phosphorus 3d-orbitals are important in the metal-phosphorus bonding based on their studies of Pd(0) phosphine complexes (6).

The larger size and lower electronegativity of phosphorus atom as

compared to nitrogen atom leads to higher polarizability of the lone pair on the phosphorus atom. Phosphine ligands tend to form stable complexes with large polarizable metal atoms and ions. Gold(I) is a typical example.

1.2 The Inorganic Chemistry of Monovalent Gold

Gold is one of the most noble metals. Common oxidation states of gold compounds are 0, +1, and +3. In aqueous solution, The Au(I) ion is extremely unstable with respect to the disproportionation (11):

$3Au^{+}(aq) = Au^{3+}(aq) + 2Au(s)$ $K = 10^{10}$

This can be derived from the following half cell electropotentials (14):

$Au \longrightarrow Au^{+}(aq) + e^{-}$ $E = 1.7 + 0.059\log[Au^{+}]$

$Au \longrightarrow Au^{3+}(aq) + 3e^{-}$ $E = 1.5 + 0.0197\log[Au^{3+}]$

However, the +1 oxidation state can be stabilized by the presence of a complexing ligand. This is exemplified by the equilibrium constant K for the following reactions:

$3(AuL_2)^{+} \longrightarrow (AuL_4)^{3+} + 2Au + 2L$ where L is a neutral ligand, and

$3(AuL_2)^{-} \longrightarrow (AuL_4)^{-} + 2Au + 2L^{-}$ where L is a monoanionic ligand.

For $L = H_2O$, $K = 10^{10}$; $L = Cl^{-}$, $K = 5x10^{7}$; $L = Br^{-}$, $K = 10^{5}$; $L = SCN^{-}$, $K = 2.1$; for $L = CN^{-}$, K is estimated to be about 10^{-25} (14).

Monovalent gold forms complexes with a number of ligands. The more

polarizable the ligand the more stable the complex. The general trend of stability is given below (14):

anionic, $[AuX_2]^-$: $CN^- >> I^- > Br^- > Cl^- \sim NCS^- > NCO^-$;

cationic, $[AuL_2]^+$: $PMe_2Ph > PMePh_2 > PPh_3 > NH_3 > py > SMe_2 > OPPh_3$;

neutral, [AuXL]: $PMe_2Ph > PMePh_2 > PPh_3 > SMe_2 >> OMe_2$.

This is in agreement with the classification of gold as a class b metal or Au(I) as a soft acid (11).

Monovalent gold forms a large number of stable complexes with trivalent phosphorus and thiolate sulphur ligands (15, 16, 17). The phosphorus atom in such complexes is always terminal while the sulphur atom can be either bridging or terminal. The importance of such complexes will be discussed in the following section. Gold(I) also forms complexes with carbon, selenium and nitrogen donor ligands (14).

Compared to copper(I) and silver(I), gold(I) complexes have a greater tendency to adopt linear two coordination geometry. The reason for this is still under dispute. Some possible explanations are (14):

(1) Polarizability of M^+ ions. Larger metal ions are more polarizable, and such ions tend to form complexes with lower coordination number. The size of M^+ is, $Au^+ > Ag^+ >> Cu^+$.

(2) Energy separation of s and p orbitals. The larger the energy separation, the more difficult the hybridization of s and p orbitals, the less p character in the

hybrids and the smaller the coordination number. The s-p energy separation of M^+ is, $Au^+ >> Ag^+ > Cu^+$.

(3) Energy separation of s and d orbitals. The smaller the energy separation of nd and (n+1)s orbitals, the easier the s-d hybridization. One of the s-d hybrids can further hybridize with ligand orbitals to form a linear coordination complex. The d-s energy separation is $Au^+ < Ag^+ < Cu^+$.

All these factors predict the dominance of linear two coordination for gold(I) complexes.

The trend of s-d separation can also be predicted by the relativistic effect (18). Increasing the charge on the nucleus will lead to a contraction of the s-orbitals which will give more shielding to the d-orbitals, hence narrowing the energy separation between nd and (n+1)s orbitals (19). Such an effect is typical for post-lanthanide metals and reaches maximum at gold. Gold chemistry is dominated by the relativistic effect, which is exemplified in the large ionization potential and electron affinity, the formation of stable diatomic Au_2, anionic Au^{-1}, and the existence of a large number of homonuclear and heteronuclear clusters (20, 21). This also explains why there are relatively short gold-gold contacts in many gold complexes (22).

Gold(I) complexes are usually prepared by the following methods:

(1) Oxidation of gold metal in the presence of a complexing ligand, such as:

$4Au + 8CN^- + O_2 + 2H_2O \longrightarrow 4[Au(CN)_2]^- + 4OH^-$ (23)

(2) Reduction of gold(III) complexes, such as:

$Na(AuCl_4) + 2PPh_3 \longrightarrow Ph_3PAuCl + Ph_3PCl_2$ (24)

$[AuCl_4]^- + 2R_2S + H_2O \longrightarrow R_2SAuCl + R_2SO + 2H^+ + 3Cl^-$ (25)

$nH(AuCl_4) + 3nRSH \longrightarrow (AuSR)_n + nRSSR + 4nHCl$ (26)

(3) Directly from gold(I) halides, such as:

$AuCl + PCl_3 \longrightarrow Cl_3PAuCl$ (27)

(4) Ligand substitution reaction, such as:

$Me_2SAuCl + PPh_3 \longrightarrow PPh_3PAuCl + Me_2S$ (28)

$PPh_3PAuCl + LiN_3 \longrightarrow Ph_3PAuN_3 + LiCl$ (29)

$Et_3PAuCl + PhSH + OH^- \longrightarrow Et_3PAuSPh + Cl^- + H_2O$ (30)

The last method is the most popular and versatile one because gold(I) has a d^{10} electronic configuration, which results in zero ligand field stabilization energy, so gold(I) complexes are kinetically labile.

In solution, gold(I) complexes undergo rapid ligand scrambling and exchange reactions (31). These reactions are thought to go through higher coordination intermediates (32). This is supported by NMR studies (33) and the structural characterization of a number of three and four coordination gold(I) complexes (34, 35) even with monodentate ligands (36-38).

1.3 Medicinal Applications of Gold(I) Phosphine Complexes

Gold is one of the transition metal elements that have been used

successfully in medicine (15, 39). The use of gold in medicine can be traced back as far as the Chinese in 2500 B.C. (40). Today, the most important application of gold compounds is in the treatment of rheumatoid arthritis (RA) (31). This was first introduced by Landé in 1927 (41), although Forestier is regarded as the father of treatment of RA with gold compounds (42).

Rheumatoid arthritis is a complex, exclusively human disease (43). The mechanism of action of gold compounds on RA is still not clear, and there are conflicting reports about the efficacy of gold drugs. It is believed, however, that gold drugs are as effective as any other available drugs, and are among the few drugs that actually induce remission of the disease (31, 44). Gold compounds have been found to affect many biological processes that were thought to be related to RA (45), such as inhibition of fibroblast proliferation (46), inhibition of cytokine induced release of granule proteins from adherent neutrophils (47), suppressive effect on the generation of superoxide radicals (48), *etc.*

There are a number of gold complexes currently in clinical use (49). Among them, sodium thiosulphate-S-aurate(I) (Sanochrysine), disodium thiomalato-S-aurate(I) (Myochrysine) and thioglucosato-S-aurate(I) (Solganol) are the most widely used. These drugs are water soluble and are given parenterally to the patients. Common problems associated with these drugs are that they are poorly characterized, and when in use, can cause toxic side effects, such as skin rashes, diarrhoea, proteinuria and thrombocytopenia (50).

One new drug, triethylphosphinegold(I) 2,3,4,6-tetra-O-acetyl-1-thio-β-glucopyranoside (Auranofin) was developed by Smith, Kline and French Laboratories recently, with the aim of reducing the toxic side effects (51). This drug is lipid soluble and can be given orally. When using such a drug, the blood and urine gold level can be maintained at a desired value by a low daily dose, thus reducing the toxicity caused by the accumulation of gold in certain tissues and organs (52). It was found that about 5% of the absorbed gold administered as auranofin is excreted through the kidneys and about 95% is excreted through the feces. By contrast, 70% of the excreted gold from Myochrysine injections is found in urine, and 30% in the feces (53). Even with Auranofin, toxic side effects, especially diarrhoea, are still a problem (52). Some studies also indicate that Auranofin is less effective than other injectable gold drugs (54). Unlike the polymeric gold(I) thiol complexes mentioned above, auranofin is monomeric. Its structure has been fully characterized by X-ray crystallography (55) (**Figure 1.1**).

Some gold(I) phosphine complexes, including auranofin, are cytotoxic. They have *in vitro* and *in vivo* antitumour activities (7, 56). They are potential anticancer drugs. Gold(I) complexes with ligands other than phosphine show marginal activities. The reason for this is probably that gold(I) phosphine complexes are neutral and

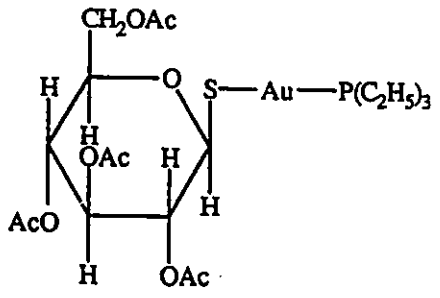

Figure 1.1 The structure of auranofin

lipophilic, they can penetrate the cell membrane readily, bringing gold to some reactive SH groups inside the cell and/or delivering toxic phosphines to certain cellular targets (7, 56).

1.4 The Biological Role of Imidazole

Imidazole is a planar, five membered ring with two nitrogen and three carbon atoms. As a result of the delocalized π system, there is considerable double bond character in the bonds between all the ring atoms (57). It can be considered as having both pyrrole and pyridine properties. It is an amphoteric molecule with a basic pyridine type nitrogen atom and a weakly acidic pyrrole type nitrogen atom (58). The ring carbon atoms of imidazole compounds are subject to both electrophilic and nucleophilic attack. Electrophilic attack takes place preferably at the C-5(4) carbon atom and nucleophilic attack at the C-2 carbon atom (59). Another characteristic of imidazole compounds is that they undergo rapid tautomerization (60). This is shown by the following scheme (**Scheme 1**).

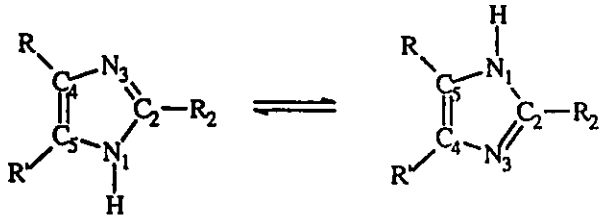

Scheme 1

Imidazole is an important ligand in chemical and biological systems. It occurs in proteins as the active site of histidine and the benzimidazole ring, and in nucleic acids as part of the purine rings of adenine, guanine and hypoxanthine.

Imidazole can function as a proton donor and/or acceptor site for hydrogen bonding, as a specific/general base or nucleophilic catalyst, and as a site for metal ion coordination (61). Metal imidazole complexes are found in a number of metalloenzymes and metalloproteins. Some examples are, copper proteins (62, 63), zinc proteins (64), manganese biomolecules (65), iron proteins (66, 67).

1.5 Objectives

Some tertiary imidazole phosphine ligands have been synthesized through literature procedures (68-70). They are: tris(imidazol-2-yl)phosphine (TIP), tris(4,5-dimethylimidazol-2-yl)phosphine (TDMIP), tris(1-methylimidazol-2-yl)phosphine (TMIP), and tris(2-ethyl-4(5)-methylimidazol-5(4)-yl)phosphine (TEMIP) (**Figure** 1.2). These ligands have binding sites for both hard and soft metal ions.

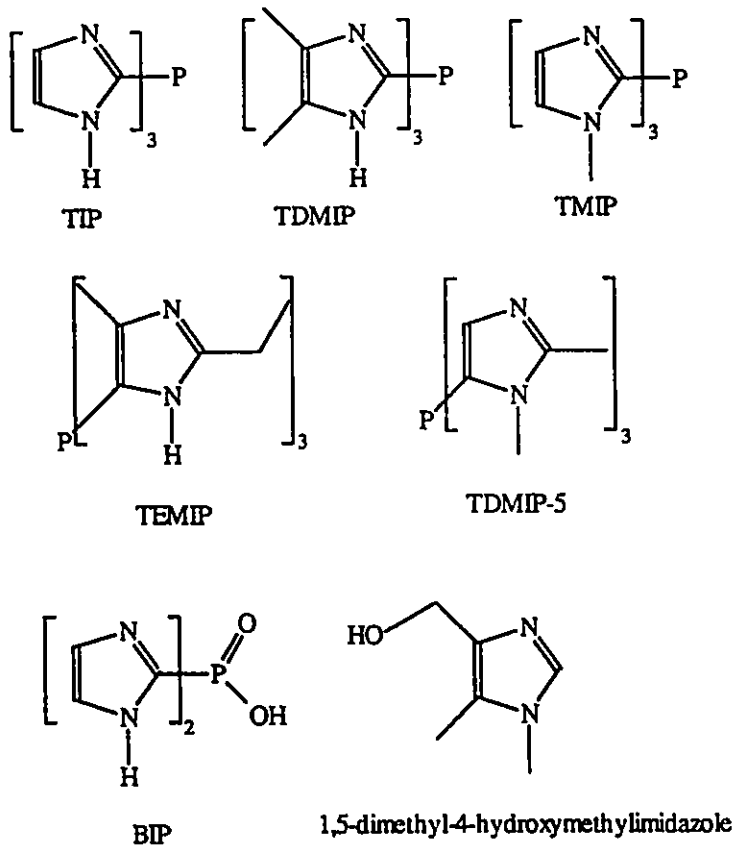

Figure 1.2 Ligands in this work

They are potential candidates for substituting the Et_3P moiety in the antirheumatoid arthritis drug auranofin. By use of such ligands, it is possible to introduce two different kinds of metals into the biological system at once, and it is also possible to change the physical and chemical properties of the drug, hence altering the pharmacodynamics and pharmacokinetics of the drug. These ligands are useful for studying the coordination chemistry of the transition metal elements, for preparing model compounds to model the structural, physical and chemical properties of some metalloproteins. For example, a zinc protein carbonic anhydrase model and an iron protein hemerythrin model have been prepared by use of such phosphine ligands (69, 71). Synthesis of another new phosphine ligand, tris(1,2-dimethylimidazol-5-yl)phosphine (TDMIP-5)(**Figure 1.2**) was unsuccessful. Several attempts gave extremely low and unreproducible yields.

In this work, a number of gold(I) and other transition metal complexes with tertiary imidazole phosphine ligands and their derivatives were prepared, some of them were characterized by X-ray crystallography and other spectroscopic methods. Their chemical properties related to the phosphine ligands were investigated.

A platinum(II) complex with the oxidation product of TIP (BIP), and gold(I) complexes with the decomposition products of TIP and TDMIP will also be described.

Chapter 2

Experiments

2.1 Chemical Reagents

All commercially available chemicals were purchased and used without further purification. Gold was obtained as pure metal chips or recovered from laboratory residues. The recovery procedure was as follows: The residue was heated to dryness and the resulting solid was burned over a Bunsen burner for 5-10 hours. The burnt solid was extracted with 6M hydrochloric acid, water, concentrated nitric acid and water respectively. The solid was separated by filtration and burned again. The process was repeated three times. The recovered metals were then dissolved in *aqua regia* and any insoluble materials were removed by filtration. The same method was also used for recovering platinum from laboratory residues.

Tetrachloroauric acid, $HAuCl_4$, was prepared by the method of Block (72). The final product was dried over containers of NaOH and P_2O_5 in an evacuated desiccator.

Gold(I) iodide was prepared by the method of Faltens and Shirley (73). To a solution of $HAuCl_4$ (0.13g) in a 3:1 methanol/water mixture (10mL), 3 equivalent KI (0.16g) in water (2mL) was added dropwise with continuous stirring. The precipitated product was separated by filtration, washed with

methanol, and used directly for further reaction (90-95% yield).

(Dimethylsulphide)chlorogold(I), Me_2SAuCl, was prepared according to Bonati *et al.* (25). To a solution of $HAuCl_4$ (4g) in methanol (10mL), a solution of 2.1 equivalent (1.5mL) of Me_2S in methanol (5mL) was added dropwise with continuous stirring. The precipitated product was separated by filtration, washed with methanol, then ether, and air dried. Yield 2.6-2.7g (90-95%). In contrast to the literature method, only a slight excess of Me_2S was added to avoid possible side reactions.

Potassium tetrachloroplatinate(II), K_2PtCl_4, was prepared by the method of Keller (74) (80% yield).

4,5-Dimethylimidazole was prepared by the method of Satoru *et al.* (75). The raw product (50g) was purified by washing through a silica gel column with acetone (300mL). The main by-product, hexamethylenetetramine, was retained on the column. The purified product was obtained by evaporation of the solvent acetone (70% overall yield).

2.2 X-ray Crystallography

Single crystal X-ray diffraction was the most important analytical tool used in this work to identify compounds from various chemical reactions and to investigate structural and chemical properties of these compounds. The theoretical basis of single crystal X-ray crystallography has been treated in detail by Buerger (76), Luger (77), and Stout and Jensen (78).

2.2.1 Crystal Preparation

Most of the crystals suitable for X-ray diffraction experiments were prepared by slow evaporation of solutions of the compounds with appropriate solvents or mixtures of solvents. For those compounds having very low solubility, the low temperature dilution method was used in some cases. By this method, dilute solutions of the reactants were prepared separately, cooled to about -40°C, and mixed at that temperature. The mixture was sealed in a beaker and kept at -10 to -20°C. Suitable crystals were obtained after 2 to 4 days.

The size of crystals chosen for X-ray data collection was between 0.02 to 0.5mm, to ensure enough diffraction power and uniform bathing in the X-ray beam. Crystals larger than 0.5mm were cut by a razor blade. The quality of the crystals was judged according to cleanness, uniformity, and extinction property. Sharp, complete extinction upon each 90° rotation of the crystal under crossed polarisers should be observed for those crystals which do not have a three fold axis as a symmetry element.

The chosen crystals were mounted on a 0.05 to 0.2mm diameter glass fibre with epoxy-cement. In the cases where crystals decomposed because of loss of lattice solvents, the cystals were sealed in a 0.2 to 0.3mm diameter glass capillary with the presence of a small amount of mother liquor.

Crystal densities were measured by suspending the crystals in a mixture of two liquids, one less and one more dense than the crystal. The measured

density D_m was compared to the calculated density D_x.

$$D_x = M \cdot Z / 0.6022V \ (g \cdot cm^{-3})$$

where M is the gram molecular weight, Z is the number of molecules in a unit cell, and V is the volume of the unit cell in $Å^3$.

Good agreement between D_m and D_x was observed, otherwise either D_m or the unit cell was remeasured to correct errors in the experiment or in the formulation of the compound.

2.2.2 Data Collection

Unit cell determination and intensity data collection were performed on Nicolet P3, Rigaku AFC6R, Siemens P3/V or Siemens P4 diffractometers. Crystals were centred optically and, if possible, with the longest axis aligned close to the ω-2θ axis on the diffractometer, in order to minimize errors in absorption correction.

When a Nicolet diffractometer was used, a full ϕ-rotation polaroid photograph was taken with all diffractometer angles set to zero. Fifteen reflections with a 2θ range from 18 to 38° were selected from the photograph and entered into the diffractometer computer. These reflections were used to determine the unit cell parameters and the orientation matrix, which was used by the computer to drive the diffractometer to appropriate angles for hkl data collection. The polaroid photograph procedure was omitted when the Rigaku and Siemens diffractometers were used. A random search was done by the diffractometer to

find 25-30 reflections. A search for possible supercells, determination of accurate cell parameters, orientation matrix, and Laue group were all done automatically.

Intensities were measured by use of graphite monochromatized CuKα (λ = 1.54180Å), MoKα (λ = 0.71073Å) or AgKα radiation (λ = 0.56086Å) with coupled ω(crystal)-2θ(counter) scans. When the unit cell dimension was too large, an ω-scan was used to avoid intensity overlap between neighbouring reflections. An upper value of 2θ was selected, depending on the scattering power of the crystal. Scans were made from 1.0° below the $K\alpha_1$ position to 1.0° above the $K\alpha_2$ position. The scan rate for each reflection was determined by the diffractometer computer. Two or three standard reflections, chosen either manually or automatically, were measured repeatedly every 50 or 100 reflections, to monitor crystal and instrument stability. Sometimes, a ψ-scan data collection was performed at the end. The data were stored in a separate file and used for absorption correction in some cases.

Intensities (I) and standard deviations (σ_I) were calculated as:

$$I = N_p - N_b$$

$$\sigma_I = (N_p + N_b)^{1/2}$$

where N_p is the peak count and N_b is the background count.

More details about data collection can be found in the diffractometer operation manual supplied by the manufacturer.

2.2.3 Data Reduction

Reflections with $-3\sigma_I \leq I \leq 3\sigma_I$ were treated by the method of French and Wilson (79). Intensities and standard deviations were reduced to observed structure factors $|F_o|$ and errors in F_o, $\sigma(F)$.

$$|F_o| = (I \cdot A/Lp)^{1/2}$$

$$\sigma(F) = [\sigma(I) \cdot A]/(2F_o \cdot Lp)$$

where Lp is the Lorenz polarization factor and A is the absorption factor.

$$Lp = (1 + \cos^2 2\theta)\cos\psi/\sin 2\theta(1 + \cos\psi)$$

where ψ is the crystal monochromator 2θ angle.

Absorption corrections were made by use of the empirical ψ-scan method (80), or the analytical DIFABS method (81).

Symmetry equivalent reflections were averaged and an R_{int} was calculated to evaluate the internal consistency of the data set.

$$R_{int} = \{\Sigma N[\Sigma w(\langle F\rangle - F)^2]/\Sigma(N-1)\Sigma w \cdot F^2\}^{1/2}$$

where the inner summations are over the N equivalent reflections averaged and the outer summations are over unique reflections. Where $\langle F\rangle$ is the averaged mean, N is the number of equivalent reflections averaged, and w is a weighting factor, $w = 1/[\sigma(F)]^2$ for normal cases.

2.2.4 Structure Solution and Refinement

The scattering factor of an atom (f) is

$$f = f_0 \exp[-B(\sin^2\theta)/\lambda^2]$$

where f_0 is the scattering factor of a spherical atom. It is a function of atom type

and $\sin\theta/\lambda$. Values of f_0 against $\sin\theta/\lambda$ for all stable elements have been tabulated with anomalous dispersion corrections (82). B is the temperature factor, which is related to the mean-square amplitude of atomic vibration.

For a crystal with a known structure, the structure factors can be calculated (F_c) for each reflection at hkl.

$$F_c(hkl) = \sum f_j \exp[2\pi i(hx_j + ky_j + lz_j)]$$

where f_j is the scattering factor of the jth atom, and x_j, y_j, z_j are the positional parameters of that atom. The sum is over all atoms in a unit cell.

On the other hand, if all the structure factors of the hkl reflections are known, the electron density at any point (x,y,z) inside the unit cell can be calculated by a Fourier synthesis.

$$\rho(x,y,z) = (1/V)\sum\sum\sum F_{hkl} \exp[-2\pi i(hx + ky + lz)]$$

or $$\rho(x,y,z) = (1/V)\sum\sum\sum |F_{hkl}| \exp[-2\pi i(hx + ky + lz - \alpha_{hkl})]$$

where V is the volume of the unit cell, α_{hkl} is the phase angle. The summations are over all h, k, and l.

In practice, it is the moduli of the structure factors $|F_{hkl}|$ that have been observed. Phases of each reflection have to be determined. In this work, two methods, the Patterson method and the direct method, were used for phase determination.

The Patterson method is based on the Patterson synthesis.

$$P(u,v,w) = (1/V)\sum\sum\sum (F_o)^2 \cos 2\pi(hu + kv + lw)$$

where (u,v,w) is an interatomic vector. Such a synthesis will give all possible interatomic vectors between atoms in a unit cell. Vectors between heavy atoms will have high peak heights on a Patterson map. The positions of such atoms can be located and used as a starting model for phase calculation.

The direct method uses probability arguments to assign phases directly to some structure factors for which the assignments are highly probable. These phased structure factors are then used in a Fourier synthesis to build a model.

In both cases, a starting model was built up and all the F_cs were calculated according to this model. The phases of these F_cs were assigned to the corresponding F_os. An improved solution was obtained from another Fourier synthesis which used all the assigned F_os. A complete structure solution was usually obtained after difference Fourier syntheses, which were carried out after least squares refinement.

$$\Delta\rho = (1/V)\Sigma\Sigma\Sigma(|F_o| - |F_c|)\exp[-2\pi i(hx + ky + lz - \alpha_c)]$$

where α_c is the phase of F_c. Missing atoms from the original model will appear as peaks on the density map.

Raw structures were refined by the method of least-squares. Full-matrix least-squares minimized $\Sigma\omega(|F_o| - |F_c|)^2$. Atomic positional parameters, temperature factors and an overall scaling factor were varied. A difference Fourier synthesis was performed after each refinement. Peaks from the difference map can be picked up to assemble a new model for phase calculation. The process was

repeated until all the parameters were scarcely varying, and the difference map was almost flat. For all the structures in this work, hydrogen atoms were placed in calculated positions and not refined. Qualities of the structure refinements were judged according to the R and S values.

$$R = \Sigma | |F_o| - |F_c| | / \Sigma |F_o|$$

$$R_w = [\Sigma w(|F_o| - |F_c|)^2 / \Sigma (F_o)^2]^{1/2}$$

$$S = [\Sigma w(|F_o| - |F_c|)^2 / (M - N)]^{1/2}$$

where w is the weight, M is the number of observed reflections and N is the number of parameters refined. The sums are over all reflections.

Details about structure solution and refinement can be found in the references mentioned above.

2.2.5 Computer Programs

Calculations were performed on VAX 3100, Laser 386 and IBM 486 computers. SHELXTL PLUS (83) was used for data reduction, ψ-scan absorption correction, structure solution and refinement, geometry calculation, and molecular diagram preparation. Atomic scattering factors with anomalous dispersion corrections were compiled into the program and used automatically. For those DIFABS absorption corrections, computations were performed on a Silicon Graphics IRIS INDIGO computer.

2.3 NMR Spectroscopy

Samples for NMR spectroscopy were dissolved in appropriate deuterated

solvents and sealed in 5mm NMR tubes. TMS was used as an internal reference for ^{1}H and ^{13}C spectra and 85% H_3PO_4 in D_2O was used as an external reference for ^{31}P spectra. Preliminary ^{1}H spectra were recorded on a Varian EM-390 continuous wave spectrometer, operating at a frequency of 90MHz. The sweep width was set up to 10ppm down field from TMS and the sweep time was set up to 2 or 5 minutes. Other ^{1}H and ^{13}C spectra were recorded on a Bruker AC-200 Fourier transform spectrometer with spectrometer frequencies of 200.133MHz for ^{1}H, and 50.324MHz for ^{13}C. Sweep widths were 2500.00Hz for ^{1}H and 12195.122Hz for ^{13}C (down field from TMS). ^{31}P spectra were recorded on a Bruker AC-300 Fourier transform spectrometer with a spectrometer frequency of 121.497MHz and sweep width of 50000.00Hz (25000 down and 25000 up from H_3PO_4). Deuterated solvents were used as internal locks. The free induction decays were processed by use of Gaussian multiplication for resolution enhancement, with 16384 memory locations. Chemical shifts were reported in ppm relative to TMS for ^{1}H and ^{13}C, and relative to H_3PO_4 for ^{31}P. Coupling constants were reported in Hz.

2.4 Vibrational Spectroscopy

Infrared spectra were recorded on Perkin Elmer 283 or Bio Rad FTS-40 spectrometers. Solid samples were prepared as KBr pellets (1-5%). Spectra were calibrated against a polystyrene calibrant. Raman spectra were recorded on a Spex 14018 spectrometer. Samples were prepared as powder and excited with λ = 514.5nm radiation from a Coherent Radiation Argon Laser Model 52. Spectra were

calibrated against powdered $HgCl_2$.

2.5 Mass Spectroscopy

Chemical ionization (CI) and electron impact (EI) mass spectra were recorded on a VG Analytical ZAB-E double focusing mass spectrometer. Low resolution spectra were recorded for routine sample analysis. Typical experimental conditions were: resolution 1000, electron energy 70eV, source temperature 200°C, source pressure $2x10^{-6}$ mbar, for EI and $4x10^{-5}$ mbar for CI. Spectra were reported in m/e (relative intensity).

2.6 Qualitative Elemental Analysis

A method was developed to perform qualitative elemental analysis for gold. The method consists of burning a small amount of sample (about a few milligrams) on a piece of porcelain crucible to above the melting point of gold (1063°C) by use of a natural gas-oxygen flame. All of the organic materials were burned off and metallic gold was melted. If the sample contained gold, golden shining droplets were left on the porcelain. In cases when other metals were present (such as copper or iron), extraction of the residue with a few droplets of concentrated HCl revealed the shining droplets of gold. Some other metal ions could be characterized by the colour of their aqua-complexes or by addition of a complexing agent, such as 1,10-phenanthroline for Fe^{2+} and KSCN for Fe^{3+}, to form a coloured complex. When relatively large amount of sample (more than 10mg) was tested, the gold residue could be scraped off the porcelain and

weighed to obtain a semi-quantitative result. Qualitative analysis for Cl^- was performed by dissolving a small amount of sample (about 1mg) in some suitable solvent mixtures (any solvent mixture which contains water or MeCN) and adding $AgNO_3$ (a few milligrams) after acidifying the solution with concentrated HNO_3. If a white precipitate was formed, the sample probably contained Cl^-. If no white precipitate was formed, the sample probably contained no Cl^-.

Chapter 3

Syntheses and Characterization of the Organic Ligands

3.1 Introduction

In this chapter, syntheses and characterization of the organic ligands related to this work will be discussed. Method (i) mentioned in the first chapter was used to synthesize the five phosphine ligands, TIP, TDMIP, TMIP, TEMIP and TDMIP-5. This is a very convenient method for synthesizing symmetric tertiary phosphines. Syntheses of the first three ligands have been reported before (68, 70); only modifications to the methods will be described. Synthesis of the new phosphine, TEMIP will be described in detail. Attempt to synthesize a new phosphine ligand, tris(1,2-dimethylimidazol-5-yl)phosphine (TDMIP-5) gave extremely low and unrepeatable yield of the product. Neither NMR nor infrared data of this ligand were recorded. The ligand bis(imidazol-2-yl)phosphinic acid (BIP), is the product of oxidation and hydrolysis of TIP (84). A method to synthesize this ligand directly from imidazole and $POCl_3$ is described. Synthesis of a new imidazole derivative is also described.

A full set of NMR data were obtained for the four phosphine ligands and will be discussed in a separate section. Some compounds have also been characterized by infrared and mass spectroscopy. Tentative assignments of the NMR spectra were made. Structures of TIP and BIP have been determined before,

together with the assignments of the NMR, infrared and mass spectra (84, 85, 86). Structures of TEMIP and TDMIP-5 are reported here.

3.2 Syntheses of the Organic Ligands

3.2.1 Tris(imidazol-2-yl)phosphine (TIP) and Tris(4,5-dimethylimidazol-2-yl)phosphine (TDMIP)

The method of Curtis and Brown (68) was used to synthesize these ligands. Reactions were carried out in ether solutions. The time for stirring the reaction mixture with concentrated NH_4OH was kept as short as possible, just enough to dissolve all of the solid materials (about 5 minutes). This revision was made by Copping (86).

In the case of TIP, the ligand was deprotected by dissolving the residue from the ether layer in a 1:10 water/acetone mixture (about 100mL for 4g product). The mixture was allowed to stand in a sealed container for 2 hours. The product crystallized during that period, and was separated by filtration. It was recrystallized from a 1:1 methanol/water. Yield 50-65%; m.p. 230-231°C, [229-231°C (68)].

In the case of TDMIP, the residue from the ether layer was dissolved in a 1:1 water/acetone mixture (about 50mL for 4g product), which was stirred under nitrogen for 1 hour, then evaporated to dryness *in vacuo*. The remaining solid was extracted with 30mL of each of the following solvents one after another, water, acetone, and CH_2Cl_2. Pure product was obtained by recrystallization from a 1:1:1

water/methanol/acetone mixture. Yield 47-59%; m.p. 227-228°C, [255-257°C (68)]; mass spectrum 317(MH^+, 72), 221(MH^+ - Me_2imH, 55), 127(Me_2imP^+, 13), 97($Me_2imH_2^+$, 100) (Me_2imH = 4,5-dimethylimidazole).

3.2.2 Tris(1-methylimidazol-2-yl)phosphine (TMIP)

The synthesis of this ligand has been described by Kurtz *et al* (69). It is essentially the same as that for TIP and TDMIP. With a methyl group on the N1 nitrogen atom, protection and deprotection steps are not needed. Reaction was carried out in THF solution (200mL THF for 8.2g starting imidazole). After the reaction, the THF solution was stirred with concentrated NH_4OH as before. The aqueous layer was back extracted with 2x100mL dichloromethane. The organic layers were combined, dried over anhydrous Na_2SO_4 and evaporated to dryness *in vacuo*. The product was recrystallized from 1:5 CH_2Cl_2/acetone. Yield 5.48g (60%); m.p. 194-195°C, [203-205°C (87)]; mass spectrum 301(19), 275(MH^+, 100), 217(20), 194(MH^+ - Meim + H, 23), 91(39), 83($MeimH^+$, 68) (Meim = 1-methylimidazole).

It was found that THF is a convenient solvent for the reaction. When ether was used as a solvent (69), almost no product was obtained. This was probably caused by some solubility problems. Moore and Whitesides reported unsuccessful attempts to synthesize this ligand by use of the above method in ether. They developed a more complicated synthetic method to make this ligand (87).

3.2.3 Tris(2-ethyl-4(5)-methylimidazol-5(4)-yl)phosphine (TEMIP)

Syntheses of tris-imidazole phosphines having the phosphorus atom attached to the imidazole C4 or C5 atom are more difficult. Reactions of 1,2-dimethylimidazole and N-protected 2-methylimidazole with n- or t-butyllithium at temperatures up to room temperature and prolonged times (up to four hours) followed by stirring with PCl_3 at room temperature for two days gave no separable products. Much of the starting imidazoles were recovered after reaction work up. The ligand TEMIP was synthesized by analogy to the method of Boggess and Zatko for the preparation of tris(2-pyridyl)phosphine (70).

2-Ethyl-4(5)methyl-5(4)bromoimidazole was synthesized as follows. To a stirred solution of 2-ethyl-4(5)-methylimidazole (Aldrich)(12g) in $CHCl_3$ (150mL) cooled in an ice bath, one equivalent of Br_2 in $CHCl_3$ (30mL) was added dropwise. The addition was stopped once the bromine colour persisted for a few minutes. After the addition, the solvent was removed *in vacuo*. The residue was washed with ether (150mL) and then dissolved in water (50mL). The bromide was precipitated out when concentrated NH_4OH (20mL) was added. The precipitate was separated by filtration, washed with water (50mL), and recrystallized twice from 1:2 acetone/water. Yield 13g (63%); m.p. 151-152°C; mass spectrum 188,190(M^+, 69,69), 173,175(M^+ - CH_3, 88,88), 43($CH_3CH_2CH^+$, 100); $\delta_H(CDCl_3)$ 1.26(t, 3H, $^3J_{H\text{-}H}$ 7.00, ring C2-$CH_2C\underline{H}_3$), 2.19[s, 3H, ring C4(5)-$C\underline{H}_3$], 2.72(q, 2H, $^3J_{H\text{-}H}$ 7.00, ring C2-$C\underline{H}_2$); $\delta_C(CDCl_3)$ 9.71[s, ring C4(5)-$\underline{C}H_3$], 12.72(s, ring C2-$CH_2\underline{C}H_3$), 21.86(s, ring C2-$\underline{C}H_2$), 110.23[s, ring $\underline{C}$5(4)], 123.94[s, ring $\underline{C}$4(5)], 148.82(s, ring $\underline{C}$2).

Because of the tautomerization of imidazole compounds, the bromine atom can be regarded as attached to the C5 or C4 carbon atom. The same is also true for the methyl group.

The bromoimidazole was N-protected through the following procedures. 2-ethyl-4(5)-methyl-5(4)bromoimidazole (10g) was added to triethylorthoformate (50mL), and the reaction mixture was heated to boiling for 4 hours. Any volatile materials were distilled off. Additional triethylorthoformate (about 30mL) was added to the reaction mixture to keep the volume of the reaction mixture no less than 20mL. The resulting mixture was purified by vacuum distillation. The high temperature fraction (115-125°C, 2-3mmHg) was collected as a colourless liquid, which crystallized upon cooling down to room temperature. Yield 14g (91%), m.p. 52-54°C; mass spectrum 290,292(M^+, 12,11), 245,247(M^+ - OCH_2CH_3, 60,63), 189(70), 173,175(M^+ - [$CH(OCH_2CH_3)_3$ + CH_3], 98,100); $\delta_H(CDCl_3)$ 1.25(t, 6H, $^3J_{H\text{-}H}$ 7.05, -$OCH_2C\underline{H}_3$), 1.30(t, 3H, $^3J_{H\text{-}H}$ 7.56, ring C2-$CH_2C\underline{H}_3$), 2.26[s, 3H, ring C4(5)-$C\underline{H}_3$], 2.78(q, 2H, $^3J_{H\text{-}H}$ 7.56, ring C2-$C\underline{H}_2$), 3.55(m, 4H, $_3J_{H\text{-}H}$ 7.05, -$OC\underline{H}_2$), 5.89(s, 1H, ring N1-C$\underline{H}$); $\delta_C(CDCl_3)$ 10.17[s, ring C4(5)-$\underline{C}H_3$], 12.44(s, ring C2-$CH_2\underline{C}H_3$), 14.69(s, -$OCH_2\underline{C}H_3$), 21.28(s, ring C2-$\underline{C}H_2$), 62.82(s, -$O\underline{C}H_2$), 102.17(s, ring N1-$\underline{C}$H), 113.70[s, ring $\underline{C}$5(4)], 124.00[s, ring $\underline{C}$4(5)], 148.52(s, ring $\underline{C}$2).

Acid catalyst was not necessary for the above reaction. The use of p-toluenesulfonic acid catalyst (68) resulted in lower yield and contaminated product. The imidazole nitrogen atoms, to which the protecting group was

attached, was not determined. It is likely that both isomers coexist, with one predominant. Signals of most of the alkyl groups were split into two peaks with intensity ratios about 1:10 in both ^{1}H and ^{13}C spectra. Further complications of the signals from the methylene protons of the ethoxy group were observed in the ^{1}H spectrum. These proton signals appear as two sets of multiplets, each composed of a number of quartets with different intensities.

The ligand TEMIP was synthesized as follows. To a stirred solution of the N-protected bromoimidazole (5.5g) in anhydrous ether (150mL) cooled at -40°C, one equivalent (7.5mL) of n-butyllithium (2.5M in hexane) was added dropwise over a time of about 10 minutes. The solution was warmed to -20 to -10°C for 2 hours with continuous stirring. A solution of PCl_3 (0.55mL) in anhydrous ether (40mL) was added in a time of about 15 minutes. The reaction mixture was warmed to room temperature and stirred overnight. All of these steps were carried out under nitrogen. After this, concentrated NH_4OH (40mL) was added quickly and the mixture stirred for about 5-10 minutes, until almost all of the solid materials were dissolved. The layers were separated and the aqueous layer was extracted with 2x100mL of ether. All the ether layers were combined and evaporated to dryness *in vacuo*. Deprotection was achieved by dissolving the residue in a 1:1 acetone/water mixture (30mL) and evaporating the solution to dryness *in vacuo*. The resulting solid was washed with the following solvents one after another, hexane (20mL), ether (20mL), acetone (10mL), and water (10mL),

then recrystallized from a 1:2 methanol/water mixture. Yield 1.0-1.2g (44-53%); m.p. 207-208°C; mass spectrum 496(M + EtMeimP$^+$ -3H, 8), 387(M + P$^+$ - 2H, 12), 359(MH$^+$, 100), 249(MH$^+$ - EtMeimH, 82), 111(EtMeimH$_2^+$, 43) (EtMeimH = 2-ethyl-4(5)methylimidazole).

3.2.4 Tris(1,2-dimethylimidazol-5-yl)phosphine (TDMIP-5)

1,2-Dimethyl-5-bromoimidazole was synthesized by analogy to the method of El Borai *et al.* for making 1-methyl-5-bromoimidazole (88). To a continuously stirred solution of 1,2-dimethylimidazole (4.8g) in $CHCl_3$ (150mL), N-bromosuccinimide (8.9g) was added in small amounts over a period of about 30 minutes. The reaction mixture was refluxed for two hours, then washed with saturated aqueous Na_2CO_3 solution (50mL). The $CHCl_3$ layer was collected, dried over anhydrous Na_2SO_4, and evaporated to dryness *in vacuo*. The remaining solid materials were extracted with hexane (10 x 70mL). The hexane was removed *in vacuo* and the product recrystallized from CH_2Cl_2/hexane. Slow addition of just one equivalent N-bromosuccinimide gave mainly mono brominated product. Yield 6.74g (77%); m.p. 92.5-93.5°C; $\delta_H(CDCl_3)$ 2.39(s, 3H, ring C2-C$\underline{H}_3$), 3.50(s, 3H, ring N1-C$\underline{H}_3$), 6.87(s, 1H, ring C4-$\underline{H}$); $\delta_C(CDCl_3)$ 14.25(s, ring C2-$\underline{C}H_3$), 31.50(s, ring N1-$\underline{C}H_3$), 102.53(s, ring $\underline{C}$5), 127.20(s, ring $\underline{C}$4), 145.70(s, ring $\underline{C}$2).

The method of making the ligand TEMIP was used for the preparation of TDMIP-5, except that THF was used as the reaction solvent for solubility reasons. The protection and deprotection steps are not needed. A yellowish hygroscopic

solid was obtained, which was found by mass spectroscopy to be contaminated. Three recrystallizations from CH_2Cl_2/hexane gave a very small amount of product. Yield 0.13%; m.p. 145-147°C.

3.2.5 Bis(imidazol-2-yl)phosphinic Acid (BIP)

Direct synthesis of BIP from imidazole and $POCl_3$ has been described by Seidel (89). The method was similar to that of preparing TIP with the addition of an ether solution of 2 equivalents of lithiated N-protected imidazole to an ether solution of $POCl_3$. It was found that this method gave a very small amount of product (<2% yield). The ligand was successfully synthesized by addition of $POCl_3$ to an ether solution of 3 equivalents of the lithiated N-protected imidazole. Similar to the preparation of TIP, the stirring time after the addition of concentrated NH_4OH to the ether solution was carefully controlled. Deprotection in 1:10 water/acetone gave a white precipitate which was separated by filtration, washed with methanol, and recrystallized from water. Yield 55%; m.p. 258-259°C [230°C (84)]. The reaction probably proceeded through the tri-substituted intermediate, R_3PO, followed by hydrolysis with loss of an R group during the deprotection reaction.

3.2.6. 1,5-Dimethyl-4-hydroxymethylimidazole

To a continuously stirred suspension of ethyl 4-methyl-5-imidazole carboxylate (5g) in THF, metallic sodium (2g, about 0.5g per piece) was added. The suspension was refluxed for 10 hours and stirred overnight. About one

equivalent sodium was consumed during this period. The remaining sodium was then picked out and methyl iodide (6g) was added. Almost all of the insoluble materials dissolved after stirring for a few minutes. Volatile materials were removed *in vacuo* and the resulting solid was dissolved in water (30mL). The aqueous solution was extracted with CH_2Cl_2 (2x100mL). The CH_2Cl_2 solution was dried over anhydrous Na_2SO_4 and evaporated to dryness in vacuo. The resulting solid was recrystallized from a 1:10 CH_2Cl_2/hexane mixture; m.p. 86-87°C; $\delta_H(CDCl_3)$ 1.39(t, 3H, $^3J_{H\text{-}H}$ 4.74, -$OCH_2C\underline{H}_3$), 2.51(s, 3H, ring C5-$C\underline{H}_3$), 3.59(s, 3H, ring N1-$C\underline{H}_3$), 4.35(q, 2H, $^3J_{H\text{-}H}$ 4.75, -$OC\underline{H}_2$), 7.39(s, 1H, ring C2-$\underline{H}$); $\delta_C(CDCl_3)$ 9.53(s, ring C5-$\underline{C}H_3$), 14.47(s, -$OCH_2\underline{C}H_3$), 31.45(s, ring N1-$\underline{C}H_3$), 60.02(s, -$O\underline{C}H_2$), 129.30(s, ring $\underline{C}$5), 135.87(s, ring $\underline{C}$4), 136.98(s, ring $\underline{C}$2), 163.83[s, -$\underline{C}$(O)OEt].

This solid (about 5g) was added to a suspension of $LiAlH_4$ (5g) in THF (200mL). The mixture was refluxed for 3 hours and stirred overnight. Water (15mL) was added dropwise very carefully. The resulting mixture was saturated with CO_2 and filtered. The insoluble materials were suspended in methanol (100mL, saturated with CO_2) and filtered afterwards. The filtrates were combined and evaporated to dryness *in vacuo*. The resulting solid product was washed with ether and recrystallized from a 1:5 methanol/toluene mixture. Total yield 2.1g (51%); m.p. 159-160°C; $\delta_H(CDCl_3)$ 2.21(s, 3H, ring C5-$C\underline{H}_3$), 3.51(s, 3H, ring N1-$C\underline{H}_3$), 4.53(s, 2H, ring C4-$C\underline{H}_2$), 7.35(s, 1H, ring C2-$\underline{H}$); $\delta_C(CDCl_3)$ 8.17(s, ring C5-$\underline{C}H_3$), 31.30(s, ring N1-$\underline{C}H_3$), 56.84(s, ring C4-$\underline{C}H_2$), 124.56(s, ring $\underline{C}$5), 136.11(s, ring

C2), 137.96(s, ring C4).

The reduction procedure was similar to the method of Jones and McLaughlin for the preparation of 5-hydroxymethylimidazoles (90). It is interesting that the methylation occurred almost exclusively on the original N3 nitrogen atom of the imidazole. This was verified by determination of the structure of a gold(I) complex with this ligand (**Chapter 7**) and the fact that no extra signals with significant intensity were observed in the NMR spectra for all of the methylated products.

3.3 The NMR Spectra of the Phosphines

NMR data of the phosphines are listed in **Table 3.3** together with tentative assignments. Signs of the phosphorus-carbon coupling constants were not determined. DMSO-d_6 was used as the solvent for TIP, TDMIP, and TMIP, methanol-d_4 for TEMIP.

Unambiguous assignments to the ^1H and ^{13}C spectra of TMIP have been made by use of NOE and selective decoupling experiments. Irradiating the resonance frequency of the ring N1-methyl protons at 3.48ppm gave intensity enhancement of the ring C5-proton signal through the NOE effect. This signal appeared to be the low field aromatic proton signal at 7.38ppm. The other aromatic proton signal at 7.03ppm was assigned to the ring C4-proton. Selectively irradiating the resonance frequencies of the aromatic protons will enhance the ^{13}C signal intensities of the carbon atoms which are coupled to these protons. Also,

Table 3.3 NMR data of the phosphines

TIP	TDMIP	TMIP	TEMIP
^{1}H			
7.22,s,2H,ring C4,C5-H	1.86,s,6H,ring C4,C5-CH_3	3.48,s,3H,ring N1-CH_3	1.26,t,3H,-CH_2CH_3, $^{3}J_{H\text{-}H}$=7.64
		7.03,s,1H,ring C4-H	2.19,s,3H,ring C4-CH_3
		7.38,s,1H,ring C5-H	2.68,q,2H,-CH_2, $^{3}J_{H\text{-}H}$=7.64
^{13}C			
	10.16,s,ring C4,5-CH_3	33.62,d,ring N1-CH_3, $^{3}J_{P\text{-}C}$=±5.06	12.07,d,ring C4(5)-CH_3, $^{3}J_{P\text{-}C}$=±7.99
			13.20,s,ring C2-CH_2CH_3
			22.51,s,ring C2-CH_2
124.96,s,ring C4,5	129.67,s,ring C4,5-CH_3	125.62,s,ring C5	122.65,s,ring C4(5)
141.01,d,ring C2-P, $^{1}J_{P\text{-}C}$=±8.83	137.69,d,ring C2-P, $^{1}J_{P\text{-}C}$=±12.3	129.56,d,ring C4, $^{3}J_{P\text{-}C}$=±9.58	141.48,d,ring C5(4)-P, $^{1}J_{P\text{-}C}$=±37.54
		139.88,d,ring C2-P, $^{1}J_{P\text{-}C}$=±12.38	153.20,s,ring C2
^{31}P			
-72.91,s	-73.18,s	-59.02,s	-99.93,s

the proton-carbon coupling of the proton under irradiation will collapse while other proton-carbon couplings will be observed. Irradiating the resonance frequency of the ring C4-proton at 7.03ppm gave enhancement of the original ^{13}C doublet at 129.56ppm, which remained as a doublet. Such a splitting was caused by the three bond coupling with the phosphorus atom. The original singlet at 125.62ppm split into a doublet and the doublet at 32.62ppm split into a quartet of doublets. The doublet at 139.88ppm was unaffected. Irradiating the resonance frequency of the ring C5-proton at 7.38ppm gave enhancement of the original ^{13}C singlet at 125.62ppm, still as a singlet. The original doublet at 129.56ppm split further into a doublet of doublets. Again, the original doublet at 32.62ppm split into a quartet of doublets, and the doublet at 139.88ppm was unaffected. Based on these observations, assignment of the ^{13}C spectrum was straight forward.

Assignments to the ^{13}C spectra of other phosphines were made by analogy to TMIP. The most down field signals were assigned to the ring C2 carbon atoms. One bond phosphorus-carbon couplings were all observed. Further evidence for the assignments came from line broadening of the ^{13}C signals. For the N-unsubstituted imidazoles, proton transfer between the ring nitrogen atoms followed by redistribution of the ring π electrons will cause the ring C4 and ring C5 carbon atoms to be exchangeable, hence broadening the ^{13}C signals of these carbon atoms. Such a proton transfer will have no effect to the ring C2 carbon atoms of TIP and TDMIP, and have little effect to the ring C2 carbon atom of

TEMIP. For these phosphines, the observed half peak widths were 50-150Hz for the upfield aromatic carbon atom signals, much broader than the downfield carbon atom signals with half peak widths of 7-9Hz. The line broadening effect was also observed from the ^{31}P spectra. Half peak width was 7.3Hz for TMIP, 21.9Hz for TIP, 58Hz for TDMIP and 110Hz for TEMIP.

An upfield shift of the ^{31}P signal usually means more shielding about the phosphorus nucleus (91). The shielding effect about the phosphorus nucleus is related to a number of factors. When all other conditions are very similar, a more shielded phosphorus atom will be more electron rich and hence a better σ-base. According to the δ_P values of the tris-imidazole phosphines studied in this work, the phosphorus atom of TEMIP is much more shielded than the others. As will be discussed in the following chapters, the phosphorus σ-basicity of TEMIP is better than the other imidazole phosphines.

The ^{31}P chemical shifts of triply coordinated phosphorus with three P-C bonds cover a range of more than 100ppm, such as PMe_3, -62ppm (92), PEt_3, -20.1ppm (92), PPh_3, -5.6 - -8ppm (93), P(2-pyridyl)$_3$, -0.33ppm (94), and P^tBu_3, 61.9ppm (95). As will be shown below, the upfield shift of the ^{31}P signals of the tertiary imidazole phosphines relative to those tertiary phenyl and pyridyl phosphines is correlated with the P-C bond distances.

3.4 The Vibrational Spectra of the Phosphines

Major infrared frequencies of the four phosphines have been listed in **Table**

3.4, together with tentative assignments. Assignments were made in accord with references 84, 86, 96, 97.

3.5 The Structures of TEMIP and TDMIP-5

Structures of the two new phosphine ligands, TEMIP and TDMIP-5 have been characterized by single crystal X-ray diffraction method. The crystal densities were measured by suspension in CCl_4/hexane. The crystal of TEMIP was mounted by gluing to the end of a glass fibre and the crystal of TDMIP-5 was mounted by gluing in a sealed glass capillary for X-ray diffraction experiment. Unit cell determination and intensity data collection were performed on a Rigaku AFC6R diffractometer with use of Cu Kα radiation. Unit cell parameters were refined by least-squares fit of angular parameters for 24 reflections ($50.4° \leq 2\theta \leq 66.4°$) for TEMIP, and 20 reflections ($20.2° < 2\theta \leq 29.4°$) for TDMIP-5. Intensities were measured with a θ(crystal) - 2θ(counter) scan. Three standards were measured every 100 reflections. Absorption corrections were made with DIFABS (81). The structures were solved by direct methods and refined by the method of least-squares, which minimized $\Sigma w(|F_o| - |F_c|)^2$. Hydrogen atoms were placed in calculated positions and not refined, except for the water molecules and the disordered ethyl group of TEMIP, to which no H atoms were added. The occupancies of the two disordered sites of the methyl carbon from the ethyl group on imidazole ring(1) were found to be 0.5 and 0.5. This was determined by fixing the temperature factors of the two atoms at the disordered sites with a value

Table 3.4 Major infrared frequencies of TIP, TDMIP, TEMIP, and TMIP

TIP	TDMIP	TEMIP	TMIP	Assignment
3500-2300vs,br	3500-2300vs,br	3500-2300vs,br		νO-H,νN-H,νC-H
			3400m,br 3110s 2925s	νC-H
1724m			1720w 1650w,br	- -
1607w,br	1650sh	1630w,br		δO-H
1530m,br	1605vs	1568vs 1523m	1505s	νring
1406s	1395s 1370s	1445vs 1428vs	1450vs 1410s	νP-C
1335m	1280m	1378w 1314vs 1280m	1350s 1285vs	γC-H
1242s	1210s	1280w	1165w 1150m	δC-H
1157w,sh	1170w	1197m		δN-H
1107s,br	1010s	1097w 1069m 1042m	1120s 1075m	δC-H
965m	930m,br	990w		δring
918w,br		901m,br 850m,br 790m	905s 865m 785vs 770vs	γC-H
757s,br	750m	749m	745vs 700vs	δP-C
707s,br		670vs	690s 680vs	γC-H
628w				-
548w	535w	528m	520vs	-
492vs	470vs	493m 473m	495vs 475s	- -

Table 3.4 (continued)

TIP	TDMIP	TEMIP	TMIP	Assignments
352w	390w		415w	-
			405w	-

Bands in cm^{-1}, s=strong, m=medium, w=weak, br=broad, sh=shoulder, v=very, ν=stretching, δ=deformation, γ=bending.

equal to that of the adjacent methylene carbon atom during refinement. Such site of occupancies were fixed and the temperature factors refined isotropically afterwards. Temperature factors of other non-H atoms were refined anisotropically. Details of crystal data and structure solution are listed in **Table 3.5.1**. Atomic positional parameters are given in **Table 3.5.2** and selected interatomic distances and angles are given in **Table 3.5.3** for both ligands. The molecule and packing diagrams are given in **Figure 3.5.1, Figure 3.5.2** and **Figure 3.5.3, Figure 3.5.4** for TEMIP and TDMIP-5 respectively.

Large residuals of the R values are probably caused by weak reflections and crystal instability. The later case is particularly true for the crystal of TEMIP. Large intensity variations of the standards were observed during data collection, although corrections were made for such variations.

The P-C bond distances are not significantly different in the case of TDMIP-5, but in the case of TEMIP, the P-C bond to ring(3) is significantly shorter than the bonds to ring(1) and ring(2). The mean P-C bond length (Å) of TEMIP 1.815(10) is longer, but not significantly, than that of TDMIP-5 1.801(7). These values are compared to the mean values (Å) of PPh_3 1.828(9) (98), P(o-tolyl)$_3$ 1.835(5) (99), P(m-tolyl)$_3$ 1.835(13) (100), P(2-pyridyl)$_3$ 1.837(4) (94), and TIP 1.811(7) (85). The trend of PPh_3 ~ P(tolyl)$_3$ ~ P(2-pyridyl)$_3$ > TEMIP ~ TIP > TDMIP-5 is observed. This is probably caused by the larger steric demand of the six membered ring compared to the five membered rings. The mean value of the

Table 3.5.1 Crystal data of TEMIP·H_2O and TDMIP-5·0.5H_2O

	TEMIP·H_2O	TDMIP-5·H_2O
Formula	$C_{18}H_{29}N_6OP$	$C_{15}H_{22}N_6O_{0.5}P$
Formula weight	376.5	325.3
Crystal colour, shape, size (mm)	colourless plate, 0.15x0.17x0.20	colourless plate, 0.16x0.20x0.25
Space group, λ (Å)	$P2_1/n$, 1.54180	C2/c, 1.54180
Unit cell parameters (Å and °)	a = 10.085(2) b = 21.728(4) c = 10.293(3) β = 94.60(3)	a = 22.930(5) b = 6.117(1) c = 25.855(5) β = 109.93(3)
Volume ($Å^3$)	2248.1(11)	3409.3(17)
Z	4	8
ρ_{cal}, ρ_{obs} (Mg m^{-3})	1.112, 1.13(2)	1.268, 1.27(2)
Max. 2θ, indices range	116°, $-10 \le h \le 11$, $-23 \le k \le 19$, $-10 \le l \le 0$	119°, $0 \le h \le 25$, $0 \le k \le 6$, $-28 \le l \le 26$
Temperature, °C	23	23
Absorption coefficient mm^{-1}	1.220	1.509
Absorption correction factors, range	0.799 - 1.168	0.851 - 1.329
Number of variables	235	201
Standard reflections (e.s.d.)	-1 4 -1 (0.140), -1 1 -2 (0.140), 1 2 -2 (0.154)	-1 1 5 (0.010), 3 1 1 (0.014), 5 1 2 (0.014)
Number of reflections measured	3411	2974
Number of independent reflections, used	2993	2541
R_{int}	0.0541	0.0184
Final R, R_w	0.1143, 0.0940	0.0846, 0.0557
Final Δ/σ, max., ave	0.054, 0.010	0.004, 0.001
Final difference map, max., min., e A^{-3}	0.60, -0.45	0.39, -0.31
Weighting	$(\sigma_F^2)^{-1}$	$(\sigma_F^2)^{-1}$
Goodness of fit, S	2.57	2.08
F(000)	780	1376

Table 3.5.2 Atomic coordinates ($x10^4$) and equivalent isotropic displacement coefficients ($Å^2x10^3$) of TEMIP·H_2O and TDMIP-5·0.5H_2O

TEMIP·H_2O:

	x		y		z		U(eq)	
P	484	(2)	3793	(1)	2709	(1)	45	(1)
N(11)	-2104	(4)	3778	(2)	3587	(5)	53	(2)
N(12)	1101	(4)	4010	(2)	5509	(4)	47	(2)
N(33)	2946	(5)	2379	(2)	2245	(5)	55	(2)
N(13)	1647	(4)	2679	(2)	3774	(4)	46	(2)
C(51)	-1089	(5)	3443	(2)	3087	(5)	42	(2)
C(52)	1034	(5)	4214	(2)	4196	(5)	42	(2)
N(32)	1934	(5)	4952	(2)	5562	(5)	56	(2)
C(42)	1559	(5)	4797	(2)	4250	(6)	48	(2)
C(23)	2505	(6)	2237	(3)	3380	(6)	49	(2)
N(31)	-2959	(5)	2883	(2)	3013	(5)	62	(2)
C(43)	2352	(6)	2931	(3)	1854	(5)	51	(2)
C(53)	1537	(6)	3129	(2)	2785	(5)	45	(2)
C(41')	-1106	(6)	2330	(2)	2096	(6)	60	(2)
C(21)	-3206	(7)	3431	(3)	3537	(7)	71	(3)
C(41)	-1654	(5)	2885	(2)	2740	(5)	45	(2)
C(22)	1644	(6)	4468	(3)	6271	(6)	55	(2)
C(42')	1803	(7)	5224	(3)	3127	(7)	75	(3)
C(43')	2614	(8)	3238	(3)	555	(6)	90	(3)
C(22')	1901	(9)	4419	(4)	7737	(7)	90	(3)
C(23')	2860	(8)	1686	(3)	4174	(7)	75	(3)
C(22")	2997	(15)	4652	(5)	8318	(11)	298	(12)
C(21')	-4521	(8)	3600	(4)	4012	(12)	147	(6)
O	403	(4)	2836	(2)	6303	(4)	56	(2)
C(23")	1777	(11)	1328	(4)	4604	(11)	156	(6)
C(21A)*	-5077	(18)	4121	(8)	3697	(18)	102	(5)
C(21B)*	-4689	(23)	3916	(10)	4959	(23)	139	(8)

Table 3.5.2 (continued)

TDMIP-5·0.5H_2O:

	x		y		z		U(eq)	
P	3481	(1)	1649	(2)	4045	(1)	46	(1)
N(13)	2363	(1)	2881	(5)	3227	(1)	43	(1)
N(11)	3541	(1)	2348	(5)	5132	(1)	45	(1)
N(12)	4551	(1)	1430	(5)	3750	(1)	48	(1)
N(32)	4499	(2)	4213	(6)	3196	(1)	54	(1)
C(23)	1942	(2)	4554	(7)	3104	(2)	49	(2)
C(53)	2832	(2)	3422	(7)	3709	(1)	44	(1)
C(22)	4811	(2)	2474	(7)	3422	(2)	50	(2)
C(21)	3784	(2)	3800	(8)	5551	(2)	54	(2)
C(52)	4030	(2)	2619	(7)	3739	(1)	43	(1)
C(42)	4015	(2)	4305	(7)	3395	(1)	52	(2)
N(31)	4144	(2)	5260	(7)	5431	(1)	65	(2)
C(51)	3753	(2)	2954	(7)	4708	(1)	48	(2)
N(33)	2112	(2)	6106	(6)	3479	(1)	60	(2)
C(43)	2666	(2)	5407	(7)	3850	(2)	55	(2)
C(13')	2314	(2)	919	(7)	2907	(2)	64	(2)
C(11')	3153	(2)	473	(7)	5129	(2)	65	(2)
C(41)	4124	(2)	4719	(8)	4910	(2)	61	(2)
C(23')	1369	(2)	4560	(8)	2610	(2)	66	(2)
C(22')	5372	(2)	1622	(8)	3323	(2)	72	(2)
C(21')	3652	(2)	3699	(8)	6079	(2)	74	(2)
C(12')	4804	(2)	-486	(8)	4083	(2)	80	(2)
O	0		1821	(8)	2500		76	(2)

Equivalent isotropic U defined as one third of the trace of the orthogonalized U_{ij} tensor.

* A disordered carbon atom was refined at these positions with occupancies of 0.5 respectively.

Table 3.5.3 Selected bond lengths (Å) and angles (°) of TEMIP·H_2O and TDMIP·0.5H_2O

TEMIP·H_2O:

P-C(51)	1.828	(6)	P-C(52)	1.830	(5)
P-C(53)	1.788	(6)	N(11)-C(51)	1.387	(7)
N(11)-C(21)	1.340	(8)	N(12)-C(52)	1.418	(7)
N(12)-C(22)	1.355	(7)	N(33)-C(23)	1.319	(8)
N(33)-C(43)	1.385	(8)	N(13)-C(23)	1.375	(7)
N(13)-C(53)	1.411	(7)	C(51)-C(41)	1.374	(7)
C(52)-C(42)	1.374	(7)	N(32)-C(42)	1.413	(8)
N(32)-C(22)	1.326	(8)	C(42)-C(42')	1.517	(9)
C(23)-C(23')	1.477	(9)	N(31)-C(21)	1.338	(8)
N(31)-C(41)	1.368	(8)	C(43)-C(53)	1.381	(8)
C(43)-C(43')	1.537	(9)	C(41')-C(41)	1.503	(8)
C(21)-C(21')	1.50	(1)	C(22)-C(22')	1.515	(9)
C(22')-C(22")	1.32	(2)	C(23')-C(23")	1.44	(1)
C(21')-C(21A)	1.29	(2)	C(21')-C(21B)	1.22	(2)
C(21A)-C(21B)	1.40	(3)			

C(51)-P-C(52)	103.9	(2)	C(51)-P-C(53)	100.3	(2)
C(52)-P-C(53)	103.1	(2)	C(51)-N(11)-C(21)	109.0	(5)
C(52)-N(12)-C(22)	108.0	(4)	C(23)-N(33)-C(43)	106.9	(5)
C(23)-N(13)-C(53)	106.6	(5)	P-C(51)-N(11)	122.7	(4)
P-C(51)-C(41)	131.2	(4)	N(11)-C(51)-C(41)	104.8	(5)
P-C(52)-N(12)	129.0	(4)	P-C(52)-C(42)	125.8	(4)
N(12)-C(52)-C(42)	105.1	(5)	C(42)-N(32)-C(22)	106.4	(5)
C(52)-C(42)-N(32)	109.3	(5)	C(52)-C(42)-C(42')	128.2	(5)
N(32)-C(42)-C(42')	122.4	(5)	N(33)-C(23)-N(13)	111.3	(5)
N(33)-C(23)-C(23')	126.6	(5)	N(13)-C(23)-C(23')	122.1	(5)
C(21)-N(31)-C(41)	107.1	(5)	N(33)-C(43)-C(53)	109.6	(5)
N(33)-C(43)-C(43')	121.9	(5)	C(53)-C(43)-C(43')	128.4	(5)
P-C(53)-N(13)	127.1	(4)	P-C(53)-C(43)	127.3	(4)
N(13)-C(53)-C(43)	105.5	(5)	N(11)-C(21)-N(31)	109.5	(6)
N(11)-C(21)-C(21')	127.2	(6)	N(31)-C(21)-C(21')	123.3	(6)
C(51)-C(41)-N(31)	109.6	(5)	C(51)-C(41)-C(41')	131.6	(5)
N(31)-C(41)-C(41')	118.8	(5)	N(12)-C(22)-N(32)	111.2	(5)
N(12)-C(22)-C(22')	123.6	(6)	N(32)-C(22)-C(22')	125.2	(6)
C(22)-C(22')-C(22")	119.8	(8)	C(23)-C(23')-C(23")	116.9	(7)

Table 3.5.3 (continued)

C(21)-C(21')-C(21A)	121	(1)	C(21)-C(21')-C(21B)	126	(1)
C(21A)-C(21')-C(21B)	68	(1)	C(21')-C(21A)-C(21B)	54	(1)
C(21')-C(21B)-C(21A)	59	(1)			

TDMIP-5·0.5H_2O:

P-C(53)	1.806	(4)	P-C(52)	1.800	(4)
P-C(51)	1.798	(4)	N(13)-C(23)	1.369	(5)
N(13)-C(53)	1.381	(4)	N(13)-C(13')	1.439	(5)
N(11)-C(21)	1.363	(5)	N(11)-C(51)	1.393	(6)
N(11)-C(11')	1.450	(6)	N(12)-C(22)	1.352	(6)
N(12)-C(52)	1.390	(5)	N(12)-C(12')	1.453	(6)
N(32)-C(22)	1.303	(5)	N(32)-C(42)	1.373	(6)
C(23)-N(33)	1.317	(5)	C(23)-C(23')	1.487	(5)
C(53)-C(43)	1.359	(6)	C(22)-C(22')	1.488	(6)
C(21)-N(31)	1.322	(6)	C(21)-C(21')	1.499	(6)
C(52)-C(42)	1.355	(6)	N(31)-C(41)	1.372	(6)
C(51)-C(41)	1.364	(6)	N(33)-C(43)	1.374	(5)
C(53)-P-C(52)	100.2	(2)	C(53)-P-C(51)	98.8	(2)
C(52)-P-C(51)	101.8	(2)	C(23)-N(13)-C(53)	107.5	(3)
C(23)-N(13)-C(13')	125.4	(3)	C(53)-N(13)-C(13')	127.1	(3)
C(21)-N(11)-C(51)	107.1	(3)	C(21)-N(11)-C(11')	127.1	(4)
C(51)-N(11)-C(11')	125.8	(3)	C(22)-N(12)-C(52)	107.5	(3)
C(22)-N(12)-C(12')	125.5	(4)	C(52)-N(12)-C(12')	126.8	(4)
C(22)-N(32)-C(42)	104.9	(4)	N(13)-C(23)-N(33)	111.1	(3)
N(13)-C(23)-C(23')	123.2	(4)	N(33)-C(23)-C(23')	125.7	(4)
P-C(53)-N(13)	123.4	(3)	P-C(53)-C(43)	131.9	(3)
N(13)-C(53)-C(43)	104.7	(3)	N(12)-C(22)-N(32)	111.9	(4)
N(12)-C(22)-C(22')	122.3	(4)	N(32)-C(22)-C(22')	125.8	(4)
N(11)-C(21)-N(31)	111.9	(4)	N(11)-C(21)-C(21')	122.8	(4)
N(31)-C(21)-C(21')	125.2	(4)	P-C(52)-N(12)	122.9	(3)
P-C(52)-C(42)	132.4	(3)	N(12)-C(52)-C(42)	103.9	(4)
N(32)-C(42)-C(52)	111.8	(4)	C(21)-N(31)-C(41)	104.5	(4)
P-C(51)-N(11)	122.2	(3)	P-C(51)-C(41)	133.3	(3)
N(11)-C(51)-C(41)	104.3	(3)	C(23)-N(33)-C(43)	105.1	(4)
C(53)-C(43)-N(33)	111.6	(3)	N(31)-C(41)-C(51)	112.1	(4)

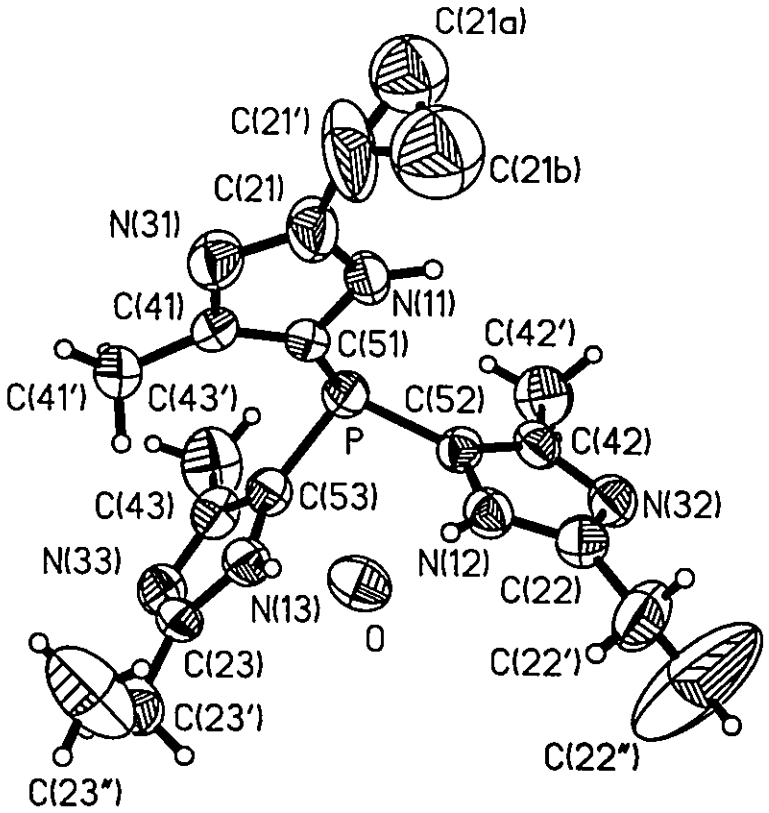

Figure 3.5.1 The molecule of TEMIP·H_2O

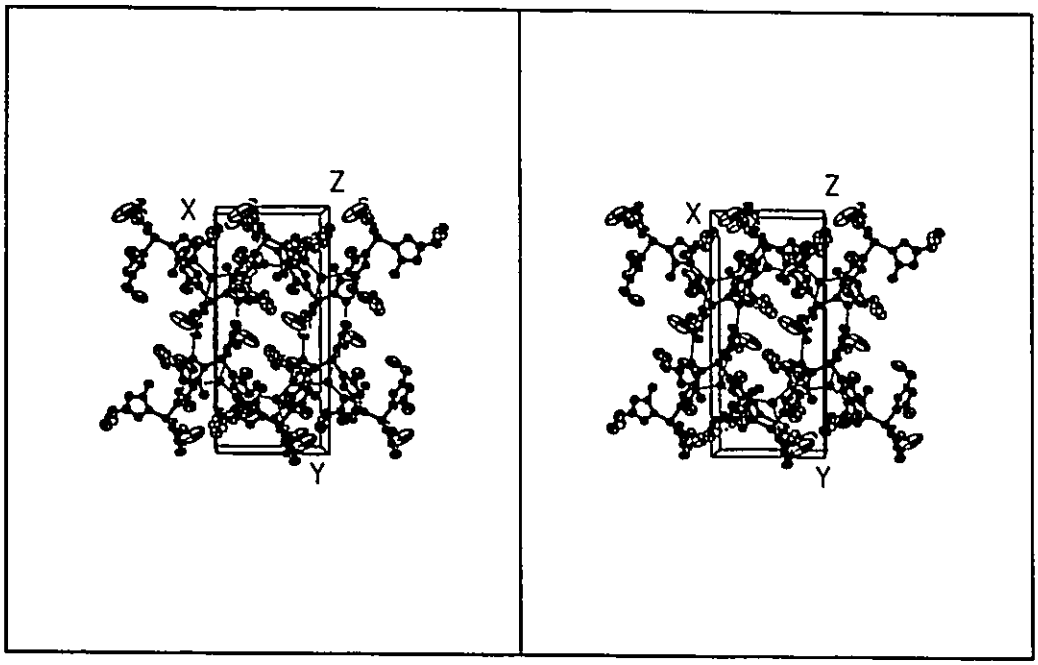

Figure 3.5.2 A stereoview of the packing of TEMIP·H_2O in a unit cell

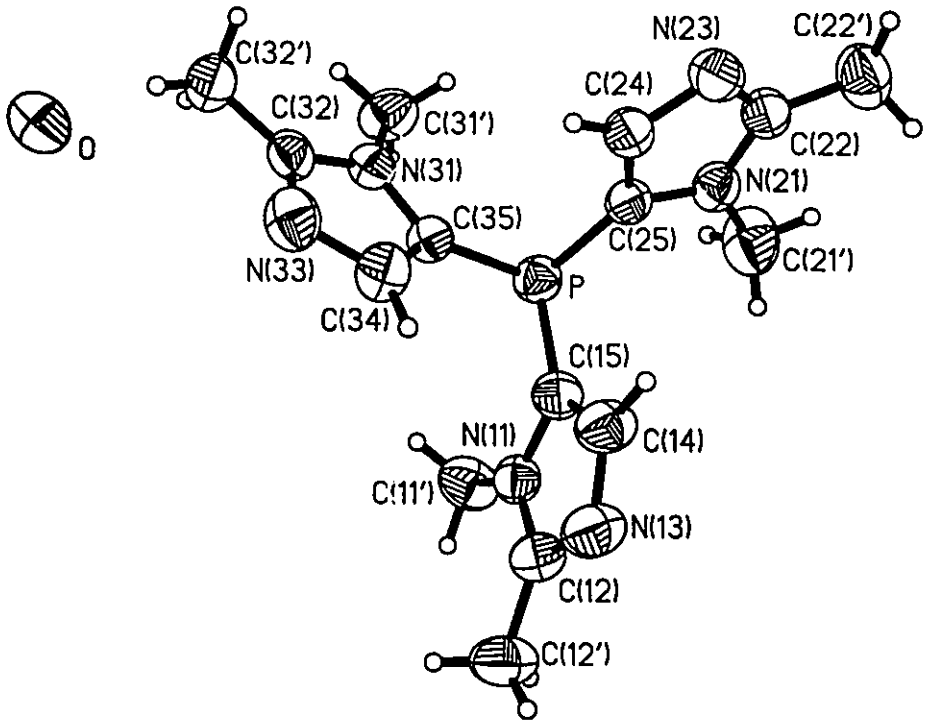

Figure 3.5.3 The molecule of TDMIP-5·0.5H_2O

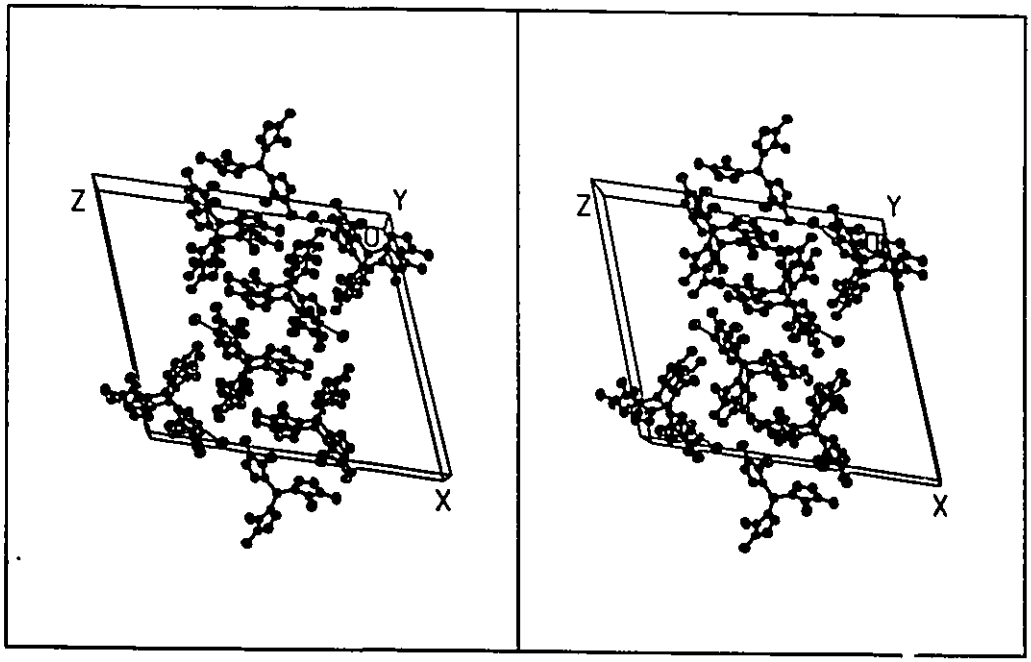

Figure 3.5.4 A stereoview of the packing of TDMIP-5·0.5H_2O in a unit cell

C-P-C' bond angles (°) of TEMIP 102.4(4) is not significantly different from other phosphines, PPh_3 103(4), P(o-tolyl)$_3$ 102.4(2), P(m-tolyl)$_3$ 101.7(5), P(2-pyridyl)$_3$ 101.5(2), and TIP 101.6(4), while the mean value of TDMIP-5 100.3(4) is significantly smaller. No information about the phosphine chemical properties can be derived from these P-C bond distances and C-P-C' bond angle values.

The imidazole rings in both ligands are essentially planar. The largest displacements (Å) are 0.008(4) for N11 and -0.007(4) for C21 out of the plane of TEMIP ring(1). The largest displacements (Å) of the phosphorus atom from those imidazole planes are 0.300(10) out of TEMIP ring(1) and -0.227(6) out of TDMIP-5 ring(1). Displacements of other substituent atoms are < 0.1Å.

In the case of TDMIP-5, the molecule is arranged like a propeller, with all methyl groups on the ring nitrogen pointing up towards the phosphorus lone pair. Such an arrangement enables the molecules to pack like chains on top of each other, along the crystallographic b axis. The ligand itself has a three fold symmetry, with the rotation axis parallel to the b axis, passing through the phosphorus atom. This symmetry is destroyed by the presence of water molecules, hydrogen bonded to the ligand molecules. Like the case of TIP, the water molecule in TDMIP-5 occupies a special position with a 0.5 site occupancy, but the hydrogen bonding patterns are different. The water molecule in TDMIP-5 acts only as a hydrogen donor, and is weakly bonded to two ring(3) nitrogen atoms from two ligand molecules, with O...N distances of 2.921(4)Å. The water

molecule in TEMIP occupies a general position with a full occupancy. It is hydrogen bonded to all three imidazole rings from different ligand molecules, with O...N distances from 2.775(6)Å to 3.002(6)Å. There is also a hydrogen bond between a ring(1) nitrogen atom of one ligand molecule and a ring(3) nitrogen atom of another ligand molecule, with a N...N distance of 2.899(7)Å.

The molecule of TEMIP does not adopt the propeller arrangement. Two imidazole rings are oriented with their methyl group on the ring C-4 carbon atom up towards the phosphorus lone pair while the methyl group of the other ring is down, probably to avoid steric interaction or to afford effective hydrogen bonding.

Chapter 4

Metal Complexes with Tris(imidazol-2-yl)phosphine (TIP)

4.1 Introduction

The ligand TIP readily forms two to one molar ratio complexes with $M(NO_3)_2$ (M = Co, Ni, Cu, Zn). These complexes are highly insoluble in common solvents. Structures of the Ni(II), Cu(II) and Zn(II) complexes have been determined. Unlike the ligands with sterically hindered groups, such as tris(4,5-diisopropylimidazol-2-yl)phosphine and tris(3,5-diisopropylpyrazolyl)borate, which form 1:1 complexes with the above metal ions (71, 101, 102), the metal ions in these complexes are octahedrally coordinated to six nitrogen atoms from the imidazole rings. By such coordination, the metal binding sites are saturated with the chelating ligand. Metal complexes with such ligands are not useful in modelling metal centres in biological systems. The 2:1 complexes still dominated the reaction, even when excess metal nitrate was added (up to 5-fold). This is probably caused by the thermodynamic stability and low solubility of the bis-ligand chelated complexes. Either 1:1 or 2:1 ligand/metal complexes with the ligand tris(2-pyridyl)phosphine are usually more soluble. When using such a ligand, bis-chelation can be avoided when the metal salt is in excess (70, 94).

Bis-ligand metal complexes with MCl_2 (M = Co, Ni, Zn) can also be prepared, of which no structural characterization has been done. The reaction of

the ligand with $CuCl_2$ is different. No 2:1 complex has been obtained. When the ligand was reacted with excess $CuCl_2$, a polymeric mixed valent Cu(I)/Cu(II) TIP complex was obtained. The structure of this complex has been determined. The starting Cu(II) must be reduced to Cu(I) before the formation of such a complex. Since phosphines are good reducing agents, some of the ligand probably acted as a reductant during the reaction. No other product has been separated from this reaction.

Reactions with gold were carried out in polar solvents (methanol and water) because of solubility reasons, but no separable product of gold(I) complex with TIP was obtained. Nucleophilic attack on the phosphorus atom by the solvent molecules might have occurred during the reaction. This is supported by the following observation: when a solution of MCl_2 (M = Cu, Ni) in methanol was added to a 1:1 molar ratio mixture of TIP and Me_2SAuCl in methanol, a colourless crystalline product was obtained. This product was characterized by ^1H, ^{13}C and ^{31}P NMR as a gold(I) complex with trimethylphosphite. This complex will be discussed in **Chapter 7**.

4.2 Preparations

Bis[tris(imidazol-2-yl)phosphine-N^3,$N^{3'}$,$N^{3''}$]M(II) dinitrate (M = Ni, Cu, Zn): TIP (0.2g) and a half stoichiometric amount of $M(NO_3)_2$ (M = Ni, Cu, Zn) were dissolved in separate 1:1 methanol/water mixtures (10mL). These solutions were cooled to -40°C and mixed at that temperature. The resulting solutions were

sealed in a glass container and kept at -15°C for a week. Crystalline products were formed during that period, which were separated by filtration, washed with acetone (10mL) and air dried. Yield: 0.06g (21.5%) for the Ni(II) complex [m.p. 301-302°C (decompose)], 0.10g (35.6%) for the Cu(II) complex [m.p. 245-246°C (decompose)], and 0.21g (74.5%) for the Zn(II) complex [m.p. 255-256°C (decompose)].

Polymeric Cu(I)/Cu(II) TIP complex: TIP (0.5g) and $CuCl_2$ (0.55g) were dissolved in separate 1:1 methanol/water mixtures (10mL). The solutions were cooled to -40°C and mixed at that temperature. The resulting solution was sealed in a glass container and kept at -15°C for a week. A yellowish green crystalline product formed during that period, and was separated by filtration, washed with methanol (5mL), acetone (5mL) and air dried. Yield 0.15g (47%), m.p. 227-228°C (decompose).

4.3 The Structures of the Bis-ligand Metal Complexes

The crystals used for X-ray diffraction experiment were mounted by gluing to the end of glass fibres. The crystal densities were measured by suspension in $CCl_4/CHBr_3$. Unit cell determination and intensity data collection were performed on a Nicolet P3 diffractometer for the Ni(II) and Cu(II) complexes and on a Siemens P4 diffractometer for the Zn(II) complex, with use of Mo Kα radiation. Unit cell parameters were refined by least-squares fit of angular parameters of 15 reflections ($19.32° \leq 2\theta \leq 27.12°$) for the nickel complex, 15 reflections ($20.61° \leq 2\theta$

$\leq 37.79°$) for the copper complex, and 25 reflections ($15.83° \leq 2\theta \leq 28.04°$) for the zinc complex. Intensities were collected with the θ(crystal)- 2θ(counter) scan method. Two standards were measured every 50 reflections for the Ni(II) and Cu(II) complexes and three standards were measured every 100 reflections for the Zn(II) complex. No instrument instability and crystal decay were observed during data collection. No absorption corrections were made for the Ni(II) and Cu(II) complexes; this will cause maximum errors in F_o of 3.8% and 4.6% respectively. A ψ-scan absorption correction (80) was made for the Zn(II) complex ($1.399 \leq A^* \leq 1.560$). Structures were solved by the Patterson method. Hydrogen atoms were placed in calculated positions and not refined. Anisotropic full-matrix least-squares refinement minimized $\Sigma w(|F_o| - |F_c|)^2$. Scale, positional parameters for all atoms and anisotropic temperature factors for non-H atoms were varied. Hydrogen atoms were refined with fixed temperature factors. Details of crystal data collection and structure solution are listed in **Table 4.3.1**. Atomic positional parameters are given in **Table 4.3.2** and selected interatomic distances and angles are given in **Table 4.3.3**. The cation and molecular packing diagrams of the Cu(II) complex are given in **Figure 4.3.1** and **Figure 4.3.2**. Diagrams of the other two complexes are essentially the same and will not be presented.

The three metal complexes are isostructural. They crystallize in the same space group, with the same molecular arrangement and the same hydrogen bonding pattern. There are two independent metal centres in one asymmetric

Table 4.3.1 Crystal data of $[(TIP)_2M](NO_3)_2$ (M = Ni, Cu, Zn)

	$[(TIP)_2Ni](NO_3)_2$	$[(TIP)_2Cu](NO_3)_2$	$[(TIP)_2Zn](NO_3)_2$
Formula	$C_{18}H_{18}N_{14}O_6P_2Ni$	$C_{18}H_{18}N_{14}O_6P_2Cu$	$C_{18}H_{18}N_{14}O_6P_2Zn$
Formula weight	647.1	651.9	653.8
Crystal colour, shape, size (mm)	purple prism, 0.25x0.27x0.27	blue prism, 0.20x0.25x0.25	colourless prism 0.20x0.30x0.30
Space group, λ (Å)	Pa-3, 0.71073	Pa-3, 0.71073	Pa-3, 0.71073
Unit cell parameters (Å)	a = 19.639(2)	a = 19.760(2)	a = 19.800(2)
Volume ($Å^3$)	7575(4)	7715(4)	7762(1)
Z	12	12	12
ρ_{cal}, ρ_{obs} ($Mg\ m^{-3}$)	1.702, 1.67(2)	1.684, 1.67(2)	1.678, 1.69(2)
Max. 2θ, indices range	45°, 0 ≤h ≤ 14, 0 ≤ k ≤ 12, -21 ≤ l ≤ -1	45°, 0 ≤ h ≤ 12, -1 ≤ k ≤ 15, -1 ≤ l ≤ 21	50°, 0 ≤ h ≤ 16, 0 ≤ k ≤ 13, -23 ≤ l ≤ -2
Temperature, °C	-65	23	23
Absorption coefficient mm^{-1}	0.963	1.040	1.139
Number of variables	186	186	188
Standard reflections	9 8 1, -1 9 8	1 -1 3, 3 -1 -1	6 0 0, 0 6 0, 0 0 6
Correction factors for standard, range	1.0042-1.0167	1.0101-1.0319	1.0000-1.0262
Number of reflections measured	954	1016	1420
Number of independent reflections, used	954	970	1302
R_{int}		0.0074	0.0000
Final R, R_w	0.0544, 0.0360	0.0683, 0.0254	0.0563, 0.0205
Final Δ/σ, max., ave	0.022, 0.004	0.035, 0.009	0.000, 0.000
Final difference map, max., min., e A^{-3}	0.44, -0.53	0.40, -0.54	0.32, -0.46
Weighting	$(\sigma_F^2)^{-1}$	$(\sigma_F^2)^{-1}$	$(\sigma F^2)^{-1}$
Goodness of fit, S	1.65	1.64	0.92
F(000)	3960	3972	3984

Table 4.3.2 Atomic coordinates ($x10^4$) and equivalent isotropic displacement coefficients ($Å^2x10^3$) of $[(TIP)_2M](NO_3)_2$ (M = Ni, Cu, Zn)

$[(TIP)_2Ni](NO_3)_2$:

	x		y		z		U(eq)	
Ni(1)	1641	(1)	1641	(1)	1641	(1)	15	(1)
P(1)	603	(1)	603	(1)	603	(1)	19	(1)
P(2)	2682	(1)	2682	(1)	2682	(1)	20	(1)
Ni(2)	5000		5000		5000		13	(1)
P(3)	6043	(1)	6043	(1)	6043	(1)	17	(1)
N(32)	2700	(3)	1796	(3)	1551	(2)	19	(2)
N(31)	1532	(2)	1700	(2)	581	(3)	18	(2)
C(21)	1128	(3)	1269	(3)	234	(3)	19	(2)
C(22)	3030	(3)	2263	(3)	1926	(3)	19	(2)
C(42)	3158	(3)	1601	(3)	1046	(3)	24	(2)
C(41)	1842	(3)	2114	(3)	100	(3)	25	(2)
N(11)	1168	(3)	1390	(3)	-445	(3)	25	(2)
N(12)	3664	(3)	2375	(3)	1680	(3)	23	(2)
C(52)	3749	(3)	1954	(3)	1124	(3)	27	(2)
C(51)	1616	(4)	1928	(3)	-542	(3)	30	(3)
N(33)	6067	(2)	5099	(2)	4960	(2)	15	(2)
C(23)	6411	(3)	5477	(3)	5415	(3)	16	(2)
C(43)	6549	(3)	4754	(3)	4584	(3)	22	(2)
N(13)	7099	(2)	5383	(3)	5334	(2)	18	(2)
C(53)	7194	(3)	4925	(3)	4815	(3)	19	(2)
N	3520	(3)	3295	(3)	-10	(3)	30	(2)
O(1)	3522	(2)	2935	(2)	-557	(2)	28	(2)
O(2)	2958	(2)	3469	(2)	248	(3)	41	(2)
O(3)	4074	(2)	3475	(2)	259	(2)	33	(2)

Table 4.3.2 (continued)

$[(TIP)_2Cu](NO_3)_2$:

	x		y		z		U(eq)	
Cu(1)	1638	(1)	1638	(1)	1638	(1)	36	(1)
Cu(2)	5000		5000		5000		33	(1)
P(2)	604	(1)	604	(1)	604	(1)	41	(1)
P(3)	3960	(1)	3960	(1)	3960	(1)	36	(1)
P(1)	2673	(1)	2673	(1)	2673	(1)	33	(1)
N(31)	1562	(3)	2710	(3)	1790	(3)	45	(2)
N(11)	1695	(3)	3662	(3)	2366	(3)	44	(2)
C(21)	1945	(3)	3033	(3)	2249	(3)	35	(2)
C(41)	1076	(4)	3171	(4)	1593	(4)	57	(3)
C(51)	1140	(4)	3752	(4)	1958	(4)	59	(3)
N(32)	563	(3)	1544	(3)	1676	(3)	50	(2)
N(33)	391	(2)	4882	(3)	5041	(3)	47	(2)
C(22)	230	(3)	1123	(3)	1249	(4)	42	(3)
C(23)	3596	(3)	4516	(3)	4585	(3)	36	(2)
C(42)	85	(5)	1826	(4)	2082	(4)	65	(3)
C(43)	3438	(4)	5223	(4)	5408	(3)	55	(3)
N(12)	-437	(3)	1150	(3)	1383	(3)	48	(2)
N(13)	2915	(3)	4611	(3)	4657	(3)	46	(2)
C(52)	-541	(4)	1591	(4)	1916	(4)	68	(3)
C(53)	2822	(4)	5062	(4)	5171	(4)	55	(3)
N	6702	(3)	4975	(4)	1490	(4)	59	(3)
O(1)	7077	(2)	4447	(3)	1488	(2)	63	(2)
O(2)	6531	(3)	5218	(3)	2046	(3)	81	(3)
O(3)	6530	(2)	5231	(3)	947	(3)	70	(2)

Table 4.3.2 (continued)

$[(TIP)_2Zn](NO_3)_2$:

	x		y		z		U(eq)	
Zn(1)	1639	(1)	1639	(1)	1639	(1)	27	(1)
P(1)	602	(1)	602	(1)	602	(1)	29	(1)
N(11)	-448	(2)	1145	(2)	1379	(2)	35	(1)
C(21)	227	(2)	1121	(2)	1254	(2)	27	(1)
N(31)	553	(2)	1543	(2)	1672	(2)	31	(1)
C(41)	69	(2)	1832	(2)	2081	(2)	38	(2)
C(51)	-558	(2)	1582	(2)	1900	(2)	42	(2)
P(2)	2679	(1)	2679	(1)	2679	(1)	30	(1)
N(12)	2382	(2)	1702	(2)	3662	(2)	33	(1)
C(22)	2257	(2)	1945	(2)	3029	(2)	25	(1)
N(32)	1794	(2)	1565	(2)	2722	(2)	28	(1)
C(42)	1616	(2)	1070	(2)	3182	(2)	40	(2)
C(52)	1971	(2)	1152	(2)	3759	(2)	39	(2)
Zn(2)	5000		5000		5000		25	(1)
P(3)	3958	(1)	3958	(1)	3958	(1)	27	(1)
N(13)	4600	(2)	4654	(2)	2905	(1)	29	(1)
C(23)	4506	(2)	4583	(2)	3580	(2)	26	(1)
N(33)	4872	(2)	5049	(2)	3911	(1)	28	(1)
C(43)	5207	(2)	5417	(2)	3424	(2)	36	(2)
C(53)	5044	(2)	5171	(2)	2799	(2)	32	(1)
N	1710	(2)	28	(2)	-1488	(2)	47	(2)
O(1)	1537	(2)	-228	(2)	-2042	(2)	69	(2)
O(2)	1528	(2)	-234	(2)	-941	(1)	55	(1)
O(3)	2083	(1)	553	(1)	-1488	(1)	47	(1)

Equivalent isotropic U defined as one third of the trace of the orthogonalized U_{ij} tensor

Table 4.3.3 Selected bond lengths (Å) and angles (°) of $[(TIP)_2M](NO_3)_2$ (M = Ni, Cu, Zn)

$[(TIP)_2Ni](NO_3)_2$:

Ni(1)-N(32)	2.109	(5)	Ni(1)-N(31)	2.096	(5)
Ni(1)-N(32A)	2.109	(5)	Ni(1)-N(32B)	2.109	(5)
Ni(1)-N(31A)	2.096	(5)	Ni(1)-N(31B)	2.096	(5)
P(1)-C(21)	1.817	(6)	P(1)-C(21A)	1.817	(6)
P(1)-C(21B)	1.817	(6)	P(2)-C(22)	1.830	(6)
P(2)-C(22A)	1.830	(6)	P(2)-C(22B)	1.830	(6)
Ni(2)-N(33)	2.105	(4)	Ni(2)-N(33A)	2.105	(4)
Ni(2)-N(33B)	2.105	(4)	Ni(2)-N(33C)	2.105	(4)
Ni(2)-N(33D)	2.105	(4)	Ni(2)-N(33E)	2.105	(4)
P(3)-C(23)	1.811	(6)	P(3)-C(23A)	1.811	(6)
P(3)-C(23B)	1.811	(6)	N(32)-C(22)	1.343	(8)
N(32)-C(42)	1.393	(8)	N(31)-C(21)	1.344	(8)
N(31)-C(41)	1.387	(8)	C(21)-N(11)	1.358	(8)
C(22)-N(12)	1.354	(8)	C(42)-C(52)	1.361	(9)
C(41)-C(51)	1.39	(1)	N(11)-C(51)	1.387	(9)
N(12)-C(52)	1.379	(8)	N(33)-C(23)	1.343	(7)
N(33)-C(43)	1.378	(7)	C(23)-N(13)	1.373	(7)
C(43)-C(53)	1.388	(8)	N(13)-C(53)	1.372	(8)
N-O(1)	1.286	(7)	N-O(2)	1.262	(7)
N-O(3)	1.260	(7)			

N(32)-Ni(1)-N(31)	90.6	(2)	N(32)-Ni(1)-N(32A)	87.2	(2)
N(31)-Ni(1)-N(32A)	94.6	(2)	N(32)-Ni(1)-N(32B)	87.2	(2)
N(31)-Ni(1)-N(32B)	177.1	(2)	N(32A)-Ni(1)-N(32B)	87.2	(2)
N(32)-Ni(1)-N(31A)	177.1	(2)	N(31)-Ni(1)-N(31A)	87.7	(2)
N(32A)-Ni(1)-N(31A)	90.6	(2)	N(32B)-Ni(1)-N(31A)	94.6	(2)
N(32)-Ni(1)-N(31B)	94.6	(2)	N(31)-Ni(1)-N(31B)	87.7	(2)
N(32A)-Ni(1)-N(31B)	177.1	(2)	N(32B)-Ni(1)-N(31B)	90.6	(2)
N(31A)-Ni(1)-N(31B)	87.7	(2)	C(21)-P(1)-C(21A)	96.0	(3)
C(21)-P(1)-C(21B)	96.0	(3)	C(21A)-P(1)-C(21B)	96.0	(3)
C(22)-P(2)-C(22A)	96.1	(3)	C(22)-P(2)-C(22B)	96.1	(3)
C(22A)-P(2)-C(22B)	96.1	(3)	N(33)-Ni(2)-N(33A)	180.0	(1)
N(33)-Ni(2)-N(33B)	87.0	(2)	N(33A)-Ni(2)-N(33B)	93.0	(2)
N(33)-Ni(2)-N(33C)	93.0	(2)	N(33A)-Ni(2)-N(33C)	87.0	(2)
N(33B)-Ni(2)-N(33C)	180.0	(1)	N(33)-Ni(2)-N(33D)	87.0	(2)
N(33A)-Ni(2)-N(33D)	93.0	(2)	N(33B)-Ni(2)-N(33D)	87.0	(2)
N(33C)-Ni(2)-N(33D)	93.0	(2)	N(33)-Ni(2)-N(33E)	93.0	(2)
N(33A)-Ni(2)-N(33E)	87.0	(2)	N(33B)-Ni(2)-N(33E)	93.0	(2)
N(33C)-Ni(2)-N(33E)	87.0	(2)	N(33D)-Ni(2)-N(33E)	180.0	(1)
C(23)-P(3)-C(23A)	95.7	(3)	C(23)-P(3)-C(23B)	95.7	(3)
C(23A)-P(3)-C(23B)	95.7	(3)	Ni(1)-N(32)-C(22)	122.0	(4)
Ni(1)-N(32)-C(42)	131.1	(4)	C(22)-N(32)-C(42)	105.4	(5)
Ni(1)-N(31)-C(21)	121.9	(4)	Ni(1)-N(31)-C(41)	131.6	(4)

Table 4.3.3 (continued)

C(21)-N(31)-C(41)	106.5	(5)	P(1)-C(21)-N(31)	125.9	(5)
P(1)-C(21)-N(11)	123.4	(5)	N(31)-C(21)-N(11)	110.7	(5)
P(2)-C(22)-N(32)	124.8	(5)	P(2)-C(22)-N(12)	124.1	(5)
N(32)-C(22)-N(12)	111.1	(5)	N(32)-C(42)-C(52)	109.3	(6)
N(31)-C(41)-C(51)	108.9	(5)	C(21)-N(11)-C(51)	107.7	(5)
C(22)-N(12)-C(52)	107.3	(5)	C(42)-C(52)-N(12)	106.9	(6)
C(41)-C(51)-N(11)	106.2	(6)	Ni(2)-N(33)-C(23)	121.8	(4)
Ni(2)-N(33)-C(43)	131.1	(4)	C(23)-N(33)-C(43)	106.4	(4)
P(3)-C(23)-N(33)	126.2	(4)	P(3)-C(23)-N(13)	123.7	(4)
N(33)-C(23)-N(13)	110.1	(5)	N(33)-C(43)-C(53)	109.4	(5)
C(23)-N(13)-C(53)	107.9	(5)	C(43)-C(53)-N(13)	106.1	(5)
O(1)-N-O(2)	119.1	(5)	O(1)-N-O(3)	120.1	(5)
O(2)-N-O(3)	120.8	(5)			

$[(TIP)_2Cu](NO_3)_2$:

Cu(1)-N(31)	2.145	(5)	Cu(1)-N(32)	2.133	(6)
Cu(1)-N(31A)	2.145	(5)	Cu(1)-N(31B)	2.145	(5)
Cu(1)-N(32A)	2.133	(6)	Cu(1)-N(32B)	2.133	(6)
Cu(2)-N(33)	2.153	(5)	Cu(2)-N(33A)	2.153	(5)
Cu(2)-N(33B)	2.153	(5)	Cu(2)-N(33C)	2.153	(5)
Cu(2)-N(33D)	2.153	(5)	Cu(2)-N(33E)	2.153	(5)
P(2)-C(22)	1.795	(7)	P(2)-C(22A)	1.795	(7)
P(2)-C(22B)	1.795	(7)	P(3)-C(23)	1.804	(7)
P(3)-C(23A)	1.804	(7)	P(3)-C(23B)	1.804	(7)
P(1)-C(21)	1.811	(6)	P(1)-C(21A)	1.811	(6)
P(1)-C(21B)	1.811	(6)	N(31)-C(21)	1.341	(8)
N(31)-C(41)	1.38	(1)	N(11)-C(21)	1.358	(8)
N(11)-C(51)	1.371	(9)	C(41)-C(51)	1.36	(1)
N(32)-C(22)	1.356	(9)	N(32)-C(42)	1.36	(1)
N(33)-C(23)	1.318	(9)	N(33)-C(43)	1.370	(9)
C(22)-N(12)	1.344	(9)	C(23)-N(13)	1.367	(8)
C(42)-C(52)	1.36	(1)	C(43)-C(53)	1.34	(1)
N(12)-C(52)	1.38	(1)	N(13)-C(53)	1.363	(9)
N-O(1)	1.279	(9)	N-O(2)	1.247	(9)
N-O(3)	1.234	(9)			

N(31)-Cu(1)-N(32)	90.6	(2)	N(31)-Cu(1)-N(31A)	86.6	(2)
N(32)-Cu(1)-N(31A)	95.7	(2)	N(31)-Cu(1)-N(31B)	86.6	(2)
N(32)-Cu(1)-N(31B)	176.3	(2)	N(31A)-Cu(1)-N(31B)	86.6	(2)
N(31)-Cu(1)-N(32A)	176.3	(2)	N(32)-Cu(1)-N(32A)	87.2	(2)
N(31A)-Cu(1)-N(32A)	90.6	(2)	N(31B)-Cu(1)-N(32A)	95.7	(2)
N(31)-Cu(1)-N(32B)	95.7	(2)	N(32)-Cu(1)-N(32B)	87.2	(2)
N(31A)-Cu(1)-N(32B)	176.3	(2)	N(31B)-Cu(1)-N(32B)	90.6	(2)
N(32A)-Cu(1)-N(32B)	87.2	(2)	N(33)-Cu(2)-N(33A)	180.0	(1)
N(33)-Cu(2)-N(33B)	86.2	(2)	N(33A)-Cu(2)-N(33B)	93.8	(2)
N(33)-Cu(2)-N(33C)	93.8	(2)	N(33A)-Cu(2)-N(33C)	86.2	(2)

Table 4.3.3 (continued)

N(33B)-Cu(2)-N(33C)	180.0	(1)	N(33)-Cu(2)-N(33D)	86.2	(2)
N(33A)-Cu(2)-N(33D)	93.8	(2)	N(33B)-Cu(2)-N(33D)	86.2	(2)
N(33C)-Cu(2)-N(33D)	93.8	(2)	N(33)-Cu(2)-N(33E)	93.8	(2)
N(33A)-Cu(2)-N(33E)	86.2	(2)	N(33B)-Cu(2)-N(33E)	93.8	(2)
N(33C)-Cu(2)-N(33E)	86.2	(2)	N(33D)-Cu(2)-N(33E)	180.0	(1)
C(22)-P(2)-C(22A)	97.1	(3)	C(22)-P(2)-C(22B)	97.1	(3)
C(22A)-P(2)-C(22B)	97.1	(3)	C(23)-P(3)-C(23A)	95.6	(3)
C(23)-P(3)-C(23B)	95.6	(3)	C(23A)-P(3)-C(23B)	95.6	(3)
C(21)-P(1)-C(21A)	97.2	(3)	C(21)-P(1)-C(21B)	97.2	(3)
C(21A)-P(1)-C(21B)	97.2	(3)	Cu(1)-N(31)-C(21)	121.6	(4)
Cu(1)-N(31)-C(41)	131.4	(5)	C(21)-N(31)-C(41)	105.6	(5)
C(21)-N(11)-C(51)	108.1	(6)	P(1)-C(21)-N(31)	125.1	(5)
P(1)-C(21)-N(11)	124.7	(5)	N(31)-C(21)-N(11)	110.2	(5)
N(31)-C(41)-C(51)	110.1	(6)	N(11)-C(51)-C(41)	106.0	(6)
Cu(1)-N(32)-C(22)	121.0	(4)	Cu(1)-N(32)-C(42)	132.6	(5)
C(22)-N(32)-C(42)	106.3	(6)	Cu(2)-N(33)-C(23)	120.8	(4)
Cu(2)-N(33)-C(43)	130.8	(5)	C(23)-N(33)-C(43)	107.3	(5)
P(2)-C(22)-N(32)	126.3	(5)	P(2)-C(22)-N(12)	124.5	(5)
N(32)-C(22)-N(12)	109.3	(6)	P(3)-C(23)-N(33)	127.6	(5)
P(3)-C(23)-N(13)	123.2	(5)	N(33)-C(23)-N(13)	109.1	(5)
N(32)-C(42)-C(52)	110.5	(7)	N(33)-C(43)-C(53)	109.0	(6)
C(22)-N(12)-C(52)	108.6	(6)	C(23)-N(13)-C(53)	107.4	(5)
C(42)-C(52)-N(12)	105.3	(7)	C(43)-C(53)-N(13)	107.1	(6)
O(1)-N-O(2)	118.2	(7)	O(1)-N-O(3)	119.5	(6)
O(2)-N-O(3)	122.2	(7)			

$[(TIP)_2Zn](NO_3)_2$:

Zn(1)-N(31)	2.160	(3)	Zn(1)-N(32)	2.170	(3)
Zn(1)-N(31A)	2.160	(3)	Zn(1)-N(31B)	2.160	(3)
Zn(1)-N(32A)	2.170	(3)	Zn(1)-N(32B)	2.170	(3)
P(1)-C(21)	1.808	(4)	P(1)-C(21A)	1.808	(4)
P(1)-C(21B)	1.808	(4)	N(11)-C(21)	1.360	(5)
N(11)-C(51)	1.365	(5)	C(21)-N(31)	1.342	(5)
N(31)-C(41)	1.379	(5)	C(41)-C(51)	1.382	(6)
P(2)-C(22)	1.815	(4)	P(2)-C(22A)	1.815	(4)
P(2)-C(22B)	1.815	(4)	N(12)-C(22)	1.363	(5)
N(12)-C(52)	1.373	(6)	C(22)-N(32)	1.333	(5)
N(32)-C(42)	1.383	(5)	C(42)-C(52)	1.351	(6)
Zn(2)-N(33)	2.172	(3)	Zn(2)-N(33A)	2.172	(3)
Zn(2)-N(33B)	2.172	(3)	Zn(2)-N(33C)	2.172	(3)
Zn(2)-N(33D)	2.172	(3)	Zn(2)-N(33E)	2.172	(3)
P(3)-C(23)	1.809	(4)	P(3)-C(23A)	1.809	(4)
P(3)-C(23B)	1.809	(4)	N(13)-C(23)	1.357	(5)
N(13)-C(53)	1.364	(5)	C(23)-N(33)	1.344	(5)
N(33)-C(43)	1.380	(5)	C(43)-C(53)	1.369	(5)
N-O(1)	1.256	(5)	N-O(2)	1.253	(5)

Table 4.3.3 (continued)

N-O(3)	1.274	(5)			
N(31)-Zn(1)-N(32)	96.0	(1)	N(31)-Zn(1)-N(31A)	86.9	(1)
N(32)-Zn(1)-N(31A)	90.9	(1)	N(31)-Zn(1)-N(31B)	86.9	(1)
N(32)-Zn(1)-N(31B)	176.3	(1)	N(31A)-Zn(1)-N(31B)	86.9	(1)
N(31)-Zn(1)-N(32A)	176.3	(1)	N(32)-Zn(1)-N(32A)	86.4	(1)
N(31A)-Zn(1)-N(32A)	96.0	(1)	N(31B)-Zn(1)-N(32A)	90.9	(1)
N(31)-Zn(1)-N(32B)	90.9	(1)	N(32)-Zn(1)-N(32B)	86.4	(1)
N(31A)-Zn(1)-N(32B)	176.3	(1)	N(31B)-Zn(1)-N(32B)	96.0	(1)
N(32A)-Zn(1)-N(32B)	86.4	(1)	C(21)-P(1)-C(21A)	96.9	(2)
C(21)-P(1)-C(21B)	96.9	(2)	C(21A)-P(1)-C(21B)	96.9	(2)
C(21)-N(11)-C(51)	108.4	(3)	P(1)-C(21)-N(11)	123.6	(3)
P(1)-C(21)-N(31)	126.7	(3)	N(11)-C(21)-N(31)	109.7	(3)
Zn(1)-N(31)-C(21)	120.9	(3)	Zn(1)-N(31)-C(41)	132.3	(3)
C(21)-N(31)-C(41)	106.7	(3)	N(31)-C(41)-C(51)	108.8	(4)
N(11)-C(51)-C(41)	106.3	(4)	C(22)-P(2)-C(22A)	96.4	(2)
C(22)-P(2)-C(22B)	96.4	(2)	C(22A)-P(2)-C(22B)	96.4	(2)
C(22)-N(12)-C(52)	107.4	(3)	P(2)-C(22)-N(12)	123.3	(3)
P(2)-C(22)-N(32)	126.5	(3)	N(12)-C(22)-N(32)	110.3	(3)
Zn(1)-N(32)-C(22)	120.7	(3)	Zn(1)-N(32)-C(42)	131.5	(3)
C(22)-N(32)-C(42)	105.9	(3)	N(32)-C(42)-C(52)	109.8	(4)
N(12)-C(52)-C(42)	106.6	(4)	N(33)-Zn(2)-N(33A)	180.0	(1)
N(33)-Zn(2)-N(33B)	86.2	(1)	N(33A)-Zn(2)-N(33B)	93.8	(1)
N(33)-Zn(2)-N(33C)	93.8	(1)	N(33A)-Zn(2)-N(33C)	86.2	(1)
N(33B)-Zn(2)-N(33C)	180.0	(1)	N(33)-Zn(2)-N(33D)	86.2	(1)
N(33A)-Zn(2)-N(33D)	93.8	(1)	N(33B)-Zn(2)-N(33D)	86.2	(1)
N(33C)-Zn(2)-N(33D)	93.8	(1)	N(33)-Zn(2)-N(33E)	93.8	(1)
N(33A)-Zn(2)-N(33E)	86.2	(1)	N(33B)-Zn(2)-N(33E)	93.8	(1)
N(33C)-Zn(2)-N(33E)	86.2	(1)	N(33D)-Zn(2)-N(33E)	180.0	(1)
C(23)-P(3)-C(23A)	96.9	(2)	C(23)-P(3)-C(23B)	96.9	(2)
C(23A)-P(3)-C(23B)	96.9	(2)	C(23)-N(13)-C(53)	108.5	(3)
P(3)-C(23)-N(13)	124.1	(3)	P(3)-C(23)-N(33)	126.3	(3)
N(13)-C(23)-N(33)	109.6	(3)	Zn(2)-N(33)-C(23)	121.1	(2)
Zn(2)-N(33)-C(43)	131.4	(2)	C(23)-N(33)-C(43)	106.3	(3)
N(33)-C(43)-C(53)	109.3	(3)	N(13)-C(53)-C(43)	106.2	(3)
O(1)-N-O(2)	120.6	(4)	O(1)-N-O(3)	119.1	(4)
O(2)-N-O(3)	120.3	(4)			

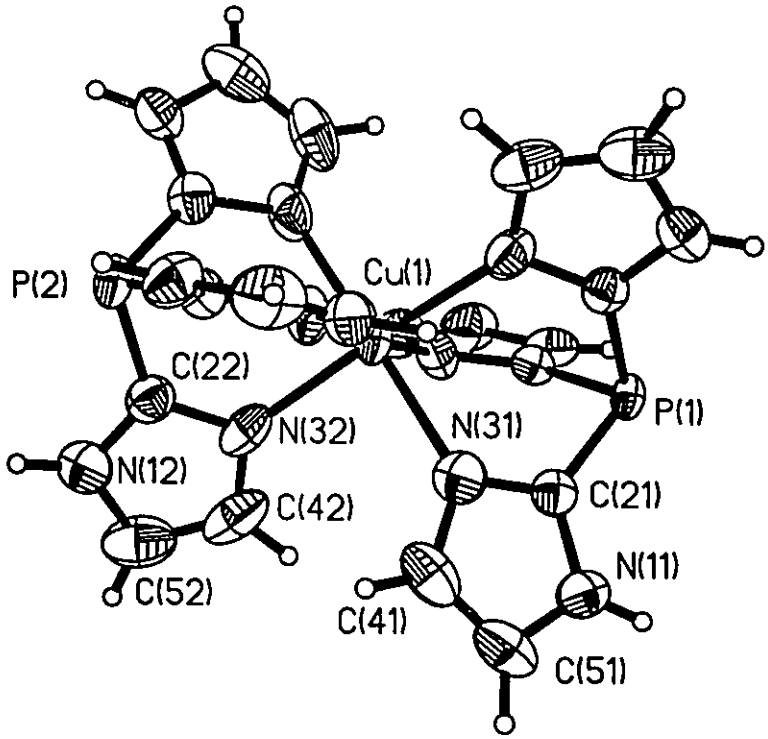

Figure 4.3.1 The cation of $[(TIP)_2Cu](NO_3)_2$

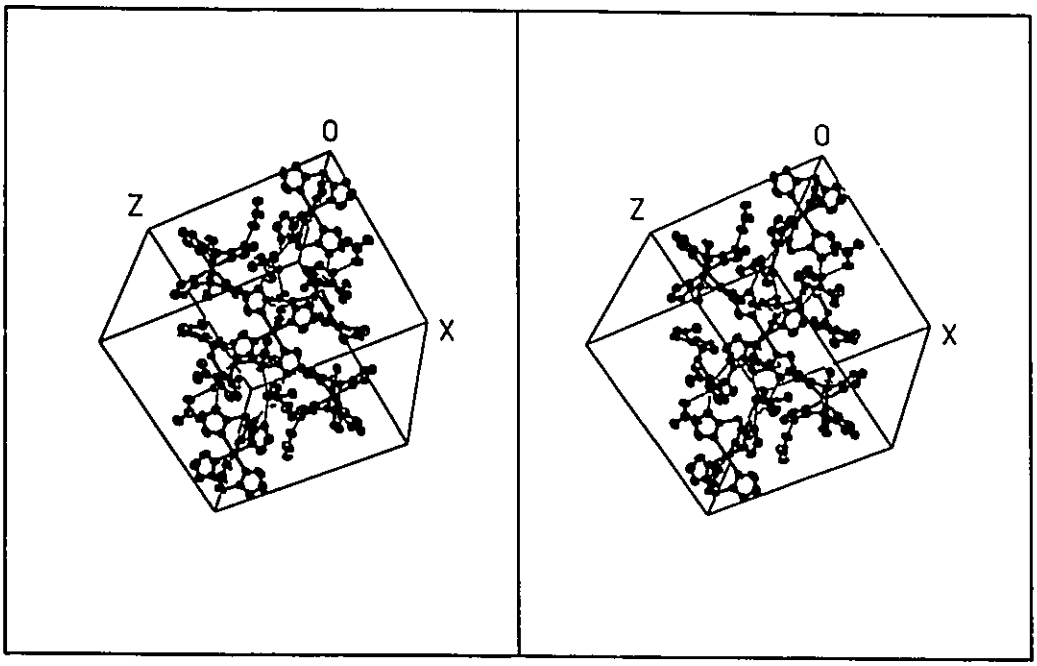

Figure 4.3.2 A stereoview of the packing of $[(TIP)_2Cu](NO_3)_2$ in a unit cell

unit. The coordination geometries around these two metal centres are essentially octahedral. Such a coordination geometry for the Cu(II) ion is an example of the dynamic Jahn-Teller effect. Further discussions about the Jahn-Teller effect will be made in **Chapter 6**.

The M-N bond distances within complexes are not significantly different. The bonds in the zinc complex are not significantly different from those of hexakis(imidazole)zinc(II) chloride 2.15(4) - 2.26(3)Å (103), but are longer than those of tris(4,5-diisopropylimidazol-2-yl)zinc(II) chloride 2.057(2)Å (71) in which the Zn(II) atom is four coordinate. The bonds in the nickel complexes are shorter than those of the hexakis(imidazole)nickel(II) complexes 2.128(4) - 2.140(2)Å (104, 105), probably because the data for the TIP complex were collected at a lower temperature. For the copper complex, the corresponding hexakis(imidazole)-copper(II) complex is distorted (106). Copper(II) complexes with other tridentate ligands with aromatic nitrogen donor atoms are also distorted (94, 107). The Cu(II)-N bonds in the TIP complex are longer than the four short bonds 1.991(2) - 2.082(2)Å but shorter than the two long bonds 2.24(1) - 2.593(3)Å in those complexes.

The imidazole rings in all complexes are essentially planar. Displacements of atoms from least-squares planes are within experimental errors. The P-C bond distances in the complexes do not differ significantly nor are they different from those in the free ligand (85) except the P-C bonds in the second molecule of the

nickel complex [1.830(6)Å], which are longer than the rest. The reason for this is not clear. All the protonated imidazole nitrogen atoms are hydrogen bonded to the nitrate oxygen atoms with the N...O distances 2.811(7)-2.956(9)Å. Two of the nitrate oxygen atoms participate in hydrogen bonding.

4.4 The Vibrational Spectra of the $[(TIP)_2M](NO_3)_2$ Complexes

Major vibrational frequencies of the bis-ligand metal nitrate complexes are listed in **Table 4.4** together with tentative assignments. Assignments were made in accord with references 84, 86, 96, 97, 108.

4.5 The Structure of the Polymeric Cu(I)/ Cu(II) TIP Complex

The crystal used for X-ray diffraction experiment was mounted by gluing to the end of a glass fibre. The crystal density was measured by suspension in $CCl_4/CHBr_3$. Unit cell determination and intensity data collection were performed on a Nicolet P3 diffractometer. No instrument instability and crystal decay were observed during data collection. The structures was solved by the Patterson method. One water molecule and one methanol molecule in the coordination sphere were found to be disordered. These molecules were refined with occupancies of 1/4 each. Hydrogen atoms were placed in calculated positions and were not refined, except for the water molecules and the disordered methanol molecule to which no hydrogen atoms were added. Anisotropic full-matrix least-squares refinement minimized $\Sigma w(|F_o| - |F_c|)^2$. Scale, positional parameters for all atoms and anisotropic temperature factors for non-hydrogen atoms were

Table 4.4 Vibrational spectra (cm^{-1}) of the $[(TIP)_2M](NO_3)_2$ (M = Ni, Cu, Zn) complexes

$[(TIP)_2Cu](NO_3)_2$		$[(TIP)_2Ni](NO_3)_2$		$[(TIP)_2Zn](NO_3)_2$		Assignments
Infrared	Raman	Infrared	Raman	Infrared	Raman	
3440-2690s,br		3440-2680s,br		3440-2680s,br		νN-H,C-H
1742w,br		1744w,br		1741w,br		-
1632w,br		1635w,br		1632w,br		
1533m	1540w,	1533m	1538w	1533m		νring
1433m	1430s	1438m	1430s	1436m	1428s	δring
1400vs		1404vs		1402vs		νNO_3
1381vs		1386vs		1383vs		νP-C
	1340vs		1340vs		1338vs	νNO_3
1314vs		1317vs		1318vs		νC-H
1262w	1272m	1262w	1268m	1260w	1268m	δC-H
1246w,br		1250w,br		1250w,br		δC-H
	1175w		1173w		1175w	νring
1153w	1160m	1156w	1160m	1152w	1160w	δN-H
	1118m		1116m		1113m	δC-H
1106s		1107s		1106s		δC-H
	1045s		1037m		1038m	-
1028w		1030w		1030w		-
972w	985w	963w	978w	961m	974w	-
951w	961w					δring
921w	932w	925w	935w	924w	938w	δC-H
865w	870w,br	866w	865w	869w,br	874w,br	γC-H
818m,br		825m		829m		γNO_3
793m,br		780m,sh		785m,br		-
765s	773w,br	768s	775w,br	769s	770w,br	δP-C
754s		752s		756s		γC-H

Table 4.4 (continued)

$[(TIP)_2Cu](NO_3)_2$		$[(TIP)_2Ni](NO_3)_2$		$[(TIP)_2Zn](NO_3)_2$		Assignments
Infrared	Raman	Infrared	Raman	Infrared	Raman	
	716w		714w		718w	-
698m		705m		701m		γC-H
	630w		630w		630w	γring
521m	538w	525m	540w	518m		γP-C
487s	490w,br	486s	485w,br	484s		-
338w,sh	342m		336m		334m	-
322m	320w	328m	320w	320m	315w	-
	280w		286w		276w	νM-N
	195s		192s		180w,br	δM-N-C

Bands in cm^{-1}, s=strong, m=medium, w=weak, br=broad, sh=shoulder, v=very.
ν=stretching, δ=deformation, γ=bending.
Assignments were made according to references 2, 5, 23, 24.

varied, except for the disordered water and methanol molecules which were refined isotropically. Hydrogen atoms were refined with fixed temperature factors. Details of crystal data and structure solution are listed in **Table 4.5.1.** Atomic positional parameters are given in **Table 4.5.2** and selected interatomic distances and angles are given in **Table 4.5.3.** Atoms of the complex in one asymmetric unit and packing diagrams are given in **Figure 4.5.1** and **Figure 4.5.2.**

In the complex, there are two copper atoms, three chloride atoms and one ligand molecule in one asymmetric unit. The oxidation states of the two copper atoms are more localized, that is, Cu(1) is more like a Cu(II) atom and Cu(2) is more like a Cu(I) atom. This is like the type I mixed valent metal complexes with localized metal centres in different oxidation states (109). In the complex, the copper(I) atom is relatively soft. It is coordinated to relatively soft chloride and phosphorus atoms only, with a pseudo-tetrahedral geometry. The Cu(I) atom is doubly bridged by two chloride atoms towards another Cu(I) atom with a Cu(I)...Cu(I) separation (Å) of 3.046(2). This value is shorter than some chloride doubly bridged Cu(I)...Cu(I) separations 3.107(1) - 3.3570(4) (110, 111), but longer than others 2.775(2) - 2.952(2) (112), and longer than the Cu(I)...Cu(I) separations with other bridging ligands 2.507(1) - 2.660(1) (113 - 115). More examples can be found in reference 116. This value is well above the sum of two covalent Cu(I) radii of 2.54Å (116, 117), and above the sum of the atomic and van der Waals radii of two Cu atoms, 2.70Å (118) and 2.8Å (119). The Cu(I)-P distance (Å) is

Table 4.5.1 Crystal data of the polymeric Cu(I)/Cu(II) TIP complex

Formula	$C_{9.25}H_{12.5}N_6O_{1.5}PCl_3Cu_2$
Formula weight	496.1
Crystal colour, shape, size (mm)	yellow needle, 0.17 0.20 0.25
Space group, λ (Å)	C2/c, 0.71073
Unit cell parameters (Å and °)	a = 16.037(3) b = 15.368(3) c = 15.597(3) β = 118.21(3)
Volume ($Å^3$)	3387.5(17)
Z	8
ρ_{cal}, ρ_{obs} ($Mg\ m^{-3}$)	1.946, 1.91(2)
Max. 2θ, indices range	45°, $0 \le h \le 17$, $0 \le k \le 16$, $-16 \le l \le 14$
Temperature, °C	23
Absorption coefficient mm^{-1}	3.090
Number of variables	205
Number of reflections measured	2133
Number of independent reflections, used	2130
R_{int}	0.0124
Final R, R_w	0.0616, 0.0478
Final Δ/σ, max., ave	0.019, 0.001
Final difference map, max., min., e A^{-3}	0.91, -0.51
Weighting	$(\sigma_F^2)^{-1}$
Goodness of fit, S	2.35
F(000)	1968

Table 4.5.2 Atomic coordinates ($x10^4$) and equivalent isotropic displacement coefficients ($Å^2x10^3$) of the polymeric Cu(I)/Cu(II) TIP complex

	x		y		z		U(eq)	
Cu(1)	1784	(1)	1343	(1)	2221	(1)	45	(1)
Cu(2)	3989	(1)	-260	(1)	4288	(1)	50	(1)
P	3623	(2)	-1581	(1)	3742	(2)	40	(1)
Cl(3)	5188	(2)	297	(1)	3937	(2)	50	(1)
Cl(2)	1922	(2)	21	(1)	1685	(2)	72	(1)
Cl(1)	2977	(2)	912	(1)	3911	(2)	67	(1)
N(31)	1529	(4)	2406	(4)	2809	(4)	38	(3)
C(52)	5690	(7)	-3084	(6)	5584	(8)	68	(6)
N(11)	3788	(4)	-1233	(4)	2074	(5)	48	(4)
C(21)	3613	(5)	-1811	(4)	2609	(5)	35	(4)
N(12)	5233	(5)	-2315	(4)	5288	(5)	53	(4)
N(13)	1896	(5)	-1811	(5)	3781	(5)	64	(4)
C(22)	4442	(6)	-2424	(5)	4434	(6)	44	(5)
C(41)	1441	(5)	2474	(5)	3637	(6)	48	(4)
C(23)	2546	(6)	-2129	(5)	3532	(6)	46	(4)
C(53)	1224	(7)	-2422	(8)	3525	(8)	86	(6)
N(32)	632	(5)	1743	(4)	850	(5)	55	(4)
N(33)	2711	(5)	2090	(4)	1867	(5)	56	(4)
C(43)	1452	(7)	-3097	(7)	3130	(8)	80	(6)
C(51)	3760	(7)	-1653	(5)	1287	(7)	66	(6)
C(42)	5134	(8)	-3654	(6)	4867	(9)	76	(7)
O(2)	1873	(5)	-285	(5)	4695	(5)	103	(5)
O(1)*	749	(12)	647	(12)	2683	(13)	130	(6)
C(1)**	0		69	(21)	2500		93	(10)

Equivalent isotropic U defined as one third of the trace of the orthogonalized U_{ij} tensor.

* The oxygen atoms of the disordered water and methanol molecules were refined at this position with occupancies of 0.5 respectively.

** The carbon atom of the disordered methanol molecule was refined at this position with an occupancy of 0.5.

Table 4.5.3 Selected bond lengths (Å) and angles (°) of the polymeric Cu(I)/Cu(II) TIP complex

Cu(1)-Cl(2)	2.247	(3)	Cu(1)-Cl(1)	2.505	(2)
Cu(1)-N(31)	2.009	(7)	Cu(1)-N(32)	2.152	(6)
Cu(1)-N(33)	2.148	(9)	Cu(1)-O(1)	2.36	(2)
Cu(2)-P	2.172	(2)	Cu(2)-Cl(3)	2.392	(3)
Cu(2)-Cl(1)	2.307	(3)	Cu(2)-Cu(2A)	3.046	(2)
Cu(2)-Cl(3A)	2.441	(2)	P-C(21)	1.793	(9)
P-C(22)	1.798	(8)	P-C(23)	1.806	(9)
Cl(3)-Cu(2A)	2.441	(2)	N(31)-C(41)	1.37	(1)
N(31)-C(21A)	1.336	(9)	C(52)-N(12)	1.35	(1)
C(52)-C(42)	1.37	(1)	N(11)-C(21)	1.34	(1)
N(11)-C(51)	1.37	(1)	C(21)-N(31A)	1.336	(9)
N(12)-C(22)	1.346	(9)	N(13)-C(23)	1.36	(1)
N(13)-C(53)	1.34	(1)	C(22)-N(32A)	1.34	(1)
C(41)-C(51A)	1.40	(1)	C(23)-N(33A)	1.32	(1)
C(53)-C(43)	1.34	(2)	N(32)-C(22A)	1.34	(1)
N(32)-C(42A)	1.35	(1)	N(33)-C(23A)	1.32	(1)
N(33)-C(43A)	1.37	(2)	C(43)-N(33A)	1.37	(2)
C(51)-C(41A)	1.40	(1)	C(42)-N(32A)	1.35	(1)
O(1)-C(1)	1.41	(3)	C(1)-O(1A)	1.41	(3)

Cl(2)-Cu(1)-Cl(1)	89.5	(1)	Cl(2)-Cu(1)-N(31)	169.3	(2)
Cl(1)-Cu(1)-N(31)	87.3	(2)	Cl(2)-Cu(1)-N(32)	94.5	(2)
Cl(1)-Cu(1)-N(32)	172.3	(3)	N(31)-Cu(1)-N(32)	87.5	(3)
Cl(2)-Cu(1)-N(33)	100.7	(2)	Cl(1)-Cu(1)-N(33)	97.7	(2)
N(31)-Cu(1)-N(33)	89.9	(3)	N(32)-Cu(1)-N(33)	88.0	(3)
Cl(2)-Cu(1)-O(1)	84.9	(5)	Cl(1)-Cu(1)-O(1)	81.7	(4)
N(31)-Cu(1)-O(1)	84.6	(5)	N(32)-Cu(1)-O(1)	92.1	(4)
N(33)-Cu(1)-O(1)	174.4	(5)	P-Cu(2)-Cl(3)	110.0	(1)
P-Cu(2)-Cl(1)	127.0	(1)	Cl(3)-Cu(2)-Cl(1)	101.9	(1)
P-Cu(2)-Cu(2A)	121.9	(1)	Cl(3)-Cu(2)-Cu(2A)	51.6	(1)
Cl(1)-Cu(2)-Cu(2A)	111.0	(1)	P-Cu(2)-Cl(3A)	109.0	(1)
Cl(3)-Cu(2)-Cl(3A)	101.9	(1)	Cl(1)-Cu(2)-Cl(3A)	104.2	(1)
Cu(2A)-Cu(2)-Cl(3A)	50.2	(1)	Cu(2)-P-C(21)	116.4	(3)
Cu(2)-P-C(22)	116.9	(2)	C(21)-P-C(22)	96.5	(4)
Cu(2)-P-C(23)	124.4	(3)	C(21)-P-C(23)	99.6	(4)
C(22)-P-C(23)	97.9	(4)	Cu(2)-Cl(3)-Cu(2A)	78.1	(1)

Table 4.5.3 (continued)

Cu(1)-Cl(1)-Cu(2)	124.7	(1)	Cu(1)-N(31)-C(41)	128.8	(5)
Cu(1)-N(31)-C(21A)	122.3	(6)	C(41)-N(31)-C(21A)	108.9	(7)
N(12)-C(52)-C(42)	104.0	(7)	C(21)-N(11)-C(51)	108.7	(7)
P-C(21)-N(11)	125.3	(5)	P-C(21)-N(31A)	125.4	(6)
N(11)-C(21)-N(31A)	109.2	(8)	C(52)-N(12)-C(22)	109.5	(7)
C(23)-N(13)-C(53)	106.2	(9)	P-C(22)-N(12)	125.7	(6)
P-C(22)-N(32A)	124.3	(5)	N(12)-C(22)-N(32A)	110.0	(6)
N(31)-C(41)-C(51A)	106.5	(8)	P-C(23)-N(13)	125.1	(6)
P-C(23)-N(33A)	124.5	(8)	N(13)-C(23)-N(33A)	110.3	(8)
N(13)-C(53)-C(43)	109	(1)	Cu(1)-N(32)-C(22A)	120.1	(5)
Cu(1)-N(32)-C(42A)	135.2	(6)	C(22A)-N(32)-C(42A)	104.7	(7)
Cu(1)-N(33)-C(23A)	120.3	(7)	Cu(1)-N(33)-C(43A)	133.1	(6)
C(23A)-N(33)-C(43A)	106.2	(9)	C(53)-C(43)-N(33A)	108.4	(9)
N(11)-C(51)-C(41A)	106.7	(9)	C(52)-C(42)-N(32A)	111.9	(8)
Cu(1)-O(1)-C(1)	152	(1)	O(1)-C(1)-O(1A)	102	(3)

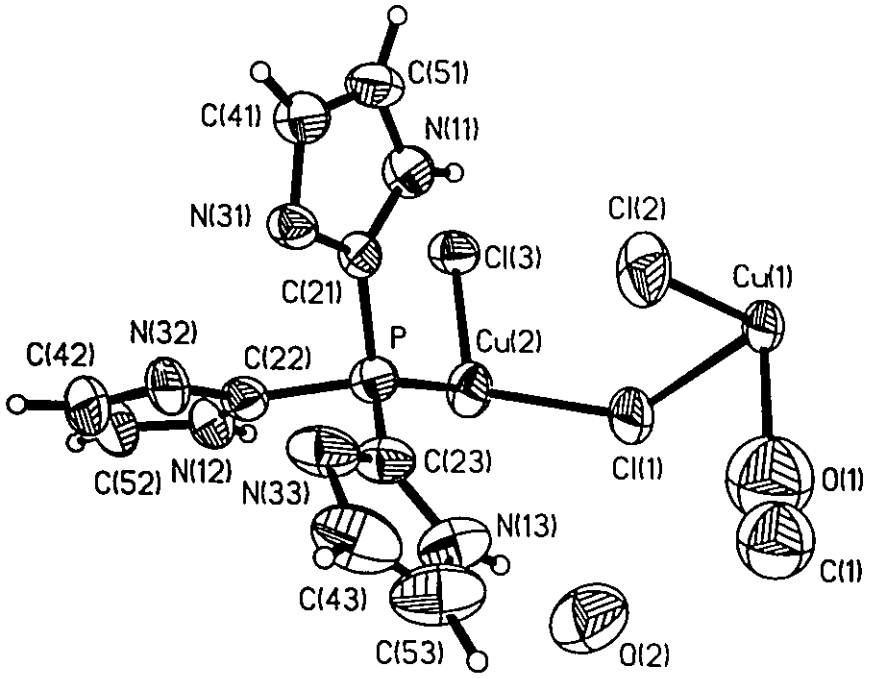

Figure 4.5.1 Atoms of the polymeric Cu(I)/Cu(II) TIP complex in one asymmetric unit

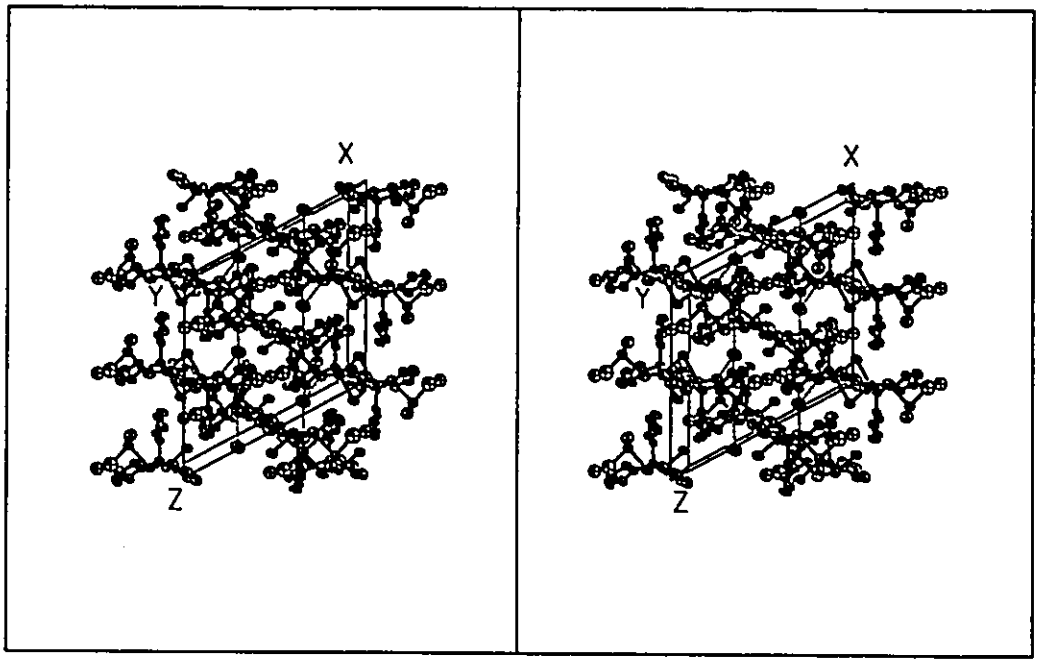

Figure 4.5.2 A stereoview of the packing of the polymeric Cu(I)/Cu(II) TIP complex in a unit cell

shorter than those of Cu(I)-P(o-tolyl)$_3$ 2.196(1), 2.206(1) (111) and Cu(I)-P(cyclohexyl)$_3$ 2.183(2) (120), but longer than the distances of other Cu(I)-P(cyclohexyl)$_3$ complexes 2.146(2) - 2.164(2) (116). The Cu(I) atom is also bridged by a chloride atom and a ligand molecule to two Cu(II) atoms. The separation between the Cu(I) and Cu(II) atoms is 4.264(3)Å. Such a multiple bridging system forms a three dimensional polymeric structure. In addition to the imidazole nitrogen atoms and bridging chloride ligands, the Cu(II) atom is also coordinated to a terminal chloride atom. Half of the sixth coordination site is filled with disordered water and methanol molecules with a weak Cu-O bond of 2.36(2)Å. The coordination geometry around the Cu(II) centre can be described as either octahedral or square-pyramidal. The Cu(II) atom is displaced by 0.156(2)Å out of the plane defined by two chloride ions and two imidazole nitrogen atoms. The other imidazole nitrogen atom occupies the apical position, trans to the oxygen atom when the Cu(II) atom is six coordinate. In the Cu(I)-Cl-Cu(II) unit, the Cl-Cu(II) bond distance is significantly longer than the Cl-Cu(I) bond distance, probably caused by the differences in coordination geometry and partially ionic nature of the complex, with the Cu(I) centre δ^- and the Cu(II) centre δ^+. Such a pattern was observed in one of the Cl bridges in a doubly bridged Cu(I)/Cu(II) system (121), and in a single Cl bridged Cu(I)/Cu(II) system (110). The Cu(II)-N distances 2.148(9) - 2.152(9)Å are not significantly different from those of $[(TIP)_2Cu](NO_3)_2$ 2.133(6) - 2.153(5)Å, except the bond trans to the terminal

chloride atom 2.009(7)Å.

All the imidazole rings are essentially planar. The mean P-C bond distance 1.80(2)Å is shorter but not significantly, than that of the free ligand 1.811(7)Å (85). A lattice water molecule is hydrogen bonded to the nitrogen atom of one of the imidazole rings with an O...N separation of 2.78(1)Å.

Chapter 5

Metal Complexes with Tris(1-methylimidazol-2-yl)phosphine (TMIP)

5.1 Introduction

In this chapter, the preparation and characterization of the gold(I) complex with TMIP is described. When the reaction was carried out in methanol or a methanol/water mixture, no product was obtained. This was probably caused by the same problem as the reaction of gold(I) with the ligand TIP (**Chapter 4**). The problem was avoided by carrying out the reaction in a less polar solvent, dichloromethane, in which both the ligand and the gold(I) complex are highly soluble. A colourless, crystalline product of TMIPAuCl was obtained. This complex was characterized by IR and NMR spectroscopy and X-ray structure determination.

A model compound of the dinuclear iron centre of hemerythrin was prepared by use of the ligand TMIP (69). In this compound the ligand is coordinated to the relatively hard iron(III) atom through its nitrogen donor atoms. It is possible to have the phosphorus donor atom on the ligand coordinated to a gold(I) atom while having the nitrogen donor atoms on the ligand coordinated to a hard metal atom. Efforts have been made to make such a complex. One product was obtained by reacting the ligand with AuI followed by addition of $Ni(NO_3)_2$. The structure of this complex has been determined and found to be

$[(TMIP)_2Ni](AuI_2)_2$. In this complex, the ligand is only coordinated to the Ni(II) atom through the nitrogen donor sites, and the gold(I) atom is coordinated to two iodide atoms. It is probable that the weak P-Au bond initially formed was attacked by an iodide anion, forming an I-Au bond, since I^- is also a good soft ligand for gold(I). The origin of the iodide anion is not clear, it is probably a product from a disproportionation reaction. The formation of such a complex reflects another weakness of such ligands having the phosphorus atom connected to the C2 carbon of the imidazole ring. Once the nitrogen atoms on the ligand are coordinated to a hard metal atom, the binding of the phosphorus atom on the ligand to gold(I) is rather weak and the ligand is easily replaced by other ligands. Other evidence about the weakness of such ligands will be discussed in the last chapter.

5.2 Preparations

Chloro[tris(1-methylimidazol-2-yl)phosphine-P]gold(I) (TMIPAuCl): To a solution of TMIP (0.1g) in CH_2Cl_2 (5mL), Me_2SAuCl (0.11g) was added quickly. The reaction mixture was stirred till almost all solid materials were dissolved, then toluene (5mL) was added. Any insoluble materials were removed by filtration. The filtrate was left to evaporate slowly at room temperature under nitrogen. A colourless crystalline product separated when almost all the CH_2Cl_2 had evaporated. This was collected by filtration, washed with diethylether (5mL) and air dried. Yield 0.15g (81%), m.p. 218-219°C (decompose).

Bis[tris(1-methylimidazol-2-yl)phosphine-N^3,$N^{3'}$,$N^{3''}$]nickel(II) di[(diiodoaurate(I)] {[(TMIP)$_2$Ni](AuI$_2$)$_2$}: Freshly prepared AuI (0.118g) was dissolved in a solution of TMIP (0.1g) in a 1:1 MeOH/MeCN mixture (10mL). To this solution, a solution of $Ni(NO_3)_2 \cdot 6H_2O$ (0.053g) in a 1:1 MeOH/MeCN mixture (5mL) was added quickly. The resulting solution was sealed in a glass container immediately after mixing and left to stand overnight at room temperature. A yellow crystalline solid precipitated out during that period, and was collected by filtration, washed with methanol (5mL) and air dried. Yield 0.06g (22%), m.p. 355-356°C (decompose).

5.3 The NMR Spectra of TMIPAuCl

Proton and ^{13}C spectra of TMIPAuCl in CD_2Cl_2 was collected on a Bruker AC 300 spectrometer. Tentative assignments to the spectra were made by analogy to the spectra of the free ligand and reported below (chemical shifts in ppm, relative to TMS, coupling constants in Hz): ^1H, 3.772, s, 3H, -C<u>H</u>$_3$, 7.228, s, 1H, ring C4-<u>H</u>, 7.288, s, 1H, ring C5-<u>H</u>; ^{13}C, 35.639, s, ring N1-<u>C</u>, 128.185, s, ring <u>C</u>5, 131.910, d, $^3J_{P\text{-}C}$ ±17.58, ring <u>C</u>4, 133.368, d, $^1J_{P\text{-}C}$ ±120.98, ring <u>C</u>2.

All the chemical shift and coupling constant values are slightly different from those of the free ligand except the one bond P-C coupling constant (signs of the $^1J_{P\text{-}C}$ were not determined, only absolute values are compared here), which increased from 12.38Hz to 120.98Hz as the ligand was coordinated to the gold. Large $^1J_{P\text{-}C}$ values have been reported for many gold(I) phosphine complexes

having the form of R_3P-Au-Y (Y refers to ligands other than phosphines). Some examples are ($^1J_{P-C}$ in Hz): 33.9 and 28.3, where R = ethyl and cyclohexyl (122); 54 - 60, where R = phenyl (123); 28.23 - 31.17, where R = ethyl, cyclohexyl, and phenyl (124); 28.38 - 58.87, where R = ethyl, cyclohexyl and phenyl (125); 61.56, where R = phenyl (126). The value found in TMIPAuCl is almost twice the largest value cited above. This is probably a reflection of the strain imposed on the P-C bond when the phosphorus atom is coordinated to the gold.

Large $^1J_{P-C}$ values (up to 200Hz) can be found in some phosphorus compounds in which the phosphorus atom has a formal oxidation state of +5 (127). With respect to the $^1J_{P-C}$ values, coordination of the phosphorus atom to the gold atom can be considered like oxidation to the +5 oxidation state. A direct consequence of this effect is the shortening of the P-C bond lengths which will be discussed below.

5.4 The Structure of TMIPAuCl

The crystal density was measured by suspension in $CCl_4/CHBr_3$ and the crystal for X-ray diffraction experiment was mounted by gluing to the end of a glass fibre. Unit cell determination and intensity data collection were performed on a Siemens P3/V diffractometer with monchromatized Ag Kα radiation. Unit cell parameters were refined by least-squares fit of angular parameters for 23 reflections ($20.07 \leq 2\theta \leq 33.06°$). Intensities were measured with a θ(crystal) - 2θ(counter) scan. Three standards were measured every 100 reflections. No signs

of crystal decay or instrumental instability were observed during data collection. An absorption correction was made with DIFABS (81). The structure was solved by the Patterson method and refined by the method of least-squares, which minimized $\Sigma w(|F_o| - |F_c|)^2$. Hydrogen atoms were placed in calculated positions and not refined. Temperature factors of non-hydrogen atoms were refined anisotropically, and those of hydrogen atoms were not refined. Details of crystal data collection and structure solution are listed in **Table 5.4.1**. Atomic positional parameters are given in **Table 5.4.2**. Selected interatomic distances and angles are given in **Table 5.4.3**. The molecule and packing diagrams are given in **Figure 5.4.1** and **Figure 5.4.2**.

The structure is normal with rectilinear two coordination around gold [P-Au-Cl bond angle 178.8(1)°]. The P-Au bond distance (Å) of 2.216(2) is similar to other phosphine gold(I) complexes, such as 2.258(1) (124), 2.240(5) (126), 2.253(2) - 2.258(1) (125), and 2.235(3) (128), for those of the Ph_3P gold(I) complexes; 2.271(1) (122) and 2.292(3) (129), for those of the $(cyclohexyl)_3P$ gold(I) complexes; 2.259(3) (55), 2.268(6) - 2.279(6) (130), 2.248(2) (131), and 2.249(5) - 2.255(5) (132) for those of the Et_3P gold(I) complexes; and 2.214(4) - 2.220(1) (133) for those of the $(2\text{-pyridyl})_3P$ gold(I) complex. The value found in the TMIPAuCl complex is most similar to those of the last example. The Au-Cl bond distance (Å) of 2.268(2) found in this complex is similar to those of Ph_3PAuCl 2.279(3) (128), Cl_3PAuCl 2.279(2) (134), $(2\text{-pyridyl})_3PAuCl$ 2.272(5) - 2.277(5) (133), and $Ph_3PSAuCl$ 2.265(2)

Table 5.4.1 Crystal data of TMIPAuCl

Formula	$C_{12}H_{15}N_6PClAu$
Formula weight	506.7
Crystal colour, shape, size (mm)	colourless needle, 0.32x0.35x0.48
Space group, λ (Å)	$P2_1/n$, 0.56086
Unit cell parameters (Å and °)	a = 7.790(2) b = 18.874(3) c = 11.408(2) β = 91.97(2)
Volume (Å^3)	1676.3(8)
Z	4
ρ_{cal}, ρ_{obs} (Mg m^{-3})	2.008, 2.02(2)
Max. 2θ, indices range	45°, $0 \le h \le 10$, $0 \le k \le 25$, $-15 \le l \le 15$
Temperature, °C	23
Absorption coefficient mm^{-1}	9.032
Absorption correction factors, range	0.565 - 1.297
Number of variables	190
Standards	4 0 0, 0 8 0, 0 0 4
Correction factors for standard, range	0.9725 - 1.0138
Number of reflections measured	4797
Number of independent reflections, used	4490
R_{int}	0.0249
Final R, R_w	0.0698, 0.0367
Final Δ/σ, max., ave	0.001, 0.000
Final difference map, max., min., e A^{-3}	1.49, -1.63
Weighting	$(\sigma_F^2)^{-1}$
Goodness of fit, S	1.89
F(000)	960

Table 5.4.2 Atomic coordinates ($x10^4$) and equivalent isotropic displacement coefficients ($Å^2x10^3$) of TMIPAuCl

	x		y		z		U(eq)	
Au(1)	116	(1)	2076	(1)	3607	(1)	48	(1)
N(33)	-311	(7)	4270	(3)	2199	(5)	54	(2)
P	1351	(2)	3101	(1)	3201	(1)	39	(1)
Cl	-1091	(3)	1016	(1)	4023	(2)	91	(1)
C(21)	3459	(7)	2970	(3)	2704	(5)	39	(2)
N(11)	4539	(7)	3455	(3)	2269	(5)	50	(2)
C(11)	4313	(9)	4216	(3)	2206	(7)	71	(3)
N(13)	80	(6)	3391	(3)	949	(5)	45	(2)
N(31)	4094	(7)	2313	(3)	2633	(5)	51	(2)
N(12)	279	(10)	3950	(3)	5067	(5)	68	(3)
C(23)	325	(7)	3620	(3)	2066	(5)	39	(2)
C(22)	1616	(9)	3695	(3)	4416	(5)	48	(2)
N(32)	3131	(8)	3893	(3)	4824	(5)	68	(2)
C(51)	5948	(9)	3095	(4)	1941	(6)	64	(3)
C(53)	-699	(9)	3929	(4)	335	(7)	64	(3)
C(13)	620	(10)	2713	(4)	486	(6)	67	(3)
C(41)	5685	(9)	2413	(4)	2152	(7)	64	(3)
C(43)	-932	(9)	4453	(4)	1116	(8)	67	(3)
C(12)	-1587	(11)	3824	(4)	4865	(8)	93	(4)
C(52)	1138	(16)	4335	(4)	5950	(8)	100	(5)
C(42)	2829	(15)	4295	(5)	5816	(8)	97	(5)

Equivalent isotropic U defined as one third of the trace of the orthogonalized U_{ij} tensor.

Table 5.4.3 Selected Bond lengths (Å) and angles (°) of TMIPAuCl

Au(1)-P	2.216	(2)	Au(1)-Cl	2.268	(2)
N(33)-C(23)	1.333	(8)	N(33)-C(43)	1.36	(1)
P-C(21)	1.772	(6)	P-C(23)	1.791	(6)
P-C(22)	1.790	(6)	C(21)-N(11)	1.351	(8)
C(21)-N(31)	1.338	(8)	N(11)-C(11)	1.448	(9)
N(11)-C(51)	1.354	(9)	N(13)-C(23)	1.353	(8)
N(13)-C(53)	1.363	(9)	N(13)-C(13)	1.454	(9)
N(31)-C(41)	1.385	(9)	N(12)-C(22)	1.39	(1)
N(12)-C(12)	1.48	(1)	N(12)-C(52)	1.39	(1)
C(22)-N(32)	1.309	(9)	N(32)-C(42)	1.39	(1)
C(51)-C(41)	1.33	(1)	C(53)-C(43)	1.35	(1)
C(52)-C(42)	1.33	(2)			

P-Au(1)-Cl	178.8	(1)	C(23)-N(33)-C(43)	104.7	(6)
Au(1)-P-C(21)	111.0	(2)	Au(1)-P-C(23)	116.3	(2)
C(21)-P-C(23)	103.9	(3)	Au(1)-P-C(22)	115.1	(2)
C(21)-P-C(22)	104.6	(3)	C(23)-P-C(22)	104.7	(3)
P-C(21)-N(11)	128.2	(5)	P-C(21)-N(31)	119.8	(4)
N(11)-C(21)-N(31)	111.7	(5)	C(21)-N(11)-C(11)	128.0	(6)
C(21)-N(11)-C(51)	106.4	(6)	C(11)-N(11)-C(51)	125.6	(6)
C(23)-N(13)-C(53)	107.0	(5)	C(23)-N(13)-C(13)	126.2	(5)
C(53)-N(13)-C(13)	126.8	(6)	C(21)-N(31)-C(41)	103.6	(5)
C(22)-N(12)-C(12)	127.7	(6)	C(22)-N(12)-C(52)	102.6	(7)
C(12)-N(12)-C(52)	129.8	(8)	N(33)-C(23)-P	125.4	(5)
N(33)-C(23)-N(13)	111.1	(5)	P-C(23)-N(13)	123.4	(4)
P-C(22)-N(12)	124.4	(5)	P-C(22)-N(32)	122.2	(5)
N(12)-C(22)-N(32)	113.3	(6)	C(22)-N(32)-C(42)	105.7	(7)
N(11)-C(51)-C(41)	107.8	(6)	N(13)-C(53)-C(43)	106.0	(6)
N(31)-C(41)-C(51)	110.5	(6)	N(33)-C(43)-C(53)	111.2	(6)
N(12)-C(52)-C(42)	109.9	(8)	N(32)-C(42)-C(52)	108.6	(8)

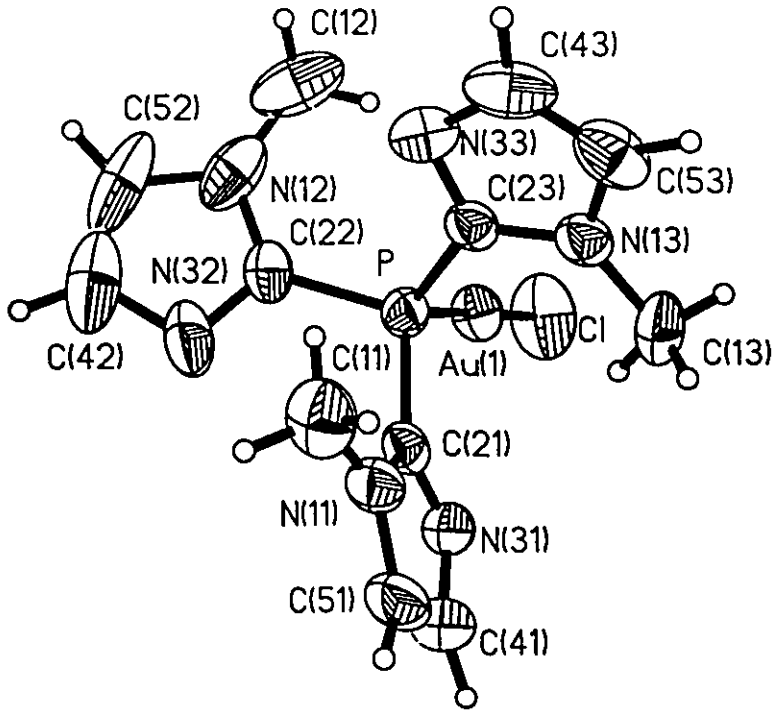

Figure 5.4.1 The molecule of TMIPAuCl

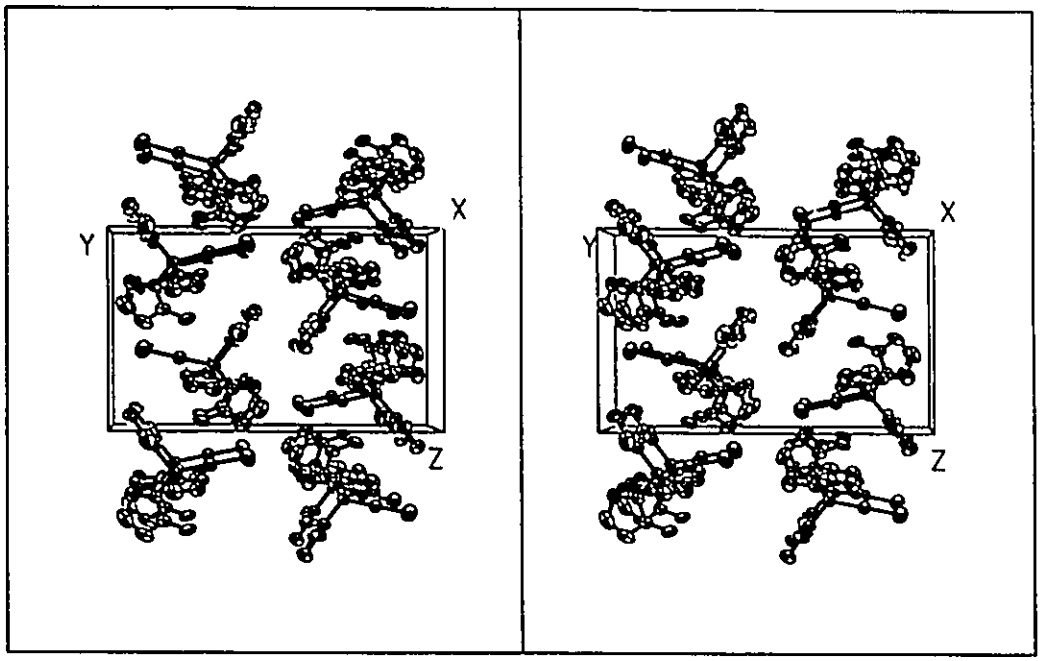

Figure 5.4.2 A stereoview of the packing of TEMIPAuCl in a unit cell

(134).

The average P-C bond distance 1.78(1)Å is shorter than those of TIP 1.811(7)Å (85) and TEMIP 1.82(1)Å. This value is also shorter than those of other gold(I) phosphine complexes, such as: 1.81(1) - 1.82(1)Å for the Ph_3P gold(I) complexes (94, 124, 125), 1.844(7)Å for the $(cyclohexyl)_3P$ gold(I) complex (122), and 1.82(2) - 1.83(5)Å for the Et_3P gold(I) complexes (55, 130). The shortening of the P-C bond distance probably accounts for the large absolute $^1J_{P\text{-}C}$ value observed in ^{13}C NMR spectra of this complex. The mean P-C distance is even shorter than that of $[(TMIP)_2Ni](AuI_2)_2$ 1.81(1)Å, in which the ligand is bonded to the nickel(II) atom through its nitrogen donor sites. No structure of the free ligand has been done to provide more information. The phosphine gold(I) complexes mentioned above having the mean P-C bond distances from 1.81(3) - 1.844(7)Å (94, 122, 124 - 126).

The imidazole rings in the molecule are essentially planer. Displacements of the ring atoms from least-square planes range from -0.027(6) to 0.036(7)Å. Substitution groups on the ring are almost coplanar with the ring. Displacements range from -0.067(19) to 0.036(15)Å for the methyl groups and -0.125(15) to -0.004(14)Å for the phosphorus atom. The molecule is packed in such a fashion that two of the three imidazole rings are oriented with their methyl groups pointing towards the phosphorus atom, while the other ring with its methyl group pointing away from the phosphorus atom. This is similar to the free ligand

TEMIP, but different from that of the free ligand TDMIP-5, which has all the methyl groups on the imidazole nitrogen atoms oriented in the same direction, pointing towards the phosphorus atom. Such a difference could be caused by packing, hydrogen bonding and steric reasons.

5.5 The Structure of $[(TMIP)_2Ni](AuI_2)_2$

The crystal density was measured by suspension in $CCl_4/CHBr_3$. The crystal for X-ray diffraction experiment was mounted by gluing to the end of a glass fibre. Unit cell determination and intensity data collection were performed on a Siemens P4 diffractometer with monchromatized Mo Kα radiation. Unit cell parameters were refined by least-squares fit of angular parameters for 32 reflections ($9.80 \leq 2\theta \leq 25.00°$). Intensities were measured with a θ(crystal) - 2θ(counter) scan. Three standards were measured every 100 reflections. No signs of crystal decay or instrumental instability were observed during data collection. An absorption correction was made by use of the empirical ψ-scan method (80). The structure was solved by the Patterson method and refined by the method of least-squares, which minimized $\Sigma w(|F_o| - |F_c|)^2$. Hydrogen atoms were placed in calculated positions and not refined. Temperature factors of non-hydrogen atoms were refined anisotropically, and those of hydrogen atoms were not refined. Details of crystal data and the structure solution are listed in **Table 5.5.1.** Atomic positional parameters are given in **Table 5.5.2.** Selected interatomic distances and angles are given in **Table 5.5.3.** The molecule and packing diagrams

Table 5.5.1 Crystal data of $[(TMIP)_2Ni](AuI_2)_2$

Formula	$C_{24}H_{36}N_{12}P_2I_4Au_2Ni$
Formula weight	1508.8
Crystal colour, shape, size (mm)	yellow needle, 0.15x0.17x0.28
Space group, λ (Å)	$P2_1/n$, 0.71073
Unit cell parameters (Å and °)	a = 11.398(1) b = 14.165(1) c = 12.364(1) β = 97.06(1)
Volume (Å^3)	1981.0(4)
Z	2
ρ_{cal}, ρ_{obs} (Mg m^{-3})	2.529, 2.54(2)
Max. 2θ, indices range	56.6°, -1 ≤ h ≤ 15, -1 ≤ k ≤ 18, -16 ≤ l ≤ 16
Temperature, °C	23
Absorption coefficient mm^{-1}	11.089
Transmission factors, range	0.056 - 0.094
Number of variables	205
Standards	0 -3 7, -5 -5 -2, -3 7 3
Correction factors for standard, range	0.9523 - 1.0438
Number of reflections measured	6122
Number of independent reflections, used	4888
R_{int}	0.0256
Final R, R_w	0.0708, 0.0324
Final Δ/σ, max., ave	0.000, 0.000
Final difference map, max., min., e A^{-3}	1.05, -1.77
Weighting	$(\sigma_F^2)^{-1}$
Goodness of fit, S	2.03
F(000)	1372

Table 5.5.2 Atomic coordinates ($x10^4$) and equivalent isotropic displacement coefficients ($Å^2x10^3$) of $[(TMIP)_2Ni](AuI_2)_2$

	x		y		z		U(eq)	
Au	1988	(1)	1017	(1)	4809	(1)	68	(1)
I(1)	1947	(1)	312	(1)	2907	(1)	72	(1)
Ni	5000		0		10000		35	(1)
I(2)	2076	(1)	1749	(1)	6701	(1)	84	(1)
P	4412	(2)	-601	(1)	7251	(1)	38	(1)
N(13)	5379	(5)	1210	(4)	6973	(4)	41	(2)
C(53)	5840	(6)	1958	(4)	7593	(5)	47	(2)
N(32)	5669	(4)	-1158	(3)	9229	(4)	39	(2)
C(23)	5080	(5)	522	(4)	7657	(5)	36	(2)
N(12)	5852	(5)	-2168	(3)	7902	(4)	39	(2)
C(21)	3211	(5)	-546	(4)	8060	(5)	40	(2)
N(31)	3346	(4)	-323	(4)	9130	(4)	40	(2)
C(52)	6474	(6)	-2517	(5)	8843	(5)	50	(3)
C(22)	5360	(5)	-1352	(4)	8176	(5)	37	(2)
C(3)	5274	(7)	1178	(5)	5799	(5)	55	(3)
N(11)	2063	(5)	-740	(4)	7733	(5)	48	(2)
C(42)	6371	(6)	-1889	(5)	9638	(6)	49	(2)
C(43)	5801	(6)	1705	(5)	8639	(6)	48	(2)
C(2)	5702	(7)	-2621	(5)	6849	(5)	61	(3)
C(41)	2241	(6)	-356	(5)	9455	(6)	56	(3)
C(51)	1456	(6)	-604	(5)	8622	(6)	57	(3)
N(33)	5333	(4)	809	(3)	8682	(4)	38	(2)
C(1)	1564	(6)	-1055	(5)	6650	(5)	59	(3)

Equivalent isotropic U defined as one third of the trace of the orthogonalized U_{ij} tensor.

Table 5.5.3 Selected bond lengths (Å) and angles (°) of $[(TMIP)_2Ni](AuI_2)_2$

Au-I(1)	2.550	(1)	Au-I(2)	2.549	(1)
Ni-N(32)	2.088	(5)	Ni-N(31)	2.103	(5)
Ni-N(33)	2.066	(5)	Ni-N(32A)	2.088	(5)
Ni-N(31A)	2.103	(5)	Ni-N(33A)	2.066	(5)
P-C(23)	1.808	(6)	P-C(21)	1.795	(7)
P-C(22)	1.817	(6)	N(13)-C(53)	1.375	(8)
N(13)-C(23)	1.360	(8)	N(13)-C(3)	1.442	(8)
C(53)-C(43)	1.35	(1)	N(32)-C(22)	1.334	(8)
N(32)-C(42)	1.366	(8)	C(23)-N(33)	1.328	(8)
N(12)-C(52)	1.378	(8)	N(12)-C(22)	1.346	(8)
N(12)-C(2)	1.443	(8)	C(21)-N(31)	1.350	(8)
C(21)-N(11)	1.350	(8)	N(31)-C(41)	1.369	(9)
C(52)-C(42)	1.34	(1)	N(11)-C(51)	1.38	(1)
N(11)-C(1)	1.459	(8)	C(43)-N(33)	1.379	(8)
C(41)-C(51)	1.33	(1)			

I(1)-Au-I(2)	178.4	(1)	N(32)-Ni-N(31)	87.1	(2)
N(32)-Ni-N(33)	87.9	(2)	N(31)-Ni-N(33)	87.5	(2)
N(32)-Ni-N(32A)	180.0	(1)	N(31)-Ni-N(32A)	92.9	(2)
N(33)-Ni-N(32A)	92.1	(2)	N(32)-Ni-N(31A)	92.9	(2)
N(31)-Ni-N(31A)	180.0	(1)	N(33)-Ni-N(31A)	92.5	(2)
N(32A)-Ni-N(31A)	87.1	(2)	N(32)-Ni-N(33A)	92.1	(2)
N(31)-Ni-N(33A)	92.5	(2)	N(33)-Ni-N(33A)	180.0	(1)
N(32A)-Ni-N(33A)	87.9	(2)	N(31A)-Ni-N(33A)	87.5	(2)
C(23)-P-C(21)	97.5	(3)	C(23)-P-C(22)	98.2	(3)
C(21)-P-C(22)	96.3	(3)	C(53)-N(13)-C(23)	108.3	(5)
C(53)-N(13)-C(3)	124.3	(5)	C(23)-N(13)-C(3)	127.4	(5)
N(13)-C(53)-C(43)	105.9	(6)	Ni-N(32)-C(22)	122.6	(4)
Ni-N(32)-C(42)	131.0	(4)	C(22)-N(32)-C(42)	106.1	(5)
P-C(23)-N(13)	125.9	(4)	P-C(23)-N(33)	124.7	(5)
N(13)-C(23)-N(33)	109.4	(5)	C(52)-N(12)-C(22)	106.5	(5)
C(52)-N(12)-C(2)	126.4	(5)	C(22)-N(12)-C(2)	127.0	(5)
P-C(21)-N(31)	123.6	(5)	P-C(21)-N(11)	127.1	(5)
N(31)-C(21)-N(11)	109.3	(6)	Ni-N(31)-C(21)	122.7	(4)
Ni-N(31)-C(41)	131.0	(4)	C(21)-N(31)-C(41)	106.3	(5)
N(12)-C(52)-C(42)	107.3	(6)	P-C(22)-N(32)	124.0	(5)
P-C(22)-N(12)	125.3	(5)	N(32)-C(22)-N(12)	110.7	(5)
C(21)-N(11)-C(51)	107.1	(5)	C(21)-N(11)-C(1)	126.3	(6)
C(51)-N(11)-C(1)	126.6	(6)	N(32)-C(42)-C(52)	109.4	(6)
C(53)-C(43)-N(33)	109.9	(6)	N(31)-C(41)-C(51)	109.8	(6)
N(11)-C(51)-C(41)	107.4	(6)	Ni-N(33)-C(23)	122.9	(4)
Ni-N(33)-C(43)	130.5	(4)	C(23)-N(33)-C(43)	106.5	(5)

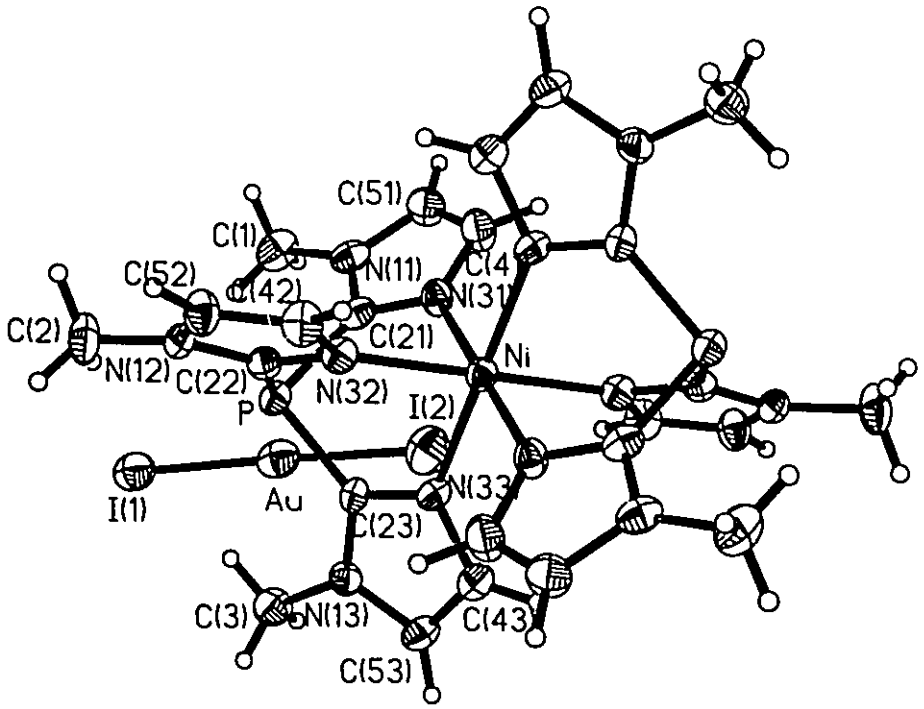

Figure 5.5.1 The molecule of $[(TMIP)_2Ni](AuI_2)_2$

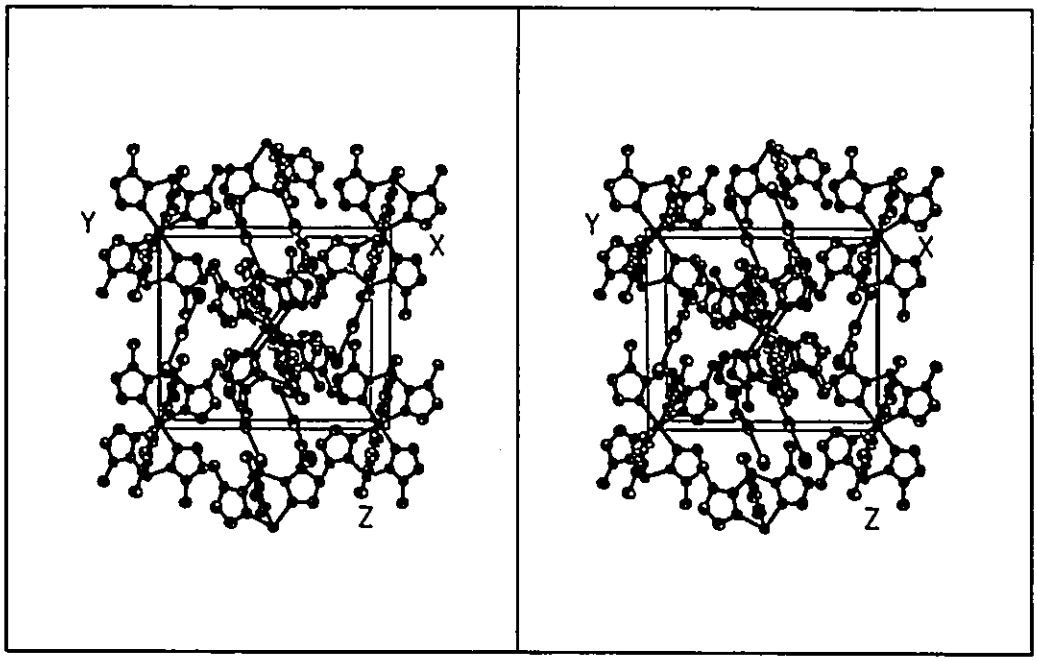

Figure 5.5.2 A stereoview of the packing of $[(TMIP)_2Ni](AuI_2)_2$ in a unit cell

are given in **Figure 5.5.1** and **Figure 5.5.2**.

The ligand forms a bis-complex with the nickel atom. The phosphorus atom on the ligand is non-coordinating. The original nitrate anions are replaced by the bigger AuI_2^- anions. Such a complex is highly insoluble and crystallized from the reaction mixture.

The AuI_2^- anion is normal as compared to those found in the literature, with Au-I bond lengths of 2.484(4) - 2.619(2)Å and I-Au-I bond angles from 175.4(3)° to straight linear (135).

The coordination geometry around the nickel atom is essentially regular octahedral, with similar M-N bond lengths and N-M-N' bond angles close to 90 and 180°. The N-Ni bond lengths 2.066(5) - 2.103(5)Å are shorter than those of the $[(imidazole)_6Ni]^{2+}$ complexes 2.128(4) - 2.140(2)Å (104, 105), but similar to those of the low temperature form of $[(TIP)_2Ni]^{2+}$ complex 2.096(5) - 2.109(5)Å discussed in **Chapter 4**.

The imidazole rings in the molecule are all planar. Displacements of the ring atoms from the least-square planes ranging from -0.010(4) to 0.010(4)Å. The methyl groups on the ring nitrogen atoms and the phosphorus atom are nearly coplanar with the rings, with displacements range from -0.03(1)Å to 0.07(1)Å. The coordination of the ring nitrogen atoms restricts the methyl groups to orient in the same direction, all pointing towards the phosphorus atom.

5.6 The Infrared Spectra of the TMIP Complexes

Table 5.6 Major infrared frequencies of TMIPAuCl and $[(TMIP)_2Ni](AuI_2)_2$

TMIPAuCl	$[(TMIP)_2Ni](AuI_2)_2$	Assignments
3600-3300s,br	3600-3300s,br	-
3122m,sh		νC-H
3114m,sh	3112m	
3104s	3102m	
1630m,br	1610w,br	-
	1650w,br	-
1500m	1515m	νring
1450vs	1468vs	νP-C
1410m	1407m	-
1353s	1341m	γC-H
1342s		
1332s		
1280vs	1285vs	δC-H
1164w	1159m	δC-H
1122w	1140m	
1075w	1076w	
914s	941m	δring
775vs	755sh	δP-C
767vs	750vs	
690s	691s	γC-H
674s		
622w	610w	-
547vs	513m	γP-C
533vs	480vs	γP-C
465-410w	434w	-
	421w	
334w		-

Bands in cm^{-1}, s=strong, m=medium, w=weak, br=broad, sh=shoulder, v=very, ν=stretching, δ=deformation, γ=bending.

Major infrared frequencies of TMIPAuCl and $[(TMIP)_2Ni](AuI_2)_2$ are listed in **Table 5.6**. Tentative assignments were made in accord with references 84, 86, 96, and 97. The obvious difference of the spectra from that of $[(TIP)_2M](NO_3)_2$ is the absence of the very strong and broad ring N-H stretching and the very strong nitrate N-O stretching bands.

Chapter 6

Metal Complexes with Tris[2-ethyl-4(5)-methylimidazol-5(4)-yl]phosphine (TEMIP)

6.1 Introduction

In this chapter, metal complexes with TEMIP will be discussed. Unlike the ligands TIP and TMIP, this ligand readily forms complexes with both soft and hard metal ions. The P-C bond is more stable towards nucleophilic attack by the solvent molecules, so reactions can be carried out in polar solvents. The ethyl group on the ring C2 carbon atom is not bulky enough to prevent the formation of the thermodynamically more favourable bis-ligand metal complexes with relatively hard transition metal ions. The structure of two complexes, $[(TEMIP)_2Cu](NO_3)_2$ and $[(TEMIPAuCl)_2Cu](NO_3)_2{\cdot}2H_2O$ have been characterized by X-ray diffraction and are discussed in this chapter. Like the $[(TIP)_2Cu](NO_3)_2$ complex, the $[(TEMIP)_2Cu](NO_3)_2$ complex does not exhibit any distortion at room temperature and it was assumed that this is another example of the dynamic Jahn-Teller effect in the coordination of the Cu(II) atom. The complex $[(TEMIPAu)_2Cu](NO_3)_2{\cdot}2H_2O$ does show a static Jahn-Teller distortion at room temperature. Possible explanations of these observations are discussed.

6.2 Preparations

Bis[tris(2-ethyl-5-methylimidazol-4-yl)phosphine-N^3,$N^{3'}$,$N^{3''}$]copper(II)

dinitrate {[(TEMIP)$_2$Cu](NO$_3$)$_2$}: A solution of Cu(NO$_3$)$_2$·3H$_2$O (0.034g) in a 1:1 methanol/water mixture (5mL) was added to a solution of TEMIP (0.1g) in a 1:1 methanol/water mixture (5mL). A blue precipitate formed immediately after mixing, and was separated by filtration, washed with water (2mL), methanol (2mL) and acetone (5mL) and air dried. Yield 0.1g (79%), m.p. 274-275°C (decompose). Crystals suitable for X-ray diffraction were prepared through the low temperature dilution method described in **Chapter 2**, where the solutions were made three times more dilute than that described above.

Bis{chloro[tris(2-ethyl-5-methylimidazol-4-yl)phosphine-P]gold(I)-N^3,$N^{3'}$,$N^{3''}$}copper(II) dinitrate dihydrate {[(TEMIPAuCl)$_2$Cu](NO$_3$)$_2$·2H$_2$O}: Solid Me$_2$SAuCl (0.082g) was dissolved in a solution of TEMIP (0.1g) in methanol (2mL). The solution was evaporated to dryness at room temperature under nitrogen and redissolved in a 1:1 methanol/water mixture (5mL). To this solution, a solution of Cu(NO$_3$)$_2$·3H$_3$O (0.034g) in a 1:1 methanol/water mixture was added. A blue precipitate formed immediately after mixing, and was separated by filtration, washed with water (2mL), methanol (2mL) and acetone (5mL) and air dried. Yield 0.11g (56%), m.p. 277-278°C (decompose). Crystals suitable for X-ray diffraction were prepared through the low temperature dilution method mentioned in **Chapter 2**, where the solutions were made three times more dilute than that described above.

6.3 The Structures of [(TEMIP)$_2$Cu](NO$_3$)$_2$ and [(TEMIP)$_2$Cu](NO$_3$)$_2$·2H$_2$O

The crystal densities were measured by suspension in hexane/CCl_4 for $[(TEMIP)_2Cu](NO_3)_2$ and $CCl_4/CHBr_3$ for $[(TEMIP)_2Cu](NO_3)_2 \cdot 2H_2O$ respectively. Crystals for X-ray diffraction experiments were mounted by gluing to the end of glass fibres. Unit cell determination and intensity data collection were performed on a Siemens P4 diffractometer with monochromatized Mo Kα radiation. For the $[(TEMIP)_2Cu](NO_3)_2$ complex, unit cell parameters were refined by least-squares fit of angular parameters for 59 reflections ($9.94 \leq 2\theta \leq 24.95°$) and intensities were measured with an ω scan. Two standards were measured every 100 reflections. For the $[(TEMIPAuCl)_2Cu](NO_3)_2 \cdot 2H_2O$ complex, unit cell parameters were refined by least-squares fit of angular parameters of 45 reflections ($8.34 \leq 2\theta \leq 24.87°$) and intensities were measured with a θ(crystal) - 2θ(counter) scan. Three standards were measured every 100 reflections. For both complexes, no signs of crystal decay or instrumental instability were observed during data collection. Absorption corrections were made with DIFABS (81). Structures were solved by the Patterson method and refined by the method of least-squares, which minimized $\Sigma w(|F_o| - |F_c|)^2$. Hydrogen atoms were placed in calculated positions and not refined. Temperature factors of non-hydrogen atoms were refined anisotropically, and those of hydrogen atoms were given fixed values of $0.08Å^2$ each and were not refined. Details of crystal data collection and the structure solution are listed in **Table 6.3.1**. Atomic positional parameters are given in **Table 6.3.2**. Selected interatomic distances and angles are given in **Table 6.3.3**. The cation

and molecular packing diagrams are given in **Figure 6.3.1**, **Figure 6.3.2** and **Figure 6.3.3**, **Figure 6.3.4** for $[(TEMIP)_2Cu](NO_3)_2$ and $[(TEMIPAuCl)_2Cu](NO_3)_2{\cdot}2H_2O$ respectively.

In the $[(TEMIP)_2Cu](NO_3)_2$ complex, the copper atom is located at a special position with one unique N-Cu bond. The other five N-Cu bonds are generated by symmetry operations. This means that the copper atom is bonded to six nitrogen atoms with identical bond distances. The six symmetry equivalent N-Cu bond distances of 2.160(6)Å in $[(TEMIP)_2Cu](NO_3)_2$ are not significantly different from those of $[(TIP)_2Cu](NO_3)_2$ [2.133(6) - 2.153(5)Å] mentioned in **Chapter 4**. Like the TIP complex, this complex can be considered as another example of the dynamic Jahn-Teller effect. The P-C bond distances in this complex [1.796(8)Å] are similar to those of the TIP complex [1.795(7) - 1.811(6)Å] and those of TMIP complexes [mean values 1.78(1) and 1.81(1)Å] mentioned in **Chapter 5**. The imidazole rings are essentially planar. Distances between the oxygen atoms of the nitrate and the nitrogen atoms of the imidazole ring are all longer than 3Å, indicating no or very weak hydrogen bonding. The methyl carbon atom of the ethyl group is disordered. The site of occupancies of the two disordered sites were found to be 0.73 and 0.27, by fixing the temperature factors of the disordered carbon atoms at $0.1Å^2$ while refining the occupancies. These partial occupancy values were fixed for subsequent refinements. The disorder of the ethyl group is probably an indication of lack of steric hindrance of the ethyl

Table 6.3.1 Crystal data of $[(TEMIP)_2Cu](NO_3)_2$ and $[(TEMIPAuCl)_2Cu](NO_3)_2 \cdot 2H_2O$

	$[(TEMIP)_2Cu](NO_3)_2$	$[(TEMIPAuCl)_2Cu](NO_3)_3 \cdot 2H_2O$
Formula	$C_{36}H_{54}N_{14}O_6P_2Cu$	$C_{36}H_{58}N_{14}O_8P_2Cl_2Au_2Cu$
Formula weight	904.4	1405.2
Crystal colour, shape, size (mm)	blue plate, 0.05x0.15x0.25	blue needle, 0.10x0.15x0.30
Space group, λ (Å)	R-3c, 0.71073	$P2_1/c$, 0.71073
Unit cell parameters (Å and °)	a = 12.578(1) c = 49.355(6)	a = 11.057(1) b = 11.805(1) c = 19.587(2) β = 101.92(1)
Volume ($Å^3$)	6762(2)	2501.5(5)
Z	6	2
ρ_{cal}, ρ_{obs} (Mg m^{-3})	1.333, 1.34(2)	1.860, 1.85(2)
Max. 2θ, indices range	45°, -1 ≤ h ≤ 13, -13 ≤ k ≤ 1, -1 ≤ l ≤ 52	55.7°, -1 ≤ h ≤ 14, -1 ≤ k ≤ 15, -25 ≤ l ≤ 25
Temperature, °C	23	23
Absorption coefficient mm^{-1}	0.614	6.503
Absorption correction factors, range	0.905 - 1.158	0.513 - 1.597
Number of variables	89	290
Standard reflections (e.s.d.)	6 0 0 (0.000), -1 2 0 (0.009)	2 0 0, 0 4 0, 0 0 6
Correction factors for standard, range		0.9048 - 1.0114
Number of reflections measured	2287	7507
Number of independent reflections, used	988	5947
R_{int}	0.0214	0.0709
Final R, R_w	0.0918, 0.0471	0.0860, 0.0529
Final Δ/σ, max., ave	0.010, 0.003	0.048, 0.004
Final difference map, max., min., e A^{-3}	0.38, -0.36	2.15, -3.19

Table 6.3.1 (continued)

	$[(TEMIP)_2Cu](NO_3)_2$	$[(TEMIPAuCl)_2Cu](NO_3)_2 \cdot 2H_2O$
Weighting	$(\sigma_F^2)^{-1}$	$(\sigma_F^2)^{-1}$
Goodness of fit, S	2.67	1.62
F(000)	2850	1374

Table 6.3.2 Atomic coordinates ($x10^4$) and equivalent isotropic displacement coefficients ($Å^2x10^3$) of $[(TEMIP)_2Cu](NO_3)_2$ and $[(TEMIPAuCl)_2Cu](NO_3)_2 \cdot 2H_2O$

$[(TEMIP)_2Cu](NO_3)_2$:

	x	y	z	U(eq)
Cu	6667	3333	833	57 (1)
P	6667	3333	129 (1)	48 (1)
N(1)	8156 (5)	1430 (4)	391 (1)	85 (3)
C(5)	7701 (5)	1805 (5)	185 (1)	70 (4)
C(4)	7299 (5)	2508 (5)	297 (1)	53 (3)
C(2)	8015 (7)	1882 (7)	624 (1)	86 (4)
N(3)	7465 (5)	2528 (5)	576 (1)	73 (3)
C(51)	7723 (7)	1454 (7)	-95 (1)	139 (7)
C(21)	8450 (8)	1714 (6)	888 (2)	142 (6)
N	0	0	349 (2)	65 (2)
O	502 (4)	-615 (4)	350 (1)	104 (3)
C(22)*	8379 (9)	561 (7)	955 (2)	116 (3)
C(23)*	9513 (17)	1527 (25)	941 (5)	116 (3)

$[(TEMIPAuCl)_2Cu](NO_3)_2 \cdot 2H_2O$:

	x	y	z	U(eq)
Au	2856 (1)	979 (1)	708 (1)	54 (1)
Cu	5000	5000	0	47 (1)
P	3684 (2)	2595 (1)	455 (1)	44 (1)
Cl	2018 (3)	-668 (2)	980 (1)	90 (1)
N(11)	7220 (6)	2061 (5)	484 (3)	54 (2)
C(42)	3025 (7)	3169 (5)	-404 (4)	48 (2)
C(41)	5296 (6)	2526 (5)	434 (3)	43 (2)
C(51)	6117 (7)	1667 (6)	614 (3)	51 (2)
C(21)	7058 (8)	3145 (7)	255 (4)	63 (3)
C(51')	6001 (8)	488 (6)	869 (4)	63 (3)
N(32)	3505 (5)	4161 (5)	-615 (3)	51 (2)
N(31)	5887 (6)	3446 (5)	214 (3)	55 (2)
O(3)	-13 (7)	6505 (6)	2633 (3)	99 (3)
N	869 (8)	6152 (8)	2415 (4)	83 (3)
N(33)	4148 (6)	4753 (5)	985 (3)	59 (2)

Table 6.3.2 (continued)

O	493 (7)	5966 (5)	4063 (4)	98 (2)
N(12)	1960 (6)	3566 (5)	-1422 (3)	59 (2)
O(2)	1799 (8)	5768 (7)	2799 (4)	116 (4)
C(43)	3554 (7)	3729 (5)	1035 (4)	50 (3)
C(52)	2038 (7)	2793 (6)	-900 (4)	56 (3)
N(13)	3153 (7)	4872 (5)	1820 (3)	64 (3)
C(53)	2933 (8)	3806 (6)	1558 (4)	57 (3)
C(52')	1195 (8)	1800 (7)	-944 (5)	76 (3)
C(22)	2820 (8)	4356 (7)	-1245 (4)	60 (3)
C(23)	3867 (8)	5419 (6)	1450 (4)	64 (3)
C(21')	8119 (9)	3805 (9)	61 (7)	108 (5)
C(23')	4235 (10)	6636 (7)	1570 (5)	85 (4)
C(22')	2961 (9)	5319 (7)	-1725 (5)	78 (4)
O(1)	855 (10)	6251 (10)	1790 (5)	182 (6)
C(53')	2123 (9)	3029 (8)	1868 (5)	93 (4)
C(23'')	4517 (12)	6990 (9)	2294 (6)	135 (7)
C(22'')	1858 (13)	5832 (9)	-2099 (6)	132 (6)
C(21'')	9237 (11)	3552 (11)	189 (10)	242 (14)

Equivalent isotropic U defined as one third of the trace of the orthogonalized U_{ij} tensor.

* A disordered carbon atom refined at these positions with partial occupancies of 0.73 and 0.27 respectively.

Table 6.3.3 Selected bond lengths (Å) and angles (°) of $[(TEMIP)_2Cu](NO_3)_2$ and $[(TEMIPAuCl)_2Cu](NO_3)_2 \cdot 2H_2O$

$[(TEMIP)_2Cu](NO_3)_2$:

Cu-N(3)	2.160	(6)	Cu-N(3A)	2.160	(5)
Cu-N(3B)	2.160	(5)	Cu-N(3C)	2.160	(6)
Cu-N(3D)	2.160	(5)	Cu-N(3E)	2.160	(5)
P-C(4)	1.796	(8)	P-C(4A)	1.796	(5)
P-C(4B)	1.796	(5)	N(1)-C(5)	1.362	(9)
N(1)-C(2)	1.335	(9)	C(5)-C(4)	1.34	(1)
C(5)-C(51)	1.457	(9)	C(4)-N(3)	1.388	(6)
C(2)-N(3)	1.33	(1)	C(2)-C(21)	1.47	(1)
C(21)-C(22)	1.45	(1)	C(21)-C(23)	1.49	(3)
N-O	1.219	(7)	N-OA	1.219	(5)
N-OB	1.219	(5)			
N(3)-Cu-N(3A)	88.9	(2)	N(3)-Cu-N(3B)	88.9	(2)
N(3A)-Cu-N(3B)	88.9	(2)	N(3)-Cu-N(3C)	179.8	(2)
N(3A)-Cu-N(3C)	91.3	(3)	N(3B)-Cu-N(3C)	90.9	(2)
N(3)-Cu-N(3D)	91.3	(3)	N(3A)-Cu-N(3D)	90.9	(2)
N(3B)-Cu-N(3D)	179.7	(2)	N(3C)-Cu-N(3D)	88.9	(2)
N(3)-Cu-N(3E)	90.9	(2)	N(3A)-Cu-N(3E)	179.8	(2)
N(3B)-Cu-N(3E)	91.3	(3)	N(3C)-Cu-N(3E)	88.9	(2)
N(3D)-Cu-N(3E)	88.9	(2)	C(4)-P-C(4A)	100.3	(2)
C(4)-P-C(4B)	100.3	(2)	C(4A)-P-C(4B)	100.3	(3)
C(5)-N(1)-C(2)	109.1	(7)	N(1)-C(5)-C(4)	106.4	(5)
N(1)-C(5)-C(51)	121.9	(7)	C(4)-C(5)-C(51)	131.6	(7)
P-C(4)-C(5)	127.8	(4)	P-C(4)-N(3)	123.6	(6)
C(5)-C(4)-N(3)	108.6	(6)	N(1)-C(2)-N(3)	109.1	(6)
N(1)-C(2)-C(21)	124.4	(9)	N(3)-C(2)-C(21)	126.4	(7)
Cu-N(3)-C(4)	119.4	(5)	Cu-N(3)-C(2)	133.5	(4)
C(4)-N(3)-C(2)	106.7	(6)	C(2)-C(21)-C(22)	120.4	(7)
C(2)-C(21)-C(23)	127	(1)	C(22)-C(21)-C(23)	54	(1)
O-N-OA	120.0	(1)	O-N-OB	120.0	(1)
OA-N-OB	120.0	(3)	C(21)-C(22)-C(23)	65	(1)
C(21)-C(23)-C(22)	61	(1)			

$[(TEMIPAuCl)_2Cu](NO_3)_2 \cdot 2H_2O$:

Au-P	2.216	(2)	Au-Cl	2.264	(2)
Cu-N(32)	2.084	(5)	Cu-N(31)	2.082	(6)
Cu-N(33)	2.333	(7)	Cu-N(32A)	2.084	(5)
Cu-N(31A)	2.082	(6)	Cu-N(33A)	2.333	(7)
P-C(42)	1.821	(7)	P-C(41)	1.793	(7)
P-C(43)	1.781	(7)	N(11)-C(51)	1.38	(1)
N(11)-C(21)	1.36	(1)	C(42)-N(32)	1.383	(9)

Table 6.3.3 (continued)

C(42)-C(52)	1.376	(9)	C(41)-C(51)	1.359	(9)
C(41)-N(31)	1.382	(9)	C(51)-C(51')	1.49	(1)
C(21)-N(31)	1.33	(1)	C(21)-C(21')	1.52	(1)
N(32)-C(22)	1.327	(9)	O(3)-N	1.22	(1)
N-O(2)	1.23	(1)	N-O(1)	1.23	(1)
N(33)-C(43)	1.389	(9)	N(33)-C(23)	1.29	(1)
N(12)-C(52)	1.36	(1)	N(12)-C(22)	1.33	(1)
C(43)-C(53)	1.35	(1)	C(52)-C(52')	1.49	(1)
N(13)-C(53)	1.362	(9)	N(13)-C(23)	1.34	(1)
C(53)-C(53')	1.50	(1)	C(22)-C(22')	1.50	(1)
C(23)-C(23')	1.50	(1)	C(21')-C(21'')	1.25	(2)
C(23')-C(23'')	1.50	(1)	C(22')-C(22'')	1.42	(2)
P-Au-Cl	179.4	(1)			
N(32)-Cu-N(31)	89.0	(2)	N(32)-Cu-N(33)	90.6	(2)
N(31)-Cu-N(33)	88.7	(2)	N(32)-Cu-N(32A)	180.0	(1)
N(31)-Cu-N(32A)	91.0	(2)	N(33)-Cu-N(32A)	89.4	(2)
N(32)-Cu-N(31A)	91.0	(2)	N(31)-Cu-N(31A)	180.0	(1)
N(33)-Cu-N(31A)	91.3	(2)	N(32A)-Cu-N(31A)	89.0	(2)
N(32)-Cu-N(33A)	89.4	(2)	N(31)-Cu-N(33A)	91.3	(2)
N(33)-Cu-N(33A)	180.0	(1)	N(32A)-Cu-N(33A)	90.6	(2)
N(31A)-Cu-N(33A)	88.7	(2)	Au-P-C(42)	115.0	(2)
Au-P-C(41)	115.1	(2)	C(42)-P-C(41)	101.9	(3)
Au-P-C(43)	114.4	(3)	C(42)-P-C(43)	103.9	(3)
C(41)-P-C(43)	105.1	(3)	C(51)-N(11)-C(21)	108.6	(6)
P-C(42)-N(32)	119.0	(5)	P-C(42)-C(52)	129.7	(6)
N(32)-C(42)-C(52)	111.1	(6)	P-C(41)-C(51)	130.0	(6)
P-C(41)-N(31)	120.6	(5)	C(51)-C(41)-N(31)	109.5	(6)
N(11)-C(51)-C(41)	105.6	(6)	N(11)-C(51)-C(51')	121.2	(6)
C(41)-C(51)-C(51')	133.1	(7)	N(11)-C(21)-N(31)	109.4	(7)
N(11)-C(21)-C(21')	120.7	(7)	N(31)-C(21)-C(21')	129.8	(7)
Cu-N(32)-C(42)	122.5	(4)	Cu-N(32)-C(22)	133.4	(5)
C(42)-N(32)-C(22)	104.1	(6)	Cu-N(31)-C(41)	121.4	(5)
Cu-N(31)-C(21)	131.4	(5)	C(41)-N(31)-C(21)	106.8	(6)
O(3)-N-O(2)	122.8	(9)	O(3)-N-O(1)	118.2	(9)
O(2)-N-O(1)	119	(1)	Cu-N(33)-C(43)	116.5	(5)
Cu-N(33)-C(23)	134.9	(5)	C(43)-N(33)-C(23)	107.1	(7)
C(52)-N(12)-C(22)	110.2	(6)	P-C(43)-N(33)	120.4	(6)
P-C(43)-C(53)	131.0	(6)	N(33)-C(43)-C(53)	108.6	(6)
C(42)-C(52)-N(12)	103.4	(6)	C(42)-C(52)-C(52')	133.7	(7)
N(12)-C(52)-C(52')	122.9	(6)	C(53)-N(13)-C(23)	108.7	(7)
C(43)-C(53)-N(13)	105.6	(7)	C(43)-C(53)-C(53')	135.1	(7)
N(13)-C(53)-C(53')	119.3	(8)	N(32)-C(22)-N(12)	111.2	(7)
N(32)-C(22)-C(22')	126.8	(7)	N(12)-C(22)-C(22')	122.0	(7)
N(33)-C(23)-N(13)	110.0	(7)	N(33)-C(23)-C(23')	126.8	(9)
N(13)-C(23)-C(23')	123.2	(8)	C(21)-C(21')-C(21'')	127	(1)
C(23)-C(23')-C(23'')	115.3	(8)	C(22)-C(22')-C(22'')	117.1	(9)

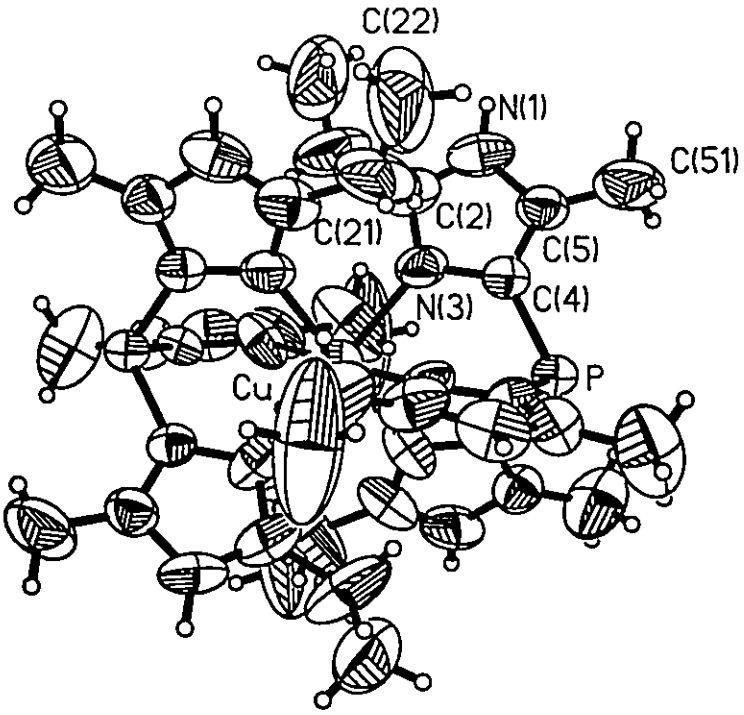

Figure 6.3.1 The cation of $[(TEMIP)_2Cu](NO_3)_2$

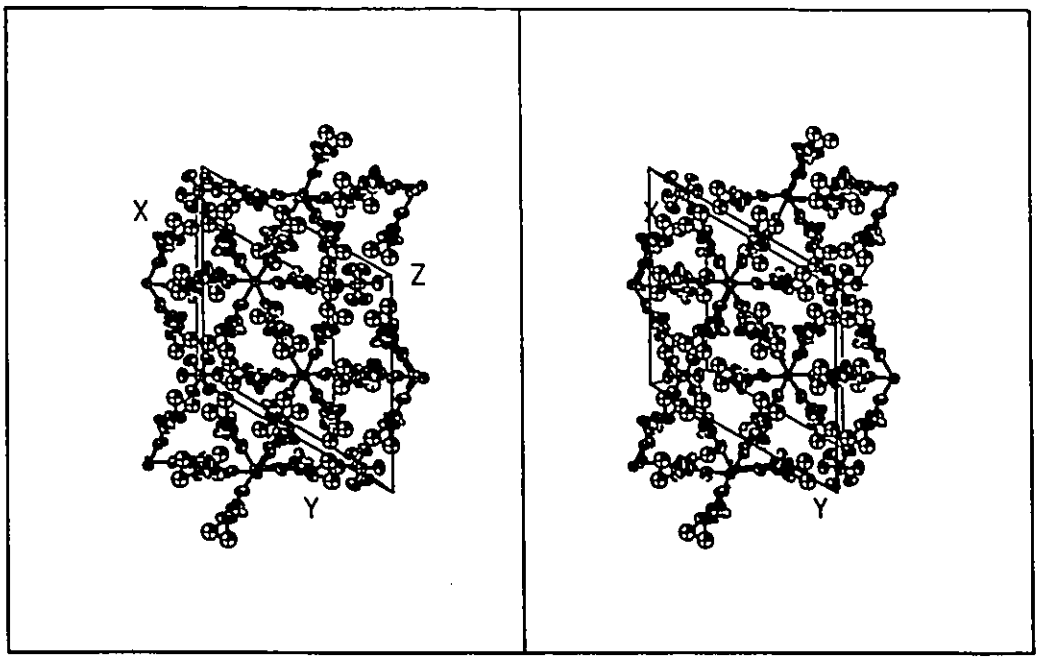

Figure 6.3.2 A stereoview of the packing of $[(TEMIP)_2Cu](NO_3)_2$ in a unit cell

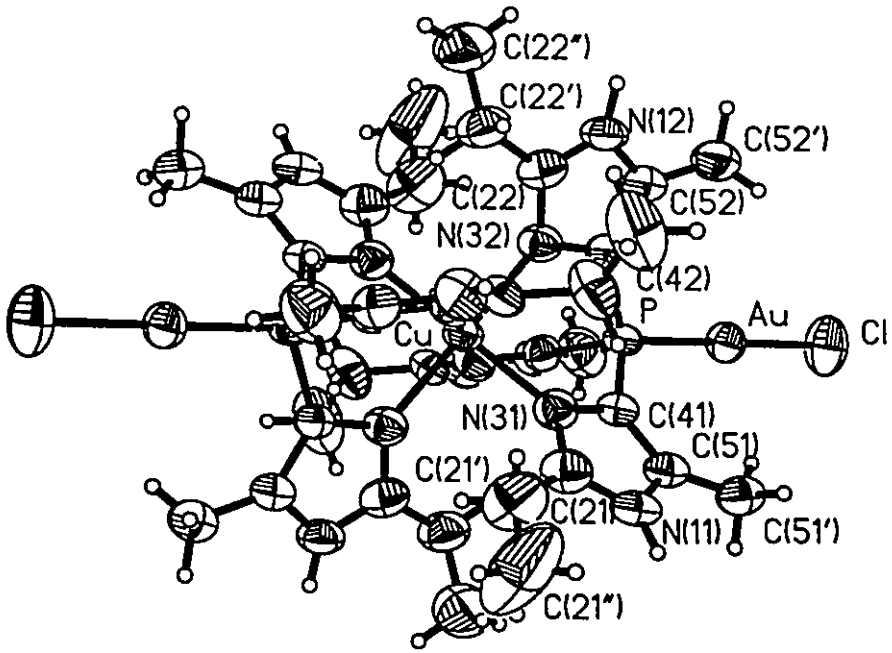

Figure 6.3.3 The cation of $[(TEMIPAuCl)_2Cu](NO_3)_2 \cdot 2H_2O$

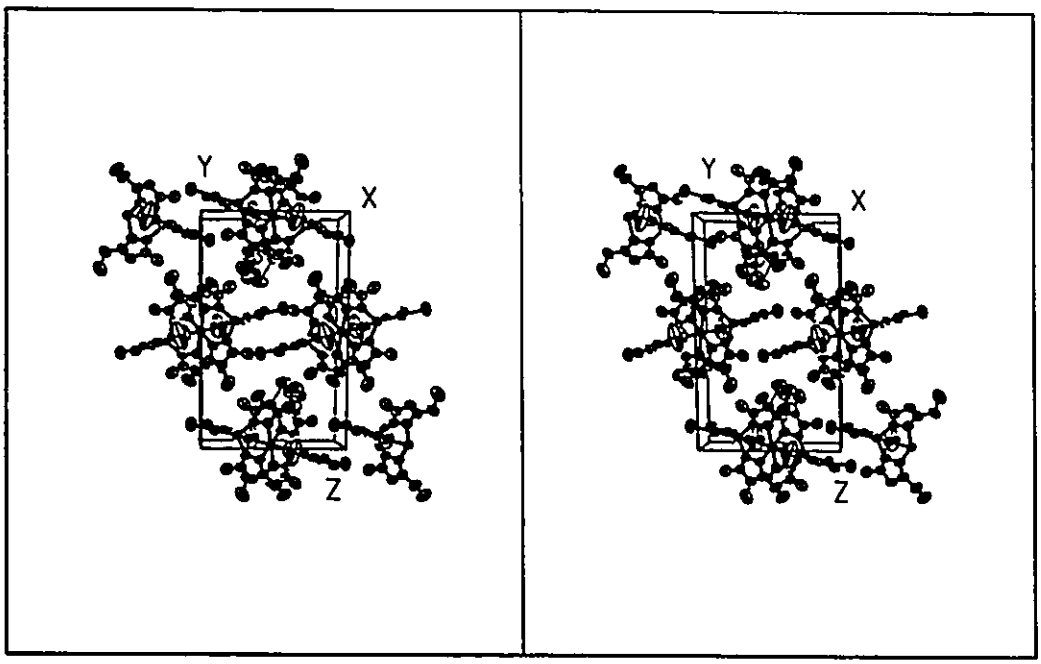

Figure 6.3.4 A stereoview of the packing of $[(TEMIPAuCl)_2Cu](NO_3)_2 \cdot 2H_2O$ in a unit cell

groups at the ring C2 position for such a ligand not to form bis-ligand chelated metal complexes.

In contrast to the $[(TEMIP)_2Cu](NO_3)_2$ complex, which shows the dynamic Jahn-Teller effect, the complex $[(TEMIPAuCl)_2Cu](NO_3)_2 \cdot 2H_2O$ is statically distorted, with two long [2.333(7)Å] and four short [2.082(6) - 2.084(5)Å] N-Cu bonds. These values (Å) are comparable to those of the copper complexes with six equivalent aromatic nitrogen donor ligands, for example, 2.31(1) and 2.06(1) - 2.08(1) for $[(TPPAuCl)_2Cu](NO_3)_2$ [TPP = tris(2-pyridyl)phosphine] (94), 2.528(4) and 1.991(2) - 2.018(3) for $Cu(HBpz_3)_2$ [$HBpz_3$ = hydrotris(1-pyrazolyl)borate] (107), 2.226(7) - 2.450(7) and 2.026(5) - 2.035(5) for $[Cu(bipy)_3](ClO_4)_2$ (bipy = 2,2'-bipyridyl) (136), 2.593(3) and 2.012(2) - 2.049(2) for $[Cu(imH)_6](NO_3)_2$ (imH = imidazole) (106) and 2.32(1) - 2.34(1) and 2.00(1) - 2.07(1) for $[Cu(phen)_6](ClO_4)_2$ (phen = 1,10-phenanthroline) (137). The coordination geometry around the gold atom is normal rectilinear. The P-Au and Cl-Au bond distances (Å), 2.216(2) and 2.264(2), are similar to those of the TMIPAuCl complex mentioned in **Chapter 5** [2.216(2) and 2.268(2)] and to those of the tris(2-pyridyl)phosphine complexes [2.214(4) - 2.222(3) and 2.267(4) - 2.277(5)] (94). No correlations between the complex stability and these values can be found. Two of the P-C bonds in the phosphine ligand are relatively short [1.781(7) and 1.793(7)Å] as compared to other gold(I) phosphine complexes (see **Chapter 5**) while the other one is significantly longer [1.821(7)Å]. The reason for this is not clear. The imidazole

rings are essentially planar. One water molecule is incorporated into the lattice and hydrogen bonded to one of the imidazole nitrogen atoms [O...N separation 2.82(1)Å]. The water molecule is also hydrogen bonded to an oxygen atom from the nitrate anion [O...O separation 2.81(1)Å]. This oxygen atom and another oxygen atom from the nitrate anion are hydrogen bonded to the other two imidazole nitrogen atoms [O...N separations 2.86(1) and 2.85(1)Å]. Such hydrogen bonding involves all three protonated imidazole nitrogen atoms of the ligand and two oxygen atoms of the nitrate anion.

6.4 The Infrared Spectra of $[(TEMIP)_2Cu](NO_3)_2$ and $[(TEMIPAuCl)_2Cu](NO_3)_2 \cdot 2H_2O$

Major infrared frequencies of $[(TEMIP)_2Cu](NO_3)_2$ and $[(TEMIPAuCl)_2Cu](NO_3)_2 \cdot 2H_2O$ are listed in **Table 6.4**. Tentative assignments were made in accord with references 84, 86, 96, and 97.

6.5 The Jahn-Teller Effect of the Copper(II) Complexes

In 1937, Jahn and Teller proposed a remarkable theorem which states: "Any nonlinear system with a degenerate ground state will undergo a distortion that lowers its energy, thereby splitting the degenerate state" (138). Copper(II) atom is a typical Jahn-Teller example. It has a d^9 electronic configuration. In an octahedral field, there will be three electrons in the doubly degenerate e_g orbitals. The Jahn-Teller theorem states that the coordination geometry around the metal atom will distort. Such a distortion will cause the degenerate orbitals to split,

Table 6.4 Major infrared frequencies (cm^{-1}) of $[(TEMIP)_2Cu](NO_3)_2$ and $[(TEMIPAuCl)_2Cu](NO_3)_2 \cdot 2H_2O$

$[(TEMIP)_2Cu](NO_3)_2$	$[(TEMIPAuCl)_2Cu]_2 \cdot 2H_2O$	Assignments
3426-2661s,br	3564-2662s,br	νO-H,N-H,C-H
1586s	1595s	γring
1519m	1520m	
1442-1384vs,br	1443-1384vs,br	νNO_3,P-C
1320s	1328s	γC-H
1263m	1267m	δC-H
1197m	1202m	δC-H
1076m	1076m	-
1046s	1046s	δring
970w	971w	-
838w	838w	γNO_3
789m	792w	δP-C
754m	755m	
711w	711w	γC-H
676w	675w	γring
606w	608w	-
554s	582s	γP-C
516s	533s	γP-C
478w	420w	-

Bands in cm^{-1}, s=strong, m=medium, w=weak, br=broad, sh=shoulder, v=very, ν=stretching, δ=deformation, γ=bending.

leaving two electrons in the lower energy orbital and one electron in the higher energy orbital, hence lowering the total energy of the system. Other strong Jahn-Teller examples are high spin d^4 and low spin d^7 atoms in an octahedral field.

Experimentally, the Jahn-Teller effect turns out to be elusive, as described by van Vleck: "It is a great merit of the Jahn-Teller effect that it disappears when not needed" (139). Copper(II) complexes having a CuL_6 (L_6 stands for any six equivalent ligands) chromophore sometimes appear to be distorted octahedral and sometimes undistorted. In the cases where almost no distortions have been observed, the dynamic Jahn-Teller effect was invoked to rationalize the violations. For structures in the solid state, two general explanations are: 1. The complex is oscillating among three equivalent (e.g., tetragonal) distortions so that on a time average the structure appears regular (dynamic Jahn-Teller); 2. Each molecule is trapped in one of the several distorted configurations. Molecules in each of these distortions are distributed at random throughout the crystal, so that on a space average, the structure appears regular (140).

Two typical examples are $[Cu(en)_3]SO_4$ (en = ethylenediamine) and $K_2Pb[Cu(NO_2)_6]$ which show regular octahedral structures at room temperature (140, 141). On lowering the temperature, both compounds undergo a phase transition and distorted structures have been observed (142, 143). This can be regarded as the freezing out of the Jahn-Teller distortion. The Jahn-Teller distortion can not always be easily frozen out however. Structural determination

showed that the octahedral CuS_6 core of the complex $[Cu(ttcn)_2](BF_4)_2(MeCN)$ (ttcn = trithiacyclononane) is hardly distorted even at 117K, while the same complex with nitromethane solvate is distorted at room temperature (144). Neutron diffraction studies of the complex $[Cu(pyO)_6](ClO_4)_2$ (pyO = pyridine N-oxide) showed that the room temperature bar-three fold symmetry around the copper atom is retained even at 20K (145). This was attributed to the second explanation mentioned above. In the room temperature structures of the three copper complexes studied in this work, the two involving copper only are almost regular octahedral while the one involving both copper and gold is tetragonally distorted. The questions one would ask about these experimental observations are: Why in some cases can the Jahn-Teller distortion be frozen out while in others it cannot? Why does a particular metal atom with the same or very similar ligands at the same temperature give distorted structures in some cases while in others the structures are undistorted?

The qualitative results obtained by Bersuker and coworkers from their studies of the Jahn-Teller effect are adapted here (146). When only an isolated Jahn-Teller species, for example, a copper(II) ion is considered, the Jahn-Teller distortion energy well is like a "Mexican hat", with no minimum along the low energy trough. That is, the ion can be distorted along any direction, and no static distortion can be observed. If the ion is coordinated, that is, the environment around the Jahn-Teller ion is not of spherical symmetry, the energy surface will

warp. To a first order approximation, three minima with equal energy will result for a Jahn-Teller ion in an octahedral field with six equivalent ligands. These three energy minima correspond to three elongated tetragonal distortions along three orthogonal axes. The energy barrier between these minima is proportional to the mean life time of a distorted configuration. If the experimental observation time is much greater than this life time, the observed populations in different distorted configurations are only dominated by the Boltzmann distribution. That is, different distortions with equal energy will be equally populated. In this case, the same number of molecules will distort along each of the three orthogonal directions and on average, an undistorted structure will be observed. This is particularly true for the X-ray structure determination which has an extremely long observation time (several days). When the second order and higher order terms are considered, the energy surface may further warp, causing the energy minima to be unequal. The inequality of the energy minima means that one or two of the distorted configurations will be more energetically favoured than the rest. As a result, static Jahn-Teller distortion will be observed.

Thus the zero and first-order Jahn-Teller distortion is dynamic in nature. Static distortion is only caused by some higher order energy perturbations. In the solid state, these energy perturbations can be lattice packing effects, hydrogen bonding, temperature, and van der Waal's interactions, *etc.* If the perturbations have the same effect on all three energy minima, a dynamically distorted

structure will result, even at very low temperatures.

Cotton *et al.* showed that at room temperature, the static Jahn-Teller distortion of the $[Cr(H_2O)_6]^{2+}$ core (a high spin d^4 system) (147) can be forced to disappear by changing to a different anion which forms a different hydrogen bonding pattern to the core (148). In the copper(II) TEMIP complexes, the addition of the AuCl tail to the phosphorus atom of the phosphine ligand can be regarded as an effective high order energy perturbation to the $(CuN_6)^{2+}$ core, which leads to the "freezing out" of the static Jahn-Teller distortion. One similar complex, $[(TPPAuCl)_2Cu](NO_3)_2$ (TPP = tris(2-pyridyl)phosphine) is also statically distorted at room temperature (94). The origin, magnitude and mechanism of the high order energy interactions are largely unknown. Further structural and spectroscopic studies are necessary.

Chapter 7

Metal Complexes with Other Ligands

7.1 Introduction

In this chapter, metal complexes with ligands other than phosphines are described. As mentioned in **Chapter 4**, the reaction of TIP with Me_2SAuCl followed by the addition of MCl_2 (M = Cu, Ni) in methanol led to the formation of $(MeO)_3PAuCl$. This complex was characterized by ^1H and ^{13}C NMR spectroscopy. The presence of gold and chlorine atoms were confirmed by qualitative elemental analysis.

When the ligand TDMIP was reacted with $HAuCl_4$ with a 2:1 ligand/Au molar ratio in a methanol/water mixture, an unexpected product, bis(4,5-dimethylimidazol-2-ylidene)gold(I) chloride was obtained. This is a bis-carbene gold(I) complex. The structure of this complex has been determined (149). The original intention of the reaction was to make a gold(I) phosphine complex, by analogy to the method used for the preparation of Ph_3PAuCl (24). Gold(I) carbene complexes have been prepared before. They are prepared from precursor isocyanide gold(I) complexes (150, 151), from cleavage of the carbon-carbon double bond in electron rich alkenes (152), carbene transfer from tungsten pentacarbonyl compounds (153), or by reacting a gold(I) starting compound with a lithiated organic molecule (154, 155). The formation of the bis-carbene gold(I)

complex in this work is through a different reaction, which involves the cleavage of at least one of the imidazole groups from the phosphine in the form of carbene and reaction of the carbene with gold.

Cleavages of the P-C bond have been observed for the tris-imidazole phosphine ligands with the phosphorus atom attached to the imidazole C2 carbon atom, when the phosphorus atom is oxidized (84, 156), and when the ligand is reacted with both a soft and a hard metal ions in polar solvents (*vide supra*). Another possible factor important to the P-C bond cleavage is protonation of the N3 nitrogen atom of the imidazole groups (149). Since the reaction was carried out in a polar solution, in the presence of an acid and an oxidizing agent, the P-C bond cleavage will be facile.

The formation of the bis-carbene gold(I) complex may proceed by trapping the intermediate carbene from the P-C cleavage reaction with a bond to a gold(I) atom or by rearranging the cleaved imidazole molecule to a carbene intermediate which then reacts with a gold(I) atom. If the reaction proceeded through the latter pathway, it should be possible to make a gold(I) carbene complex by reacting a gold(I) starting material with imidazole. Gold(I) is relatively soft and is stabilized by soft ligand atoms. In this respect, carbenes are better ligands than nitrogen donor ligands. This will favour the rearrangement of the cleaved imidazole molecule to form a gold(I) carbene complex rather than a gold(I) imidazole complex.

In aqueous solution, no gold(I) carbene complex was obtained when imidazole was reacted with Me_2SAuCl or with $HAuCl_4$ in the presence of thiodiglycol. So the first reaction pathway is more likely to be true. On the other hand, preparations of gold(I) imidazole (157), gold(I) pyrazole (158), gold(I) pyridine (159), and gold(I) bipyridine (160) complexes have been described. When Me_2SAuCl was reacted with 1,5-dimethyl-4-hydroxymethylimidazole in a methanol/toluene mixture, a crystalline product was separated. The structure of this complex was determined (161). No sign of formation of the tautomeric gold(I) carbene complex was observed during the reaction. The product was unstable towards water. When the compound was dissolved in water, metallic gold soon started to deposit. Such a decomposition reaction explains why no product was obtained when imidazole was reacted with Me_2SAuCl in aqueous solutions, and confirms that the first pathway is more pertinent.

Preparations of the other gold(I) nitrogen complexes mentioned above were all carried out in non-aqueous solvents. In aqueous solution, some imide nitrogen compounds (include imidazole and pyrazole compounds) reacted with gold(I) starting materials in the presence of a strong base to form imido-gold(I) complexes (126, 162-166).

The ligand BIP is an oxidative decomposition product of TIP, and has been characterized as a zwitterion (84). Copper(II), zinc(II) and iron(II) complexes with this ligand have been characterized before (89). A zinc(II) complex with a similar

C(4),C(5)-substituted acid from oxidative decomposition of TDMIP has also been characterized (156). In all these complexes, the metal atoms are bonded to the N(3) atom of one of the imidazole rings and to one of the oxygen atoms of the phosphonate group. In contrast to these complexes, reaction of K_2PtCl_4 with BIP resulted in deprotonation of the protonated imidazole N(3) atom of the zwitterion and a complex with a MN_4 chromophore was obtained (167).

7.2 Experiments

Chloro(trimethylphosphite-P)gold(I) [$(MeO)_3PAuCl$]: Half a stoichiometric amount of MCl_2 (M = Ni, Cu) in methanol (5mL) was added to a solution of TIP (0.1g) and Me_2SAuCl (0.127g) in methanol (5mL). The reaction mixture was left at room temperature to evaporate under nitrogen. Colourless crystals were formed after the volume of the reaction mixture was reduced to about 3mL. These were separated by filtration, washed with methanol (1mL) and air dried. Yield 0.055g (35.8%), m.p. 94-96°C (decompose).

Bis(4,5-dimethylimidazol-2-ylidene)gold(I) chloride hydrate [bis-carbene gold(I) complex]: A solution of $HAuCl_4$ (0.13g) in 1:1 methanol/water (3mL) was added to a solution of TDMIP (0.2g) in 1:1 methanol/water (5mL). The reaction mixture was left to evaporate at room temperature under nitrogen. A colorless crystalline solid was formed after the volume of the solvents were reduced to about 3mL. The product was collected by filtration, washed with methanol (5mL), acetone (10mL) and air dried. Yield 0.06g (29%), m.p. 229-230°C (decompose).

Bis(4-hydroxymethyl-1,5-dimethylimidazole-N^3)gold(I) chloride [bis-imidazole gold(I) complex]: Solid Me_2SAuCl (0.12g) was added to a solution of 4-hydroxymethyl-1,5-dimethylimidazole (0.1g) in methanol (3mL). The reaction mixture was stirred till almost all solid materials were dissolved. Toluene (5mL) was added and any insoluble materials were removed by filtration. The filtrate was left to evaporate slowly at room temperature under nitrogen. A colorless crystalline solid was formed after most of the methanol was evaporated. The product was collected by filtration, washed with toluene (5mL), ether (5mL) and air dried. Yield 0.12g (60%), m.p. 176-178°C (decompose).

Bis[di(imidazol-2-yl)phosphinato-N^3,$N^{3'}$]platinum(II) tetrahydrate [$(BIP)_2Pt{\cdot}4H_2O$]: A solution of K_2PtCl_4 (0.2g) in water (5mL) was added to a solution of BIP (0.2g) in water (10mL). The reaction mixture was left to evaporate at room temperature under nitrogen. A colorless crystalline solid was formed after the volume of the solution was reduced to about 5mL. The product was collected by filtration, washed with methanol (5mL) and air dried. Yield 0.15g (47%), m.p. 330-332°C (decompose).

The crystal densities were measured by suspension in $CCl_4/CHBr_3$ and the crystals for X-ray diffraction experiment were mounted by gluing to the end of glass fibres. Unit cell determination and intensity data collection were performed on a Siemens P4 diffractometer with monchromatized Mo Kα radiation. Unit cell parameters were refined by least-squares fit of angular parameters from 24

reflections ($20.6 \leq 2\theta \leq 38.4°$) for the bis-carbene gold(I) complex, from 39 reflections ($4.85 \leq 2\theta \leq 12.45°$) for the bis-imidazole gold(I) complex and from 38 reflections ($10.81 \leq 2\theta \leq 24.96°$) for the $(BIP)_2Pt{\cdot}4H_2O$ complex. For all three complexes, intensities were measured with a θ(crystal) - 2θ(counter) scan. Three standards were measured every 100 reflections. No signs of crystal decay or instrumental instability were observed during data collection. Absorption corrections were made by use of the empirical ψ-scan method (80). The structures were solved by the Patterson method and refined by the method of least-squares, which minimized $\Sigma w(|F_o| - |F_c|)^2$. Hydrogen atoms were placed in calculated positions and not refined except for the water molecules to which no hydrogen atoms were added. Temperature factors of non-hydrogen atoms were refined anisotropically; some of the oxygen atoms from the water molecules were refined isotropically and those of hydrogen atoms were not refined. Details of crystal data collection and structure solution are listed in **Table 7.2.**

7.3 The NMR Spectra of Chloro(trimethylphosphite-P)gold(I) [$(MeO)_3PAuCl$]

Proton and ^{13}C NMR spectra of $(MeO)_3PAuCl$ were recorded on a Bruker AC-200 spectrometer with chloroform as a solvent and TMS as an internal standard. The ^{31}P NMR spectrum was recorded on a Bruker AC-300 spectrometer, with chloroform as a solvent and 85% H_3PO_4 in D_2O as an external standard. There is only one type of proton, carbon and phosphorus atom in the complex, so the assignments are straight forward. The proton signal appears as a doublet

Table 7.2 Crystal data of bis(4,5-dimethylimidazol-2-ylidene)gold(I) chloride hydrate, bis(4-hydroxymethyl-1,5-dimethylimidazole-N^3)gold(I) chloride, and $(BIP)_2Pt{\cdot}4H_2O$

	Bis(4,5-dimethylimidazol-2-ylidene)gold(I) chloride hydrate	Bis(4-hydroxymethyl-1,5-dimethylimidazole-N^3)gold(I) chloride	Bis[di(imidazol-2-yl)phophinato-$N^3,N^{3'}$]platinum(II) tetrahydrate
Formula	$C_{10}H_{18}ClN_4OAu$	$C_{12}H_{20}ClN_4O_2Au$	$C_{12}H_{20}N_8O_8P_2Pt$
Formula weight	442.7	484.7	661.4
Crystal colour, shape, size (mm)	colourless needle, 0.15x0.20x0.35	colourless needle, 0.14x0.16x0.40	colourless plate, 0.17x0.33x0.50
Space group, λ (Å)	$P2_1/n$, 0.71073	$P2_1/n$, 0.71073	P-1, 0.71073
Unit cell parameters (Å and °)	a = 7.692(2) b = 11.351(2) c = 16.890(3) β = 97.98(2)	a = 8.115(1) b = 13.998(1) c = 13.919(1) β = 104.190(7)	a = 7.473(1) b = 7.779(2) c = 9.787(2) α = 109.46(3) β = 98.56(3) γ = 98.29(3)
Volume ($Å^3$)	1460.4(5)	1532.8(2)	518.9(3)
Z	4	4	1
ρ_{cal}, ρ_{obs} ($Mg\ m^{-3}$)	2.013, 2.01(1)	2.101, 2.12(1)	2.116, 2.11(1)
Max. 2θ, indices range	50°, $0 \le h \le 9$, $0 \le k \le 13$, $-20 \le l \le 19$	45°, $2 \le h \le 10$, $-1 \le k \le 18$, $-18 \le l \le 16$	45°, $-1 \le h \le 12$, $-11 \le k \le 11$, $-15 \le l \le 11$
Temperature, °C	23	23	23
Absorption coefficient mm^{-1}	10.25	9.779	7.038
Transmission factors, range	0.019 - 0.057	0.0362 - 0.0657	0.156 - 0.324
Number of variables	148	190	136
Standard reflections	0 -2 5, 2 2 5, 1 -3 3	3 -6 4, -3 6 4, -3 0 -5	3 1 -5, 1 3 2, 3 -3 3
Correction factors for standard, range	0.9974 - 1.0132	0.9580 - 1.0016	0.9815 - 1.0336
Number of reflections measured	2941	2790	5675

Table 7.2 (continued)

	Bis(4,5-dimethylimidazol-2-ylidene)gold(I) chloride hydrate	Bis(4-hydroxymethyl-1,5-dimethylimidazole-N^3)gold(I) chloride	Bis[di(imidazol-2-yl)phophinato-N^3,$N^{3'}$]platinum(II) tetrahydrate
Number of independent reflections, used	2581	2547	4521
R_{int}	0.018	0.0197	0.015
Final R, R_w	0.0350, 0.0394	0.044, 0.033	0.0268, 0.0324
Final Δ/σ, max., ave	0.146, 0.033	0.001, 0.000	0.001, 0.000
Final difference map, max., min., e A^{-3}	1.40, -0.83	0.65, -0.46	2.73, -1.28
Weighting	$(\sigma_F^2)^{-1}$	$(\sigma_F^2)^{-1}$	$(\sigma_F^2)^{-1}$
Goodness of fit, S	0.89	1.81	2.22
F(000)	840	928	320

at 3.791ppm with a $|^3J_{P-H}|$ of 13.96Hz. The ^{13}C signal appears as a singlet at 53.277ppm. The ^{31}P signal appears as a poorly resolved multiplet at 120.484ppm with a $|^3J_{P-H}|$ of 13.96Hz. These are compared to the values reported for the free ligand: δ_P = 139.6 - 141ppm, δ_H = 3.48ppm, $^3J_{P-H}$ = 10.8Hz (93, 168).

7.4 The Structure of Bis(4,5-dimethylimidazol-2-ylidene)gold(I) Chloride hydrate

Atomic positional parameters are given in **Table 7.4.1**. Selected interatomic distances and angles are given in **Table 7.4.2**. The cation and molecular packing diagrams are given in **Figure 7.4.1** and **Figure 7.4.2**.

In the complex, the gold atom adopts its usual linear two coordination. The C-Au-C' bond angle is slightly bent [175.8(2)], probably as a result of the Au...Au' interaction [3.372(1)Å] between two adjacent molecules. The Au-C bond distances 2.012(6)Å and 2.016(6)Å are similar to those of the other gold(I)-carbene complexes [ranging from 1.92(3)Å to 2.06(2)Å (151, 154, 155, 169 - 171)], and similar to those of the gold(I)-carbon bonds in other gold(I) complexes [ranging from 1.92(1)Å to 2.062(8)Å (172 - 175)]. All the C-N bond distances within the imidazole ring are shorter than a single C-N bond (176), which indicates the delocalization of the π electron density into the ring system. As a result of such a delocalization, the gold(I)-carbon bond will have little double bond character. This is reflected in the similarities of the gold(I)-carbon bond distances of the gold(I)-carbene complexes with the other gold(I) complexes.

In the solid state, the molecules are stacked in parallel pairs with an

Table 7.4.1 Atomic coordinates ($x10^4$) and equivalent isotropic displacement coefficients ($Å^2x10^3$) of bis(4,5-dimethylimidazol-2-ylidene)gold(I) chloride hydrate

	x	y	z	U(eq)
Au	482 (1)	967 (1)	4305 (1)	52 (1)
N(1)	-1228 (7)	-974 (4)	3230 (3)	55 (2)
C(2)	209 (8)	-389 (5)	3530 (3)	51 (2)
N(3)	1496 (8)	-874 (4)	3166 (3)	63 (2)
C(4)	870 (9)	-1784 (6)	2663 (4)	61 (2)
C(5)	-869 (8)	-1847 (5)	2690 (3)	55 (2)
C(1)	2006 (12)	-2458 (8)	2192 (5)	94 (4)
C(3)	-2288 (10)	-2625 (7)	2272 (4)	79 (3)
N(1A)	2306 (7)	2975 (5)	5250 (3)	63 (2)
C(2A)	833 (8)	2394 (5)	5020 (3)	53 (2)
N(3A)	-371 (7)	2990 (5)	5351 (3)	61 (2)
C(4A)	385 (10)	3941 (6)	5799 (4)	64 (2)
C(5A)	2054 (11)	3938 (6)	5730 (4)	69 (3)
C(1A)	-700 (12)	4759 (7)	6239 (5)	93 (3)
C(3A)	3554 (12)	4730 (8)	6046 (5)	99 (4)
O*	300 (4)	5263 (3)	8719 (2)	81 (1)
ClA*	300 (4)	5263 (3)	8719 (2)	81 (1)
Cl*	-4160 (3)	2016 (2)	4885 (1)	71 (1)
Oa*	-4160 (3)	2016 (2)	4885 (1)	71 (1)

Equivalent isotropic U defined as one third of the trace of the orthogonalized U_{ij} tensor.

* A disordered chloride ion and water molecule were refined at these sites with a 0.5 occupancy respectively.

Table 7.4.2 Selected bond lengths (Å) and angles (°) of bis(4,5-dimethylimidazol-2-ylidene)gold(I) chloride hydrate

Au-C(2)	2.012	(6)	Au-C(2A)	2.016	(6)
Au-AuA	3.372	(1)	N(1)-C(2)	1.328	(7)
N(1)-C(5)	1.400	(8)	C(2)-N(3)	1.352	(9)
N(3)-C(4)	1.381	(8)	C(4)-C(5)	1.347	(9)
C(4)-C(1)	1.48	(1)	C(5)-C(3)	1.50	(1)
N(1A)-C(2A)	1.322	(8)	N(1A)-C(5A)	1.390	(9)
C(2A)-N(3A)	1.331	(8)	N(3A)-C(4A)	1.398	(8)
C(4A)-C(5A)	1.31	(1)	C(4A)-C(1A)	1.51	(1)
C(5A)-C(3A)	1.50	(1)			
C(2)-Au-C(2A)	175.8	(2)	C(2)-Au-AuA	86.6	(2)
C(2A)-Au-AuA	97.5	(2)	C(2)-N(1)-C(5)	111.9	(5)
Au-C(2)-N(1)	129.6	(5)	Au-C(2)-N(3)	126.1	(4)
N(1)-C(2)-N(3)	104.2	(5)	C(2)-N(3)-C(4)	111.7	(5)
N(3)-C(4)-C(5)	106.4	(6)	N(3)-C(4)-C(1)	122.6	(6)
C(5)-C(4)-C(1)	131.0	(6)	N(1)-C(5)-C(4)	105.7	(5)
N(1)-C(5)-C(3)	121.7	(6)	C(4)-C(5)-C(3)	132.6	(6)
C(2A)-N(1A)-C(5A)	112.4	(6)	Au-C(2A)-N(1A)	128.0	(5)
Au-C(2A)-N(3A)	128.1	(4)	N(1A)-C(2A)-N(3A)	104.0	(5)
C(2A)-N(3A)-C(4A)	111.0	(6)	N(3A)-C(4A)-C(5A)	106.8	(6)
N(3A)-C(4A)-C(1A)	121.6	(7)	C(5A)-C(4A)-C(1A)	131.5	(7)
N(1A)-C(5A)-C(4A)	105.8	(6)	N(1A)-C(5A)-C(3A)	121.1	(7)
C(4A)-C(5A)-C(3A)	133.1	(7)			

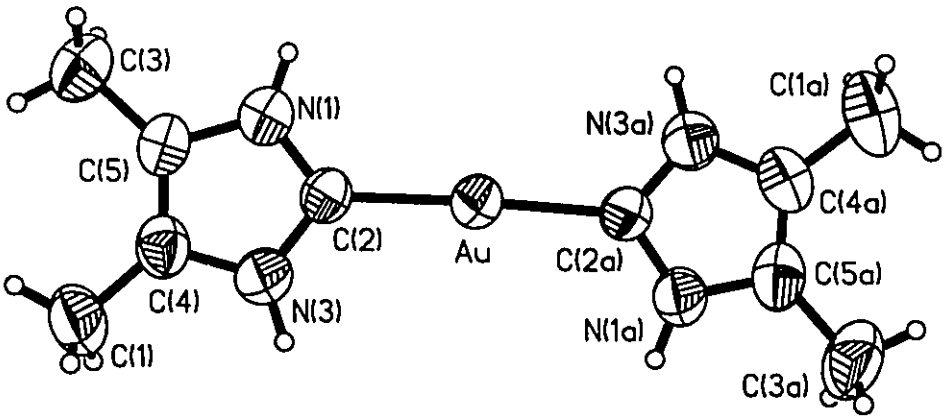

Figure 7.4.1 The cation of bis(4,5-dimethylimidazol-2-ylidene)gold(I) chloride hydrate

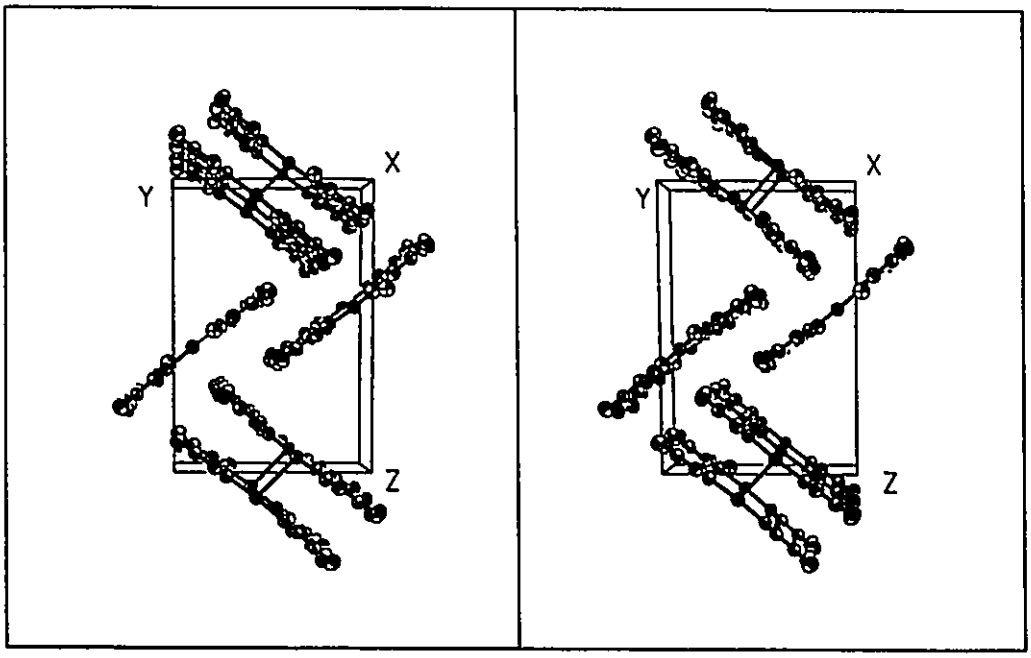

Figure 7.4.2 A stereoview of the packing of bis(4,5-dimethylimidazol-2-ylidene)gold(I) chloride hydrate in a unit cell

eclipsed fashion within each pair, to allow intermolecular Au...Au' and π-π interactions but to minimize methyl group repulsive interactions. The chloride anion and a lattice water molecule are hydrogen bonded to each other and to the imidazole nitrogen atoms, with Cl...O and Cl...N distances 3.014(8) - 3.296(8)Å.

7.5 The Structure of Bis(4-hydroxymethyl-1,5-dimethylimidazole-N^3)gold(I) Chloride

Atomic positional parameters are given in **Table 7.5.1**. Selected interatomic distances and angles are given in **Table 7.5.2**. The cation and molecular packing diagrams are given in **Figure 7.5.1** and **Figure 7.5.2**.

In the complex, the gold atom is linearly coordinated to two imidazole N3 nitrogen atoms. If the substitution groups on the imidazole ring are not considered, this complex is a tautomer of the bis-carbene gold(I) complex. Another non-tautomeric form of the gold(I) complex with imidazole, that is bond to the gold atom through the deprotonated imidazole N1 nitrogen atom, has also been prepared (166). Gold(I) imidazole complexes with the gold atom bonded to both the nitrogen and carbon atoms have been described (155, 169). In this respect, the chemistry of imidazole with gold(I) is quite versatile, although the nitrogen atom is a less effective ligand for gold(I). The Au-N bond distances in the title complex, 2.011(5), 2.000(5)Å, are similar to those of the imidazole N3 and pyridine N gold(I) complexes, 2.00(2) - 2.10(4)Å (159, 177). These values are slightly shorter than those of the gold(I) complexes with imido nitrogen ligands

Table 7.5.1 Atomic coordinates ($x10^4$) and equivalent isotropic displacement coefficients ($Å^2x10^3$) of bis(4-hydroxymethyl-1,5-dimethylimidazole-N^3)gold(I) chloride

	x	y	z	U(eq)
Au	1717 (1)	6160 (1)	2014 (1)	46 (1)
C(2')	4552 (9)	6179 (8)	3889 (6)	51 (3)
N(1)	-1397 (6)	6284 (6)	-815 (5)	44 (2)
N(3)	611 (7)	6171 (7)	554 (4)	46 (2)
C(41)	3234 (8)	6226 (10)	-78 (6)	64 (4)
C(1)	-3113 (8)	6258 (8)	-1458 (6)	58 (3)
C(4)	1349 (7)	6261 (8)	-226 (5)	46 (3)
C(5)	96 (7)	6343 (7)	-1073 (5)	40 (2)
C(51)	163 (9)	6451 (8)	-2135 (5)	59 (3)
O(4)	4080 (6)	6966 (6)	570 (5)	72 (3)
C(2)	-1075 (8)	6178 (8)	173 (5)	47 (3)
Cl	6638 (2)	5694 (2)	2014 (2)	62 (1)
N(3')	2816 (7)	6179 (7)	3466 (4)	45 (2)
N(1')	4787 (6)	6254 (6)	4840 (5)	45 (2)
C(1')	6489 (8)	6237 (9)	5533 (7)	62 (3)
C(4')	2049 (7)	6289 (7)	4256 (5)	45 (3)
C(41')	148 (8)	6276 (10)	4070 (6)	63 (4)
C(5')	3272 (8)	6337 (7)	5109 (5)	44 (3)
C(51')	3143 (10)	6471 (9)	6137 (6)	60 (3)
O(41')*	-704 (12)	6908 (12)	3408 (10)	69 (5)
O(42')*	-491 (13)	5413 (12)	3916 (10)	73 (6)

Equivalent isotropic U defined as one third of the trace of the orthogonalized U_{ij} tensor.

* O41' and O42' represent a disordered O atom and were given occupancies of 0.5.

Table 7.5.2 Selected bond lengths (Å) and angles (°) of bis(4-hydroxymethyl-1,5-dimethylimidazole-N^3)gold(I) chloride

Au-N(3)	2.011	(5)	Au-N(3')	2.000	(5)
C(2')-N(3')	1.387	(8)	C(2')-N(1')	1.30	(1)
N(1)-C(1)	1.460	(8)	N(1)-C(5)	1.347	(9)
N(1)-C(2)	1.34	(1)	N(3)-C(4)	1.37	(1)
N(3)-C(2)	1.340	(8)	C(41)-C(4)	1.493	(9)
C(41)-O(4)	1.44	(1)	C(4)-C(5)	1.360	(8)
C(5)-C(51)	1.50	(1)	N(3')-C(4')	1.40	(1)
N(1')-C(1')	1.478	(8)	N(1')-C(5')	1.376	(9)
C(4')-C(41')	1.501	(9)	C(4')-C(5')	1.349	(8)
C(41')-O(41')	1.341	(2)	C(41')-O(42')	1.311	(2)
C(5')-C(51')	1.47	(1)			
N(3)-Au-N(3')	178.8	(4)	N(3')-C(2')-N(1')	108.3	(7)
C(1)-N(1)-C(5)	128.6	(7)	C(1)-N(1)-C(2)	122.8	(6)
C(5)-N(1)-C(2)	108.5	(5)	Au-N(3)-C(4)	129.0	(4)
Au-N(3)-C(2)	124.0	(5)	C(4)-N(3)-C(2)	106.8	(5)
C(4)-C(41)-O(4)	112.3	(8)	N(3)-C(4)-C(41)	121.4	(6)
N(3)-C(4)-C(5)	108.4	(6)	C(41)-C(4)-C(5)	130.2	(7)
N(1)-C(5)-C(4)	107.1	(6)	N(1)-C(5)-C(51)	121.4	(5)
C(4)-C(5)-C(51)	131.5	(6)	N(1)-C(2)-N(3)	109.2	(6)
Au-N(3')-C(2')	125.7	(5)	Au-N(3')-C(4')	128.5	(4)
C(2')-N(3')-C(4')	105.6	(5)	C(2')-N(1')-C(1')	123.1	(6)
C(2')-N(1')-C(5')	111.5	(5)	C(1')-N(1')-C(5')	125.4	(7)
N(3')-C(4')-C(41')	120.0	(6)	N(3')-C(4')-C(5')	108.9	(6)
C(41')-C(4')-C(5')	131.0	(7)	C(4')-C(41')-O(41')	116	(1)
C(4')-C(41')-O(42')	113	(1)	O(41')-C(41')-O(42')	112.3	(9)
N(1')-C(5')-C(4')	105.7	(6)	N(1')-C(5')-C(51')	123.8	(6)
C(4')-C(5')-C(51')	130.5	(6)			

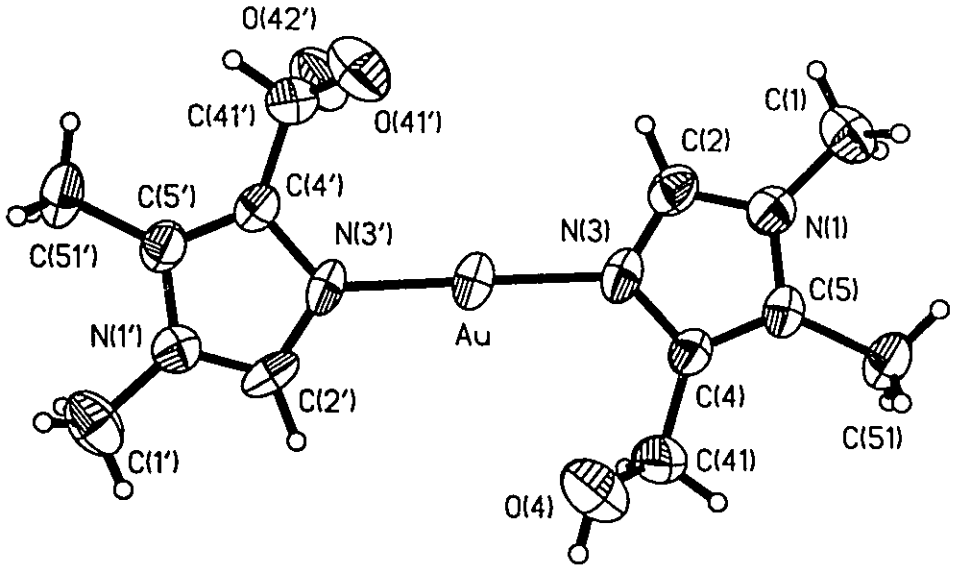

Figure 7.5.1 The cation of bis(4-hydroxymethyl-1,5-dimethylimidazole-N^3)gold(I) chloride

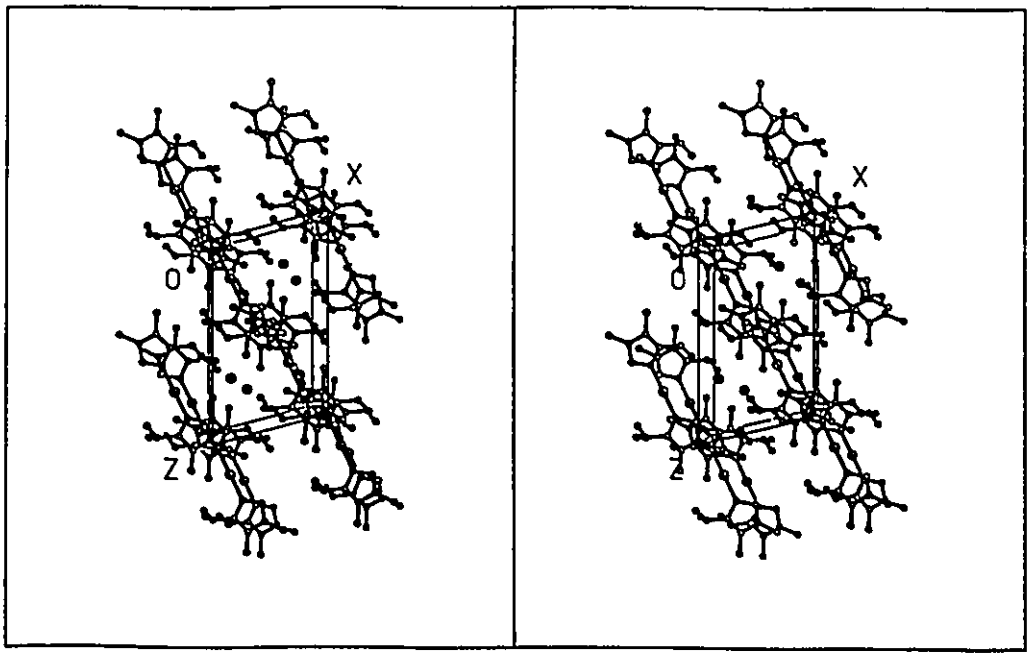

Figure 7.5.2 A stereoview of the packing of bis(4-hydroxymethyl-1,5-dimethylimidazole-N^3)gold(I) chloride in a unit cell

[ranging from 2.019(5)Å to 2.20(1)Å (126, 163 - 166)].

The complex cation is nearly planar if the hydroxy groups are excluded. The cations are packed like sheets parallel to the crystallographic ac plane. These sheets are staggered like bricks in a wall along the b axis. Cations within each sheet are linked by hydrogen bonds through the chloride anion and the hydroxy group on the ligand, with O...Cl distances 3.04(1) - 3.09(2)Å. Between the sheets, there are only π-π and van de Waal's interactions. As a result, there is no short Au...Au' contact (the shortest Au...Au' separation is greater than 6Å), so the N-Au-N' bond angle [(178.8(4)°] is closer to 180°. One of the hydroxy groups of the complex is disordered in such a fashion, that in one molecule it is pointing up from the plane defined by the imidazole rings and the gold atom while in the other it is pointing down. Such a disorder lowers the symmetry of the cation.

7.6 The Structure of Bis[di(imidazol-2-yl)phosphinato-N^3,$N^{3'}$]platinum(II) Tetrahydrate [$(BIP)_2Pt{\cdot}4H_2O$]

Atomic positional parameters are given in **Table 7.6.1.** Selected interatomic distances and angles are given in **Table 7.6.2.** The molecule and packing diagrams are given in **Figure 7.6.1** and **Figure 7.6.2.**

In the complex, the environment around the Pt atom is almost exactly square-planar, with cis-N-Pt-N' angles 89.7(1) and 90.3(1)° and a trans-N-Pt-N' angle 180° by symmetry. The Pt-N bond distances 2.023(3) and 2.014(3)Å are similar to those of other Pt-imidazole complexes 2.006(6) - 2.07(3)Å (178), and

Table 7.6.1 Atomic coordinates ($x10^4$) and equivalent isotropic displacement coefficients ($Å^2x10^3$) of $(BIP)_2Pt{\cdot}4H_2O$

	x	y	z	U (eq)
Pt	5000	0	0	21 (1)
P	1610 (1)	-3938 (1)	-2343 (1)	27 (1)
N(1)	1948 (4)	-2030 (4)	-4304 (3)	33 (1)
C(2)	2509 (4)	-2121 (4)	-2963 (3)	26 (1)
N(3)	3751 (4)	-570 (3)	-2128 (3)	25 (1)
C(4)	4007 (5)	527 (4)	-2957 (4)	31 (1)
C(5)	2887 (6)	-390 (5)	-4322 (4)	36 (1)
N(1')	-149 (4)	-2743 (4)	49 (3)	32 (1)
C(2')	1327 (4)	-2512 (4)	-544 (3)	25 (1)
N(3')	2573 (4)	-1011 (3)	394 (3)	25 (1)
C(4')	1849 (5)	-282 (5)	1623 (4)	32 (1)
C(5')	162 (5)	-1358 (6)	1425 (4)	37 (1)
O(1)	3036 (4)	-5021 (4)	-2174 (3)	42 (1)
O(2)	-260 (4)	-4901 (4)	-3279 (3)	39 (1)
O(3)	3442 (9)	3498 (8)	4692 (7)	115 (2)
O(4)*	3551 (10)	4960 (9)	756 (8)	50 (2)
O(5)*	3218 (11)	5218 (10)	1791 (9)	58 (2)

The equivalent isotropic temperature factor, U(eq), is defined as one third of the trace of the orthogonalized U_{ij} tensor.

* O(4) and O(5) were each given a site occupancy of one half.

Table 7.6.2 Selected bond lengths (Å) and angles (°) of $(BIP)_2Pt{\cdot}4H_2O$

Pt-N(3)	2.023	(3)	Pt-N(3')	2.014	(3)
P-C(2)	1.799	(4)	P-C(2')	1.803	(3)
P-O(1)	1.474	(3)	P-O(2)	1.488	(3)
N(1)-C(2)	1.346	(4)	N(1')-C(2')	1.337	(5)
C(2)-N(3)	1.334	(3)	C(2')-N(3')	1.338	(3)
N(3)-C(4)	1.372	(5)	N(3')-C(4')	1.374	(5)
C(4)-C(5)	1.362	(5)	C(4')-C(5')	1.357	(5)
C(5)-N(1)	1.371	(5)	C(5')-N(1')	1.377	(4)
O(4)...(O5)	1.04	(1)			
C(2)-P-C(2')	99.0	(1)	C(2)-P-O(2)	108.3	(2)
C(2')-P-O(2)	108.1	(2)	C(2)-P-O(1)	109.4	(2)
C(2')-P-O(1)	109.9	(2)	O(1)-P-O(2)	120.1	(2)
Pt-N(3)-C(2)	124.4	(2)	Pt-N(3')-C(2')	125.3	(3)
Pt-N(3)-C(4)	127.2	(2)	Pt-N(3')-C(4')	127.5	(2)
C(5)-N(1)-C(2)	108.4	(3)	C(5')-N(1')-C(2')	108.4	(3)
N(1)-C(2)-N(3)	108.6	(3)	N(1')-C(2')-N(3')	109.4	(3)
C(2)-N(3)-C(4)	108.4	(3)	C(2')-N(3')-C(4')	107.2	(3)
N(3)-C(4)-C(5)	107.5	(3)	N(3')-C(4')-C(5')	108.6	(3)
C(4)-C(5)-N(1)	107.0	(4)	C(4')-C(5')-N(1')	106.4	(3)
P-C(2)-N(1)	125.9	(2)	P-C(2')-N(1')	126.2	(2)
P-C(2)-N(3)	125.4	(2)	P-C(2')-N(3')	124.4	(3)
N(3)-Pt-N(3')	89.7	(1)	N(3)-Pt-N(3A)	180.0	(1)
N(3')-Pt-N(3A)	90.3	(1)			

Hydrogen bonds*

N(1)-H(1A)...O(2')	2.714	(4)	(H(1A)...O(2')	1.87	N(1)-H(1A)...O(2')	155
N(1')-H(1A')...O(4'')	2.70	(1)	(H(1A')...O(4'')	1.84	N(1')-H(1A')...O(4'')	160
N(1')-H(1A')...O(5'')	2.72	(1)	(H(1A')...O(5'')	1.86	N(1')-H(1A')...O(5'')	160
O(1)...O(4'')	2.70	(1)				
O(1)...O(5'')	2.80	(1)				
O(1)...O(3'')	2.98	(1)				
O(3)...O(3')	2.88	(1)				
O(1)...O(4'')	2.84	(1)				

N(3A) is related to N(3) by the inversion centre at 1/2,0,0. Other atoms are related to those shown in Table by a, -x,-1-y,-1-z; b, -x,-y,-z; c, 1-x,-y,-z; d, x,y-1,z-1; e, 1-x,1-y,1-z; f, x,y-1,z.

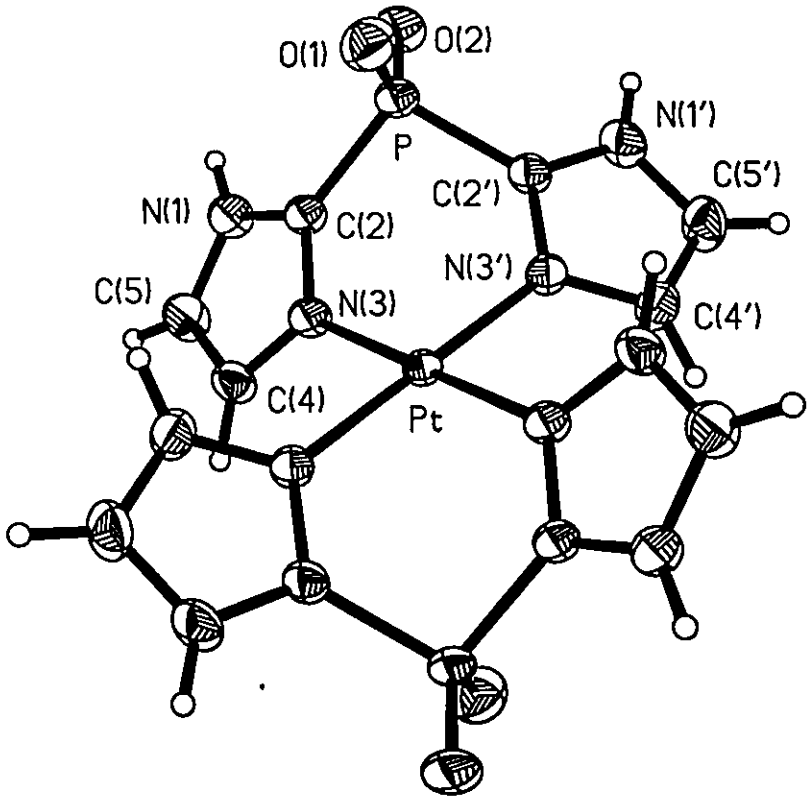

Figure 7.6.1 The molecule of $(BIP)_2Pt$

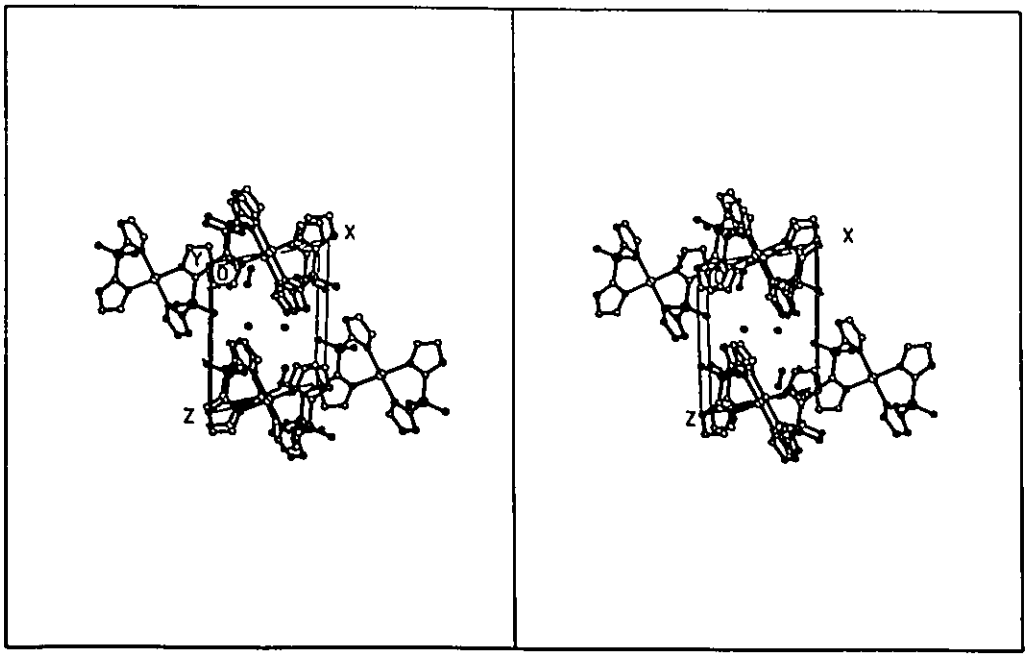

Figure 7.6.2 A stereoview of the packing of $(BIP)_2Pt{\cdot}4H_2O$ in a unit cell

those of Pt-adenine and Pt-guanine complexes 2.007(7) - 2.07(3)Å (179). The Pt atom is located at the inversion centre with one ligand molecule in one asymmetric unit. The other coordinated ligand is generated by inversion. In order to avoid unfavourable steric interactions of these two ligand molecules while still accommodating the square-planar coordination of the Pt atom, the six membered ring Pt-N(3)-C(2)-P-C(2')-N(3') of half of the molecule is folded about the Pt...P axis on one direction to adopt a boat conformation, and the two imidazole rings are folded towards each other on the other direction.

Bond lengths of the coordinated ligand are similar to those of the free ligand (84). Small differences of the C-P-C', O-P-O' and O-P-C bond angles were observed. In the solid state, the neighbouring complex molecules are linked by water molecules which are hydrogen bonded to the imidazole N(1) and oxygen atoms of the ligand [O...N and O...O' distances 2.70(1) - 2.98(1)Å].

Chapter 8

Studies of the Reaction of Phosphine Ligands with Gold(I) Thiolate Complexes

In preparing possible compounds for testing as anti-arthritic drugs, it is desirable to replace the Cl atom in the R_3PAuCl complex by a thiolate S atom. Such a complex will be more relevant to the antirheumatoid arthritis drug triethylphosphinegold(I) 2,3,4,6-tetra-O-acetyl-1-thio-β-D-glucopyranoside (Auranofin). The preparation and characterization of a number of Auranofin analogues have been reported (122 - 125, 129, 131, 132, and 180), with various tertiary alkyl and aryl-phosphines and various thiolate ligands. All the preparations of these complexes were essentially the same and involved the reaction of the R_3PAuCl complex with a thiolate ligand in aqueous solution in the presence of a strong base. The resulting products are usually insoluble and were separated by filtration and recrystallized from some non-aqueous solvent. When the R group is imidazole or its derivatives, it is possible to bind some other transition metal elements to the R group. Such a complex can serve the purpose of introducing two different metals into the biological system at once. Two thiolate ligands, 1-thio-β-D-glucose tetraacetate (TGT) and D-penicillamine (D-pen) were selected for this study. Only preliminary work was done here.

The 1:1 molar ratio reaction product of TEMIP with Me_2SAuCl is an amorphous solid. This solid is assumed to have a formulation of TEMIPAuCl.

Reaction of equimolar TEMIPAuCl with D-pen in a 1:1 methanol/water mixture in the presence of NH_4OH resulted in another amorphous solid after evaporation of the solvents. The by-product of the reaction, NH_4Cl, was not separated, because it has similar solubility to that of the gold complex. When half a mole of $Cu(NO_3)_2$ was added to the 1:1 methanol/water solution of the solid mixture of the gold complex and NH_4Cl, a blue crystalline product was obtained in about 50% yield. This product was characterized to be $[(TEMIPAuCl)_2Cu](NO_3)_2 \cdot 2H_2O$ by the fact that it had an identical infrared spectrum to a genuine sample.

Such a result was rather surprising. A thiolate sulphur atom is generally considered as a better soft ligand for gold(I) than a chloride atom. Replacing the chloride atom from gold(I) by a thiolate sulphur atom is the method used for the preparations of Auranofin and its analogues. In this reaction, the thiolate sulphur atom is replaced by the chloride atom. One possible explanation for the formation of such a product is that the ligands around the gold(I) atom are undergoing rapid exchange in solution. As one of the resulting complexes $[(TEMIPAuCl)_2Cu](NO_3)_2 \cdot H_2O$ is very insoluble, it is precipitated from the reaction mixture, driving the equilibrium towards one side. But in the case of the more soluble metal chloride complexes, similar results were also observed. The other possibility is that when the phosphine is a relatively strong σ-base, the trans-effect of the phosphorus atom labilized the trans-sulphur-gold bond, and a rather weaker Cl-Au bond was more favoured. Such a reaction may have some

relevance to the *in vivo* fate of Auranofin. When the O-acetyl groups on the thioglucose are hydrolysed in the body and the complex becomes more water soluble, the thiolate ligand could be replaced by the chloride ligand, since the body is full of Cl^- and triethylphosphine is a good σ-base.

In order to avoid further complications of the reaction and the formation of undesirable products, 1:1 molar ratio thiolate/gold(I) complexes were prepared first followed by reactions of these complexes with the phosphine ligands. By doing so, undesirable by-product, such as NH_4Cl can be readily separated out from the products by washing the mixture with excess methanol.

Gold(I) thiolate complexes have important applications as antirheumatoid arthritis drugs (15). Typical examples are Sodium thiosulphate-S-aurate(I) (Sanochrysin), disodium thiomalato-S-aurate(I) (Myochrysin), and thioglucosato-S-aurate(I) (Solganol). It is well known that gold(I) complexes usually adopt a linear two coordination. When gold(I) is coordinated to two sulphur ligands (such as Sanochrysin) or one sulphur and one phosphorus ligands (such as Auranofin), the sulphur atom and the phosphorus atom are both terminal and the complex is more likely to be monomeric. In fact, both Sanochrysin and Auranofin are monomeric compounds whose structures are well characterized (181, 55). On the other hand, when gold(I) is reacted with a sulphur ligand in a 1:1 molar ratio (such as Myochrysin and Solganol), the sulphur atom must be bridging to satisfy the preferred linear two coordination for gold(I). Such a bridging sulphur

coordination means that polymers, different oligomers or mixtures of these conformers are probably formed. In fact, most of the 1:1 gold(I)/thiolate complexes are poorly characterized. Only one structure of this type complex has been reported so far with the ligand 2,4,6-triisopropyl-thiophenol. The complex is a sulphur bridged hexamer (182). Such complexes have also been reported for 1:1 Cu(I) and Ag(I)/thiolate complexes, in which sulphur bridged tetramers and octamers are observed (183). It is unfortunate that the 1:1 gold(I) thiomalate and thioglucose complexes, as well as most of the other 1:1 gold(I) thiolate complexes are not of such simple formulations, especially when the ligand is chiral. When there are other good σ-donor ligands available, such as a phosphine or an excess of thiolate ligands, the rather weaker bridging sulphur coordination can be replaced by a terminal ligand, and monomeric complexes can be formed.

Despite the fact that bis-thiolate gold(I) complexes are more likely to be monomeric, relatively few of such type complexes have been well characterized (181, 182, 184, 185). When the ligand thiomalic acid and D-penicillamine was reacted with Me_2SAuCl in a 2:1 molar ratio in the presence of NH_4OH, crystalline products of $[Au(SR)_2]^-$ were obtained with NH_4^+ as the counter cation. The structures of these complexes have been determined and will be discussed elsewhere (186).

The 1:1 gold(I)/D-penicillamine complex (D-penAu) was prepared in about 80% yield by the following method. Equimolar amounts of D-penicillamine and

Me_2SAuCl were dissolved in a 3:1 methanol/water mixture to which excess of NH_4OH (about 5-fold) was added. A white solid precipitated when acetone was added to the reaction mixture. This solid was separated by filtration, washed with methanol and air dried. The by-product NH_4Cl was washed off with methanol. This was verified by the qualitative elemental test for Cl^-. The 1:1 TGT/gold(I) complex (TGTAu) was prepared in about 80% yield by the following method. Equimolar amount of 1-thio-β-D-glucose tetraacetate and Me_2SAuCl was dissolved in CH_2Cl_2 and the solution was evaporated to dryness under nitrogen. The resulting solid was collected, washed with ether and air dried.

Reactions of TMIP and TEMIP with TGTAu in 1:1 molar ratio gave glassy solid products of which no further characterizations were made. In the case of TMIP, addition of $M(NO_3)_2$ (M = Ni, Cu) to the reaction mixture resulted in the formation of $[(TMIP)_2M](NO_3)_2$ complexes, and most of the TGTAu complex can be extracted out from the reaction residue by CH_2Cl_2. The poor σ-basicity of this phosphine ligand is again manifested here, the bridging sulphur coordination can effectively knock off the phosphine from the gold(I) atom. In the case of TEMIP, no $[(TEMIP)_2M](NO_3)_2$ type complexes were formed, and almost no TGTAu complex can be extracted by CH_2Cl_2. Instead, a light blue needle-like crystalline product was obtained. Qualitative elemental analysis showed that this product contained both gold and copper. It can be seen that there is a significant difference between these two types of tertiary imidazole phosphines. It is

unfortunate that the poor crystallinity prevents structural characterization of this product.

The reaction of TEMIP with D-penAu also gave a glassy solid product. Addition of half a mole of $Fe(ClO_4)_2$ to a 1:1 methanol/water solution of this product gave a crystalline solid in about 70% yield (by weight). The crystal rapidly decomposed when it was separated out from the mother liquor. Qualitative elemental analysis showed that both gold and iron were present in the complex. Structural determination by X-ray diffraction showed that the complex probably has the formulation of $(TEMIPAuD\text{-}pen)_2Fe$, with the gold(I) atom linearly coordinated to a phosphorus atom of the phosphine and a sulphur atom of the D-pen molecule and the Fe(II) atom octahedrally coordinated six imidazole nitrogen atoms of the phosphine. Because the crystal decomposed during the intensity data collection (intensities of the standards drop more than 20%), the structure cannot be solved exactly, and no conclusive information can be derived.

Chapter 9

General Conclusions and Future Work

9.1 Reactions of the Phosphine Ligands with Transition Metal Elements

The tertiary imidazole phosphine ligands studied in this work are powerful tris-chelating ligands for relatively hard transition metal elements. Under normal conditions, the thermodynamically more favourable bis-ligand metal complexes are formed, having the metal atoms coordinated to six imidazole N(3) nitrogen atoms. Such complexes are not useful as model compounds of metal centres in biological systems. The bis-ligand Cu(II) complexes provided some interesting Jahn-Teller examples. The formation of the bis-ligand metal complexes are partly caused by the smaller steric demands of the ligands and partly caused by the very low solubilities of these complexes. In addition to the metal complexes discussed in previous chapters, other products were obtained when the ligands TDMIP, TMIP and TEMIP reacted with MX_2 (M = Fe, Co, Ni, or Cu; X = Cl or NO_3) in a 2:1 molar ratio. When TIP was reacted with MCl_2 (M = Co, Ni, Zn) in a 2:1 molar ratio in a 1:1 methanol/water mixture, crystalline products were obtained. These products are soluble in methanol but insoluble in water. The nickel complex has a reddish purple colour. Preliminary X-ray diffraction studies showed that the crystal had hexagonal symmetry and the complex cation probably has a structure similar to that of $[(TIP)_2Ni](NO_3)_2$ mentioned in **Chapter**

4. When TIP was reacted with 3-fold excess of $NiCl_2$, a blue crystalline product was obtained. This compound was soluble in both methanol and water. Similar results were obtained when TIP was reacted with excess $CoCl_2$ and TEMIP was reacted with excess $NiCl_2$. Products with colours and solubilities which differed from the reaction products with a 2:1 ligand/metal molar ratio were obtained. No structural and spectroscopic information was obtained for any of these complexes.

As discussed in **Chapter 4**, the reaction of TIP with excess of $CuCl_2$ is quite different as a polymeric Cu(I)/Cu(II) complex was formed. When TIP was reacted with $CuCl_2$ in a 2:1 molar ratio in a 1:1 methanol/water mixture, a transient blue crystalline solid was formed. This solid redissolved in the reaction mixture when more methanol was evaporated and an amorphous solid was obtained after the mixture was evaporated to dryness.

The reaction product of TEMIP with Me_2SAuCl in a 1:1 molar ratio is amorphous. Upon addition of half a mole of $Cu(NO_3)_2$, $CuCl_2$ or $FeCl_2$, crystalline products were obtained, of which the $Cu(NO_3)_2$ complex was characterized as discussed in **Chapter 6**. Again, the complex with metal nitrate is very insoluble while complexes with metal chlorides are soluble in methanol. Reaction of TDMIP with AuI in a 1:1 molar ratio gave an insoluble white precipitate. This precipitate can be redissolved by addition of the ligand up to a 4-fold excess. After addition of $AgNO_3$ (1 equivalent to AuI) and separation of the resulting AgI, a crystalline product was obtained. Semi-quantitative elemental analysis showed that this

compound contained gold with a gold content of about 12.4%. A crystal of the compound was found to be monoclinic with a unit cell volume of 8265(2)Å^3. Because the crystal decomposed during the intensity data collection, little structural information was obtained. According to the information obtained, this compound is probably a high coordination gold(I) complex with the formulation of $[(TDMIP)_4Au](NO_3)$ which requires a gold content of 13% and a calculated number of molecules per unit cell of 4.25, close to the reasonable value of 4.

As discussed in **Chapter 3**, the isolation of pure product of the new phosphine, TDMIP-5 was unsuccessful. Addition of $Cu(NO_3)_2$ to a methanol solution of the reaction mixture resulted in the formation of a deep blue solid precipitate. This solid was insoluble in methanol, acetone and dichloromethane. It could be washed by such solvents successively and then recrystallized from water. Since all of the other materials are more likely to be soluble in those organic solvents, this blue solid is most probably a Cu(II) complex of the ligand. It will be of interest to determine the structure of this complex because if the ligand is chelating the metal, a quite strained eight membered ring of P-C(5)-C(4)-N(3)-Cu-N'(3)-C'(4)-C'(5)-P will be formed, even if the phosphine is oxidized to the corresponding phosphine oxide. However, steric congestion will probably prevent the formation of a bis-ligand chelated complex.

Reactions of tertiary imidazole phosphine ligands with transition metal elements are not simple, and many interesting chemical studies can still be done

in this area.

9.2 Chemical Properties of Tertiary Imidazole Phosphines

Some of the reactions related to the chemical properties of the phosphine ligands are discussed below.

1. Oxidation of TIP resulted in the cleavage of one of the P-C bonds and the formation of the bis-imidazole-phosphinic acid (84). Oxidation of the phosphorus atom will probably lead to the nucleophilic attack on this atom by the solvent water molecule, followed by the breaking of the P-C bond. The resulting phosphinic acid is found as a zwitterion in the solid state (84), with the OH group on the phosphorus atom deprotonated and one of the imidazole N(3) nitrogen atom protonated. If this is also the case in solution, the negative charge on the oxygen atom will probably prevent further nucleophilic attack on the phosphorus atom. Similar reaction with the ligand TDMIP has also been observed (156). Reactions of this type are probably a reflection of the lack of electron density on the phosphorus atom. If the phosphorus atom is more electron-rich, as in Ph_3P, the corresponding phosphine oxide is formed after oxidation.

2. Reaction of TDMIP with acidic $HAuCl_4$ leads to the formation of the bis-carbene gold(I) complex (149). This is thought to be caused by protonation of the imidazole N(3) nitrogen atom followed by breaking of at least one of the P-C bonds (149). Oxidation of the phosphorus atom might occur first since the starting $HAuCl_4$ is strongly oxidizing.

3. Reaction of TIP with Me_2SAuCl and MCl_2 (M = Ni or Cu) in methanol gave the product $(MeO)_3PAuCl$ (**Chapter 4, 7**). The formation of such a product is probably caused by nucleophilic attack on the phosphorus atom by the solvent molecule followed by breaking of the P-C bonds. It is interesting that in this case, all three P-C bonds are broken. The relatively higher bond energy of the P-O bond is probably the driving force of such a reaction, which is accelerated by the presence of the metal cations.

4. Reaction of TMIP with AuI and $Ni(NO_3)_2$ gave the product $[(TMIP)_2Ni](AuI_2)_2$ (**Chapter 5**). In this complex, the ligand is only coordinated to the nickel atom through its hard binding sites. The phosphorus atom on the ligand is free without coordination. The formation of the AuI_2^- must follow the decomposition reaction of some unstable gold(I) complexes {$[(TMIPAuI)_2Ni]^{2+}$ is probably one of them}. The instability of the gold(I) TMIP complex is further manifested by the fact that the colourless complex TMIPAuCl slowly turned to yellow, brown and then black over a period of 6 months.

5. Complexes of TEMIP with both a soft and a hard metal atoms can be readily prepared, whether they are highly insoluble (with NO_3^- as the counter anion) or readily soluble (with Cl^- as the counter anion).

Some information about the chemical properties of these tertiary imidazole phosphines can be gleaned from the above reactions.

1. Phosphine ligands having the phosphorus atom attached to the

imidazole C(2) carbon atoms are not very stable. They are subject to oxidative, electrophilic and nucleophilic attacks. Such attacks eventually break the P-C bonds and hence disintegrate the ligands. This can be caused by the polarity of the P-C bonds. The P-C bonds can be considered as polarized with δ^- on the carbon atom and δ^+ on the phosphorus atom. The more electronegative the carbon atom, the more polarized the P-C bond, and the more vulnerable this bond. The imidazole C(2) carbon atom can be considered as more electronegative than imidazole C(4,5) and other aryl and alkyl carbon atoms. This is reflected in the ease of preparing these ligands. The ligands TIP, TDMIP and TMIP can be readily prepared by direct lithiation of the imidazole C(2) carbon atom with n-butyllithium while lithiation of the imidazole C(4,5) carbon atom can only proceed through the corresponding bromide (**Chapter 3**).

2. The phosphorus atom of the tris(imidazol-2-yl)phosphines is a poorer σ-base than that of the tris(imidazol-4(5)-yl)phosphines. Although the σ-basicity and the π-acidity of phosphine ligands is still a controversial subject (6), it is generally observed that phosphines having more electron-withdrawing groups attached to the phosphorus atom are poorer σ-bases and better π-acids. In stabilizing higher valent metal atoms, σ-basicity is more important than π-acidity. This is true for gold(I) complexes. The imidazole C(2) carbon atom, being adjacent to two nitrogen atoms, is more electron-withdrawing than the imidazole C4 and C5 atoms. On the other hand, the electron withdrawn from the ring C(2) carbon atom

can be more readily delocalized onto the ring N(3) nitrogen atom and into the ring π-system while that withdrawn from the ring C[4(5)] atom will be mainly concentrated on the less electronegative carbon atoms. All evidence observed in this work supports the argument that the ligands TIP, TDMIP and TMIP are poorer σ-donor ligands than TEMIP and other aryl and alkyl-phosphine ligands with respect to the phosphorus atom.

9.3 Future Work

As mentioned above, there is still a lot of chemistry to be done for transition metal complexes with tertiary imidazole phosphines. In addition to the phosphorus atom and the imidazole N(3) nitrogen atoms, these ligands have a third type binding site which can be explored, that is, the imidazole N(1) nitrogen atom. Deprotonation of this nitrogen atom followed by binding to a metal atom has been reported for a number of complexes (187). Such a type of binding has also been observed for some enzyme systems (188).

The synthesis of the new phosphine ligand TEMIP opens a method of derivatizing the biologically important imidazole molecules at their C-4(5) site. Such imidazole derivatives are more relevant to the ligands in biological systems. Especially, when there are bulky inert groups on the imidazole C(2) atom, steric blocking by these groups can produce interesting coordination complexes. One proposed tertiary imidazole phosphine ligand is tris(1-ethyl-2-isopropylimidazol-5-yl)phosphine. This ligand can be prepared from 2-isopropylimidazole by

ethylation at the N(1) site and bromination at the C(5) site followed by metallation of the bromide and reaction of the metallated imidazole with PCl_3. The larger hydrophobic groups on the imidazole, as compared to the phosphine TDMIP-5, will probably make this phosphine water insoluble, and hence simplify the purification of the final product. In fact, this ligand has been successfully synthesized by a student who is following this work, although whether the phosphorus atom is attached to the imidazole C(4) or C(5) carbon atom has not been determined. Reactions of this phosphine ligand with transition metal elements are currently under investigation. Other tri- and bi-dentate ligands with such imidazole derivatives can be prepared in the future and can be used to make interesting model complexes for some metalloenzymes.

References

1. D.F. Shriver, P.W. Atkins, and C.H. Lanford, "Inorganic Chemistry", Oxford University Press, Oxford, England, 1990.

2. a, J. Emsley and D. Hall, "The Chemistry of Phosphorus", Harper and Row, London, 1976; b, R.F. Hudson, "Organo-Phosphorus Chemistry", Academic Press, London, 1965.

3. a, L.H. Pignolet, "Homogeneous Catalysts with Metal Phosphine Complexes", Plenum Press, New York, 1983; b, E.C. Alyea ed., "Catalytic Aspects of Metal Phosphine Complexes", American Chemical Society Press, Washington, D.C., 1982; c, F.A. Cotton and B. Hong, Prog. Inorg. Chem., 1992, **40**, 179; d, C. Bianchini, A. Meli, M. Peruzzini, F. Vizza and F. Zanobini, Coord. Chem. Rev., 1992, **120**, 193.

4. D.E.C. Corbridge, "Phosphorus", Elsevier, Amsterdam, 1978.

5. a, M. Grayson, P.T. Keough, and G.A. Johnson, J. Am. Chem. Soc., 1959, **81**, 4803; b, D.P. Young, W.E. McEwen, D.C. Velez, J.W. Johnson, and C.A. Vander Werf, Tetrahedron Lett., 1964, 359.

6. G. Paccioni and P.S. Bagus, Inorg. Chem., 1992, **31**, 4391.

7. S.J. Berners-Price and P.J. Sadler, Struct. Bond., 1988, **70**, 27.

8. a, W.A. Henderson and C.A. Streuli, J. Am. Chem. Soc., 1960, **82**, 5791; b, R.C. Bush and R.J. Angelici, Inorg. Chem., 1988, **27**, 681.

9. a, J. Behan, R.A.W. Johnstone, and R.J. Puddephatt, J. Chem. Soc., Chem. Commun., 1978, 444; b, R.J. Puddephatt, G.M. Bancroft, and T. Chan, Inorg. Chim.

Acta, 1983, **73**, 83.

10. N.N. Greenwood and A. Earnshaw, "Chemistry of the Elements", Pergamon Press, England, 1986.

11. F.A. Cotton and G. Wilkinson, "Advanced Inorganic Chemistry", Harper and Row, New York, 1983.

12. a, M.J. Dewar, Bull. Soc. Chem. Fr., 1951, **18**, c71; b, J. Chatt and L.A. Duncanson, J. Chem. Soc., 1953, 2939.

13. P. Powell, "Principles of Organometallic Chemistry", Chapman and Hall, London, 1988.

14. R.J. Puddephatt, "The Chemistry of Gold", Elsevier, Amsterdam, 1978.

15. R.V. Parish, Interdisc. Sci. Rev., 1992, **17**, 221.

16. C.E. Housecroft, Coord. Chem. Rev., 1992, **115**, 117.

17. W.E. Smith, Coord. Chem. Rev., 1985, **67**, 311.

18. P. Pyykko, Chem. Rev., 1988, **88**, 563.

19. D.R. McKelvey, J. Chem. Ed., 1983, **60**, 112.

20. H. Schmidbaur, Interdisc Sci. Rev., 1992, **17**, 213.

21. P. Pyykkö and J.-P. Desclaux, Acc. Chem. Res., 1979, **12**, 276.

22. H. Schmidbaur, Gold Bull., 1990, **23**, 11.

23. a, M.I. Brittan, Am. Sci., 1974, **62**, 402; b, B.M. Chadwick and A.G. Sharpe, Adv. Inorg. Chem. Radiochem., 1968, 8; c, A.G. Sharpe, "The Chemistry of Cyno Complexes of the Transition Metals", Academic Press, London, 1976.

24. R. Roulet, N.Q. Lan, W.R. Mason, and G.P. Fenske, Helv. Chim. Acta, 1973, **56**, 2405.

25. F. Bonati and G. Mnghetti, Gazz. Chim. Ital., 1973, **103**, 373.

26. S. Åkerstrom, Ark. Kemi., 1959, **14**, 387.

27. H. Schmidbaur and A. Shiotani, Chem. Ber., 1971, **104**, 2821.

28. L.G. Vaughan, U.S. Pat. 3,661,959, 1972.

29. L.H. Jones, Inorg. Chem., 1963, **2**, 777.

30. G.E. Coates, C. Kowala, and J.M. Swan, Aust. J. Chem., 1966, **19**, 539.

31. P.J. Sadler, Struct. Bond., 1976, **29**, 171.

32. A. Shiotani, H.-F. Klein, and H. Schmidbaur, J. Am. Chem. Soc., 1971, **93**, 1555.

33. a, M.J. Mays and P.A. Vergano, J. Chem. Soc., Dalton Trans., 1979, 1112; b, C.B. Colburn, W.E. Hill, C.A. McAuliffe, and R.V. Parish, J. Chem. Soc., Chem. Commun., 1979, 218; c, R.V. Parish, A.K.H. Al-Sa'ady, C.A. McAuliffe, K. Moss, and R. Fields, J. Chem. Soc., Dalton Trans., 1984, 491.

34. O. Crespo, M.C. Gimeno, A. Laguna, and P.G. Jones, J. Chem. Soc., Dalton Trans., 1992, 1601.

35. P.G. Jones, G.M. Sheldrick, A. Fugner, F. Gotzfried, and W. Beck, Chem. Ber. 1981, **114**, 1413.

36. P.G. Jones, Acta Cryst. 1980, **B36**, 3105.

37. P.G. Jones, J. Chem. Soc., Chem. Commun., 1980, 1031.

38. R.C. Elder, E.H.K. Zeiher, M. Onady, and R. Whittle, J. Chem. Soc., Chem.

Commun., 1981, 900.

39. P.J. Sadtler, Adv. Inorg. Chem., 1991, **36**, 1.

40. G.M. Dyson, Pharm. J., 1929, **123**, 249, 266.

41. K. Landé, Munch. Med. Wochenschr., 1927, **74**, 1132.

42. J. Forestier, J. Lab. Clin. Med., 1935, **20**, 827.

43. D.J. McCarty, "Arthritis", Lea and Febiger, Philadelphia, 1985.

44. Empire Rheumatism Concil, Ann. Rheum. Dis., 1960, **20**, 315.

45. a, M. Chaffman, R.N. Brogden, R.C. Heel, T.M. Speight, and G.S. Avery, Drugs, 1984, **27**, 378; b, J.H. Leibfarth and R.H. Persellin, Agents Actions, 1981, **11**, 458.

46. T. Matsubara, Y. Saegusa, and K. Hirohata, Arthritis Rheum., 1988, **31**, 1272.

47. J. Richter, Ann. Rheum. Dis., 1991, **50**, 372.

48. K.J. Rae, C.N.N. Mackay, C.J. McNeil, D.H. Brown, W.E. Smith, D. Lewis, and H.A. Capell, Ann. Rheum. Dis., 1986, **45**, 839.

49. N.L. Gottlieb and R.G. Gray, Agents Actions, 1981, **8**, 529.

50. W.F. Kean and W.W. Buchanan, Ther. Rev., 1981, **36**, 1557.

51. B.M. Sutton, E. McGusty, D.T. Walz and M.J. DiMartino, J. Med. Chem., 1972, **15**, 1095.

52. A.A. Capell, D.S. Cole, K.K. Manghani, and R.W. Morris Ed., "Auranofin", Excerpt Medica, Amsterdam, 1983.

53. G.C. Bernhard, J. Lab. Clin. Med., 1982, **100**, 167.

54. a, J.R. Ward, H.J. Williams, E. Boyce, M.J. Egger, J.C. Reading, and E.O. Sannelson, Am. J. Med., 1983, 133; b, N.L. Gottlib and W.J. Wilbur, Am. J. Med., 1983, 1.

55. D.T. Hill and B.M. Sutton, Cryst. Struct. Commun., 1980, **9**, 679.

56. S.J. Berners-Price and P.J. Sadler, Chem. Br., 1987, 541.

57. a, S. Martinez-Carrera, Acta Cryst., 1966, **20**, 783; b, G.J. Visser and A. Vos, Acta Cryst., 1971, **B27**, 1802.

58. a, K. Schofield, M.R. Grimmett, and B.R.T. Keen, "Heteroaromatic Nitrogen Compounds: The Azoles", Cambridge University Press, Cambridge, England, 1976. pp 346-372; b, M.R. Grimmett, Adv. Heterocycl. Chem., 1980, **27**, 241.

59. M.R. Grimmett, "Comprehensive Heterocyclic Chemistry", K.T. Potts Ed., Pergamon Press, Oxford, England, 1984. pp 374-375.

60. a, J. Elgaero, C. Marzin, A.R. Katritzky, and P. Linda, Adv. Heterocycl. Chem., Suppl., 1976, **1**, 280; b, B.I. Khristich, Khim. Geterotsikl. Soedin., 1970, 1683.

61. a, G.L. Eichhorn Ed., "Inorganic Biochemistry", Elsevier, New York, 1973; b, R.J. Sundberg and R.B. Martin, Chem. Rev., 1974, **74**, 471; c, B.E. Bowler, A.L. Raphael, and H.B. Gray, Prog. Inorg. Chem., 1990, **38**, 259.

62. A.G. Sykes, Struct. Bond., 1991, **75**, 175.

63. N. Kitajima, Adv. Inorg. Chem., 1992, **39**, 1.

64. T.G. Spiro Ed., "Zinc Enzymes", Wiley, New York, 1983.

65. J.B. Vincent and G. Christou, Adv. Inorg. Chem., 1989, **33**, 197.

66. R.G. Wilkins, Chem. Soc. Rev., 1992, **21**, 171.

67. B.L. Stoddard, P.L. Howell, D. Ringe, and G.A. Petsko, Biochemistry, 1990, **29**, 8885.

68. N.J. Curtis and R.S. Brown, J. Org. Chem., 1980, 45, 4038.

69. F.-J. Wu, D.M. Kurtz, Jr., K.S. Hagen, P.D. Nyman, P.G. Debrunner, and V.A. Vankai, Inorg. Chem., 1990, **29**, 5174.

70. R.K. Boggess and M. Zatko, J. Coord. Chem., 1975, **4**, 217.

71. a, R.J. Read and M.N.G. James, J. Am. Chem. Soc., 1981, **103**, 6947; b, R.S. Brown, N.J. Curtis, and J. Hugget, J. Am. Chem. Soc., 1981, **103**, 6953.

72. B.P. Block, Inorg. Sunth., 1953, **4**, 14.

73. M.D. Faltens and D.A. Shirley, J. Chem. Phys., 1970, **53**, 4249.

74. R.N. Keller, Inorg. Synth., 1946, **2**, 247.

75. a, I. Satoru, Y. Mitsutasu, and M. Hisaya (Mitsubishi Petrochemical Co., Ltd.) Jpn. Kokai Tokkyo Koho, JP 61 30,574 (86 30,574), C.A. 104: P224902z; b, Mitsui Toatsu Chemicals, Inc., Jpn Kokai Tokkyo Koho, JP 60 56,961 (85 56,961), C.A. 103: P87878j.

76. M.J. Buerger, "X-ray Crystallography", John Wiley and Sons, New York, 1942.

77. P. Luger, "Modern X-ray Analysis on Single Crystals", Walter de Gruyter, Berlin, 1980.

78. G.H. Stout and L.H. Jensen, "X-ray Structure Determination", John Wiley and Sons, New York, 1989.

79. S. French and K. Wilson, Acta Cryst., 1978, **A34**, 517.

80. A.C.T. North, D.C. Phillips, and F.S. Mathews, Acta Cryst., 1968, **A24**, 351.

81. N. Walker and D. Stuart, Acta Cryst., 1983, **A39**, 158.

82. D.J. Cromer and T.T. Waber, "International Tables for X-ray Crystallography", Vol. IV, Kynoch Press, Birmingham, 1974.

83. G.M. Sheldrick, SHELXTL PLUS Release 4.21/V, Siemens Analytical Instrument Inc. Madison, WI, 1990.

84. H.E. Howard-Lock, C.J.L. Lock, S. Penny, and M.A. Turner, Can. J. Chem., 1989, **67**, 1051.

85. D. Copping, C.S. Frampton, H.E. Howard-Lock, and C.J.L. Lock, Acta Cryst., 1992, **C48**, 675.

86. D. Copping, Senior Thesis, McMaster University, 1990.

87. S.S. Moore and G.M. Whitesides, J. Org. Chem., 1982, **47**, 1489.

88. M. El Borai, A.H. Moustafa, M. Anwar, and F.I. Abdel Hay, Croat. Chem. Acta, 1981, **54**, 211

89. T. Seidel, Senior Thesis, McMaster University, 1990.

90. R.G. Jones and K.C. McLaughlin, J. Am. Chem. Soc., 1949, **71**, 2444.

91. D.G. Gorenstein, "Phosphorus-31 NMR", Academic Press, Orlando, Florida, 1984.

92. B.E. Mann, J. Chem. Soc., Perkin Trans., 1972, 30.

93. a, M.M. Crutchfield, C.H. Dungan, L.H. Letcher, V. Mark, and J.R. Van Wazer,

"Topics in Phosphorus Chemistry", Vol. 5, John Wiley & Sons, 1967; b, L.D. Quin and J.H. Somers, J. Org. Chem., 1972, **37**, 1217.

94. M.A. Turner, Ph.D. Thesis, McMaster University, 1988.

95. L.D. Quin and J.J. Breen, Org. Magn. Reson., 1973, **5**, 17.

96. J.B. Hodgson, G.C. Percy, and D.A. Thornton, J. Molecular Struct., 1980, **66**, 81.

97. Marcia Cordes de N.D. and J.L. Walter, Spectrachim. Acta, 1968, **A24**, 237.

98. J.J. Daly, J. Chem. Soc., 1964, 3799.

99. T.S. Cameron, and B. Dahlen, J. Chem. Soc., Perkin Trans. II, 1975, 1737.

100. T.S. Cameron, K.D. Howlett, and K. Miller, Acta Cryst., 1978, **B34**, 1639.

101. N. Kitajima, T. Koda, S. Hashimoto, T. Kitagawa, and Y. Moro-oka, J. Am. Chem. Soc., 1989, **111**, 8975.

102. N. Kitajima, K. Fujisawa, and Y. Moro-oka, J. Am. Chem. Soc., 1990, **112**, 3210.

103. C. Sandmark and C.-I. Branden, Acta Chem. Scand., 1967, **21**, 993.

104. G.J.M. Ivarsson and W. Forsling, Acta Cryst., 1979, **B35**, 1896.

105. J.P. Konopelski, C.W. Reimann, C.R. Hubbard, A.D. Mighell, and A. Santoro, Acta Cryst., 1976, **B32**, 2911.

106. D.L. McFadden, A.T. McPhail, C.D. Garner, and F.E. Mabbs, J. Chem. Soc., Dalton Trans., 1975, 263.

107. A. Murphy, B. Hathaway, and T.J. King, J. Chem. Soc., Dalton Trans., 1979, 1647.

108. B.C. Cornilsen and K. Nakamoto, J. Inorg. Nucl. Chem., 1974, **36**, 2467.

109. P. Day, Endeavour, 1970, **20**, 45.

110. B. Bremer, A. Pinkerton, and J.A. Walmsley, Inorg. Chim. Acta, 1990, **174**, 27.

111. S.K. Hadjikakou, P.d. Akrivos, P. Karagiannidis, E. Raptopoulou, and A. Terzis, Inorg. Chim. Acta, 1993, **210**, 27.

112. R.J. Baker, S.C. Nyburg, and J.T. Szymanski, Inorg. Chem., 1971, **10**, 138.

113. C.S. Arcus, J.L. Wilkinson, C. Mealli, T.J. Marks, and J.A. Ibers, J. Am. Chem. Soc., 1974, **96**, 7564.

114. C. Mealli, C.S. Arcus, J.L. Wilkinson, T.J. Marks, and J.A. Ibers, J. Am. Chem. Soc., 1976, **98**, 711.

115. J.O. Alben, L. Yen, and N.J. Farrier, J. Am. Chem. Soc., 1970, **72**, 4475.

116. G.L. Soloveichik, O. Eisenstein, J.T. Poulton, W.E. Streib, J.C. Huffman, and K.G. Caulton, Inorg. Chem., 1992, **31**, 3306.

117. P.S. Coan, K. Folting, J.C. Huffman, and K.G. Caulton, Organometallics, 1989, **8**, 2724.

118. J.C. Slater, J. Chem. Phys., 1964, **41**, 3199.

119. A. Bondi, J. Phys. Chem., 1964, **68**, 441.

120. M.R. Churchill and F.J. Rotellar, Inorg. Chem., 1979, **18**, 166.

121. W.E. Marsh, W.E. Hatfield, and D.J. Hodgson, Inorg. Chem., 1983, **22**, 2899.

122. P.D. Cookson and E.R.T. Tiekink, J. Coord. Chem., 1992, **26**, 313.

123. E. Delgado and E. Hernandez, Polyhedron, 1992, **11**, 3135.

124. V.J. Hall, G. Siasios, and E.R.T. Tiekink, Aut. J. Chem., 1993, **46**, 561.

125. P.D. Cookson and E.R.T. Tiekink, J. Chem. Soc., Dalton Trans., 1993, 259.

126. R. Faggiani, H.E. Howard-Lock, C.J.L. Lock, and M.A. Turner, Can. J. Chem., 1987, **65**, 1568.

127. D.G. Gorenstein, Prog. NMR Spectrosc., 1983, **16**, 1.

128. N.C. Baenziger, W.E. Bennett, and D.M. Soboroff, Acta Cryst., 1976, **B32**, 962.

129. F. Bonati, A. Burini, B.R. Pietroni, E. Giorgini, and B. Bovio, J. Organomet. Chem., 1988, **344**, 119.

130. S. Ahrland, B. Aurivillius, K. Dreisch, B. Noren, and A. Oskarsson, Acta Chem. Scand., 1992, **46**, 262.

131. C.S.W. Harker, E.R.T. Tiekink, and M.W. Whitehouse, Inorg. Chim. Acta, 1991, **181**, 23.

132. P.D. Cookson and E.R.T. Tiekink, J. Crystallogr. Spectrosc. Res., 1993, **23**, 273.

133. C.J.L. Lock and M.A. Turner, Acta Cryst., 1987, **C43**, 2096.

134. P.G. Jones and E. Bembenek, J. Crystallogr. Spectrosc. Res., 1992, **22**, 397.

135. a, A. Hountas, A. Terzis, and G.C. Papavassiliou, Acta Cryst., 1990, **C46**, 228; b, H.-N. Adams, W. Hiller, and J. Strahle, Z. Anorg. Allg. Chem., 1982, **485**, 81; c, P. Braunstein, A. Muller, and H. Bogge, Inorg. Chem., 1986, **25**, 2104; d, Y. Ishikawa, K. Kikuchi, K. Saito, and I. Ikemoto, Acta Cryst., 1989, **C45**, 572; e, U. Geiser, H.H. Wang, K.S. Webb, N.A. Firestone, N.A. Beno, and J.M. Williams, Acta Cryst., 1987, **C43**, 996; f, G. Helgesson and S. Jagner, Acta Chem. Scand.,

1987, **A41**, 556; g, E. Bohm, K. Dehnicke, J. Beck, W. Hiller, J. Strahle, A. Maurer, and D. Fenske, Z. Naturforsch., 1988, **B43**, 138.

136. O.P. Anderson, J. Chem. Soc., Dalton Trans., 1972, 2597.

137. O.P. Anderson, J. Chem. Soc., Dalton Trans., 1973, 1237.

138. a, H.A. Jahn and E. Teller, Proc. Roy. Soc., 1937, **A161**, 220; b, H.A. Jahn, Proc. Roy. Soc., 1938, **A164**, 117.

139. J.H. van Vleck, J. Chem. Phys., 1939, **7**, 61.

140. D.L. Cullen and E.C. Lingafelter, Inorg. Chem., 1970, **9**, 1858.

141. a, D.L. Cullen and E.C. Lingafelter, Inorg. Chem., 1971, **10**, 1264; b, N.W. Issacs and C.H.L. Kernard, J. Chem. Soc. A, 1969, 386.

142. I. Bertini, P. Dapporto, D. Gatteschi, and A. Scozzafava, J. Chem. Soc., Dalton Trans., 1979, 1409.

143. M.D. Joesten, S. Takagi, and P.G. Lenhert, Inorg. Chem., 1977, 16, 2680.

144. R.S. Glass, L.K. Steffen, D.D. Swanson, G.S. Wilson, R. de Gelder, R.A.G. de Graaff, and J. Reedijk, Inorg. Chim. Acta, 1993, **207**, 241.

145. C.P. Keijzers, R.K. McMullan, J.S. Wood, G. van Kalkeren, R. Srinivasan, and E. de Boer, Inorg. Chem., 1982, **21**, 4275.

146. a, I.B. Bersuker, Coord. Chem. Rev., 1975, **14**, 357; b, J. Gazo, I.B. Bersuker, J. Garaj, M. Kabesova, J. Kohout, H. Langfelderova, M. Melnik, M. Serator, and F. Valach, Coord. Chem. Rev., 1976, **19**, 253; c, I.B. Bersuker, The Jahn-Teller Effect and Vibronic Interactions in Modern Chemistry, Plenum, New York, 1984.

147. B.N. Figgis, E.S. Kucharski, and P.A. Reynolds, Acta Cryst., 1990, **B46**, 577.

148. F.A. Cotton, L.R. Falvello, C.A. Murillo, and J.F. Quesada, J. Solid State Chem., 1992, **96**, 192.

149. J.F. Britten, C.J.L. Lock, and Z. Wang, Acta Cryst., 1992, **C48**, 1600.

150. F. Bonati and G. Minghetti, Synth. React. Inorg. Metal-Org. Chem., 1971, **1**, 299.

151. G. Banditelli, F. Bonati, S. Calogero, G. Valle, J. Organomet. Chem., 1984, **275**, 153.

152. B. Cetinkaya, P. Dixneuf, and M.F. Lappert, J. Chem. Soc., Dalton Trans., 1974, 1827.

153. R. Aumann and E.O. Fischer, Chem. Ber., 1981, **114**, 1853.

154. H. G. Raubenheimer, F. Scott, M. Roos, and R. Otte, J. Chem. Soc., Chem. Commun., 1990, 1722.

155. F. Bonati, A. Burini, B.R. Pietroni, and B. Bovio, J. Organomet. Chem., 1989, **375**, 147.

156. R.G. Ball, R.S. Brown, and J.L. Cocho, Inorg. Chem., 1984, **23**, 2315.

157. K.C. Dash, H. Schmidbaur, and A. Schmipeter, Inorg. Chim. Acta, 1980, **41**, 167.

158. G. Banditelli, A.L. Bandini, G. Minghetti, and F. Bonati, Can. J. Chem., 1981, **59**, 1241.

159. H.-N. Adams, W. Hiller, and J. Strahle, Z. Anorg. Allg. Chem., 1982, **485**, 81.

160. W. Clegg, Acta Cryst., 1976, **B32**, 2712.

161. C.J.L. Lock and Z. Wang, Acta Cryst., 1993, **C49**, 1330.

162. Y. Rosopulos, U. Nagel, and N. Beck, Chem. Ber., 1985, **118**, 931.

163. T. Amagai, T.K. Miyamoto, H. Ichida, and Y. Sasaki, Bull. Chem. Soc. Jpn., 1989, **62**, 1078.

164. S.J. Berners-Price, M.J. DiMartino, D.T. Hill, R. Kuroda, M.A. Mazid, and P.J. Sadler, Inorg. Chem., 1985, **24**, 3425.

165. E.R.T. Tiekink, J. Cryst. Spectrosc. Res., 1990, **20**, 371.

166. B. Bovio, F. Bonati, A. Burini, and B.R. Pietroni, Z. Naturforsch., 1984, **B39**, 1747.

167. J.F. Britten, C.J.L. Lock, and Z. Wang, Acta Cryst, 1993, **C49**, 881.

168. J.B. Stothers and J.R. Robinson, Can. J. Chem., 1964, **42**, 967.

169. F. Bonati, A. Burini, B.R. Pietroni, and B. Bovio, J. Organomet. Chem., 1991, **408**, 271.

170. G. Banditelli, F. Bonati, S. Calogero, G. Valle, F.E. Wagner, R. Wordel, Organometallics, 1986, **5**, 1346.

171. a, U. Schubert, K. Ackerman, and R. Aumann, Cryst. Struct. Commun., 1982, **11**, 591; b, M. Lanfranchi, M.A. Pellingheli, A. Tiripicchio, F. Bonati, Acta Cryst., 1985, **C41**, 52.

172. W.P. Bosman, W. Bos, J.M.M. Smits, P.T. Beurskens, J.J. Bour, J.J. Steggerda, Inorg. Chem., 1986, **25**, 2093.

173. D.S. Eggleston, D.F. Chodosh, R.L. Webb, L.L. Davis, Acta Cryst., 1986, **C42**, 36.

174. R. Uson, A. Laguna, J. Vicente, J. Garcia, P.G. Jones, and G.M. Sheldrick, J. Chem. Soc., Dalton Trans., 1981, 655.

175. a, K. Kikuchi, Y. Ishikawa, K. Saito, and I. Ikemoto, Acta Cryst., 1988, **C44**, 466; b, P.G. Jones and J. Lautner, Acta Cryst., 1988, **C44**, 2091.

176. L. Pauling, The Nature of the Chemical Bond, 3rd edition, Ithaca: Cornell Univ. Press, 1960, pp221-230.

177. J.R. Lechat, R.H. de Almeida Santos, G. Banditelli, and F. Bonati, Cryst. Struct. Commun., 1982, **11**, 471.

178. a, J.R. Bales, M.A. Mazid, P.J. Sadler, A. Aggarwal, R. Kuroda, S. Neidle, D.W. Gilmour, B.J. Peart, and C.A. Ramsden, J. Chem. Soc., Dalton Trans., 1985, 795; b, B.J. Graves, D.J. Hodgson, C.G. van Kralingen, and J. Reedjik, Inorg. Chem., 1978, **17**, 3007; c, J.W. Carmichael, N. Chan, A.W. Cordes, C.K. Fair, and D.A. Johnson, Inorg. Chem., 1972, **11**, 1117.

179. a, R. Beyerle, B.E. Brown, R. Faggiani, B. Lippert, and C.J.L. Lock, Inorg. Chem., 1985, **24**, 4001; b, R. Faggiani, B. Lippert, C.J.L. Lock, and R.A. Speranzini, Inorg. Chem., 1982, **21**, 3216; c, R. Faggiani, C.J.L. Lock, and B. Lippert, J. Am. Chem. Soc., 1980, **102**, 5418; d, B. Lippert, C.J.L. Lock, and P. Pilon, Inorg. Chim. Acta, 1984, **93**, 43; e, C.J.L. Lock, R.A. Speranzini, G. Turner, and J. Powell, J. Am. Chem. Soc., 1976, **98**, 7865.

180. a, C.S.W. Harker, E.R.T. Tiekink, and M.W. Whitehouse, Inorg. Chim. Acta, 1991, **181**, 23; b, B.F. Hoskins, Z. Lu, and E.R.T. Tiekink, Inorg. Chim. Acta, 1989, **158**, 7.

181. H. Ruben, A. Zalkin, M.O. Faltens, and D.H. Templeton, Inorg. Chem., 1974, **13**, 1836.

182. I. Schroter and J. Strahle, Chem. Ber., 1991, **124**, 2161.

183. a, I. Schroter-Schmid and J. Strahle, Z. Naturforsch., 1990, **B45**, 1537; b, B. Becker, W. Wojnowski, K. Petters, E.-M. Petters, H.G. von Schnering, Polyhedron, 1990, **9**, 1659; c, W. Wojnowski, M. Wojnowski, K. Petters, E.-M. Petters, and H.G. von Schnering, Z. Anorg. Allg. Chem., 1985, **530**, 79.

184. P.A. Bates and J.M. Waters, Acta Cryst., 1985, **C41**, 862.

185. P.J.M.W.L. Birker and G.C. Verschoor, Inorg. Chem., 1982, **21**, 990.

186. J.F. Britten, D. LeBlanc, H.E. Howard-Lock, Z. Wang, and C.J.L. Lock, paper to be published.

187. a, P. Chaudhuri, I. Karpenstein, M. Winter, M. Lengen, C. Butzlaff, E. Bill, A.X. Trautwein, U. Florke, and H.-J. Haupt, Inorg. Chem., 1993, **32**, 888; b, P. Chaudhuri, I. Karpenstein, M. Winter, C. Butzlaff, E. Bill, A.X. Trautwein, U. Florke, and H.-J. Haupt, J. Chem. Soc., Chem. Commun., 1992, 321; c, G.P. Gupta, G. Lang, C.A. Koch, B. Wang, W.R. Scheidt, and C.A. Reed, Inorg. Chem., 1990, **29**, 4234.

188. a, I. Bertini, L. Banci, M. Piccioli, C. Luchinat, Coord. Chem. Rev., 1990, **100**,

67; b, J.A. Tainer, E.D. Getzoff, J.S. Richardson, and D.C. Richardson, Nature, 1983, **306**, 284.